

UCSF

UC San Francisco Electronic Theses and Dissertations

Title

Inactivation of HYAL1 in squamous cell carcinomas

Permalink

<https://escholarship.org/uc/item/59f2n76m>

Author

Frost, Gregory I.

Publication Date

1999

Peer reviewed|Thesis/dissertation

Inactivation of HYAL1 in Squamous Cell Carcinomas

by

Gregory I. Frost

DISSERTATION

Submitted in partial satisfaction of the requirements for the degree of

DOCTOR OF PHILOSOPHY

in

Oral Biology

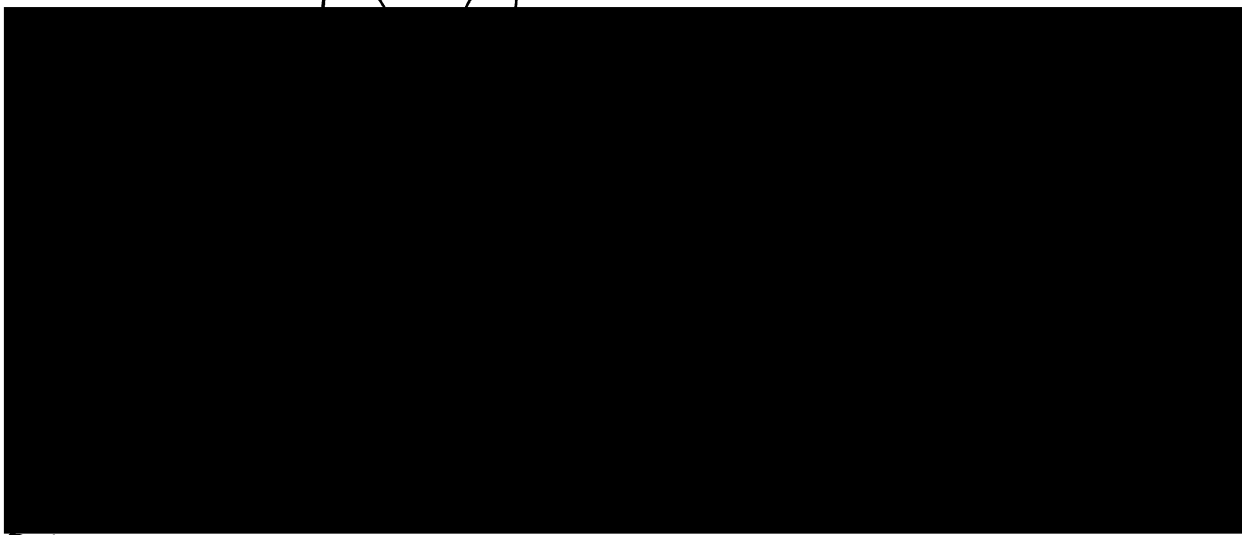
in the

GRADUATE DIVISION

of the

UNIVERSITY OF CALIFORNIA

San Francisco



Date

University Librarian

Degree Conferred:



**ACADEMIC
PRESS**

Academic Press
525 B Street, Suite 1900
San Diego, CA 92101-4495

March 9, 1999

Gregory I. Frost
Sidney Kimmel Cancer Center
10835 Altman Row
San Diego, CA 92121
Fax: 450-3251

Dear Dr. Frost:

RE: Analytical Biochemistry, Biochemical and Biophysical Research Communications, Genomics

Thank you for your request to use material from your work published in an Academic Press publication.

It is now the policy of Academic Press that authors need not obtain permission in the following cases: (1) to use their original figures or tables in their future works; (2) to make copies of their papers for their classroom teaching; and (3) to include their Papers as part of their dissertations.

Sincerely,

Cindy MacDonald
Editorial Manager

attachment

Abstract

Inactivation of HYAL1 in Squamous Cell Carcinomas

Gregory I. Frost

Hyaluronidases are a family of β ,1-4 endoglucosaminidases that degrade glycosaminoglycans, such as hyaluronan and chondroitin sulfates. The substrates for these enzymes function as structural components of the extracellular matrix and as reservoirs for growth factors. Their digestion products however, have been implicated as initiators or promoters of complex cell signaling processes such as angiogenesis, chemotaxis and apoptosis. This leaves hyaluronidases as potential regulators of pathways that play a pivotal role in wound healing, development and carcinogenesis.

Initial studies resulted in the purification, cloning and sequencing of HYAL1, the predominant hyaluronidase of human plasma. Sequence analysis revealed the hyaluronidase of human plasma to be identical to the predicted gene product of LuCa-1, a candidate tumor suppressor gene on a region of human chromosome 3p21.3 frequently deleted in malignancy. To further refine this candidate tumor suppressor gene locus on 3p21.3, and to test whether the HYAL1^{LuCa-1} gene was directly related to the chromosomal aberrations, I

examined the status of HYAL1 in head and neck squamous cell carcinoma lines, where hemizygous deletions of 3p21.3 are frequently found. A combined functional and molecular-genetic approach was used to test this hypothesis. While the HYAL1 gene product was absent in the majority of head and neck squamous cell carcinoma lines and hemizyosity of 3p21.3 was frequently detected, the two phenomena were not associated with each other. Inactivation of the HYAL1 gene product was not dependent upon gene copy number, but rather was associated with the incomplete splicing of the 5' untranslated region. This aberrant splicing was not a result of mutations within the HYAL1 gene, but may be linked to defective splicing that is epigenetic in nature. The HYAL1 gene is therefore unlikely to be directly linked to the chromosomal deletions on 3p21.3 in the majority of head and neck squamous cell carcinomas.

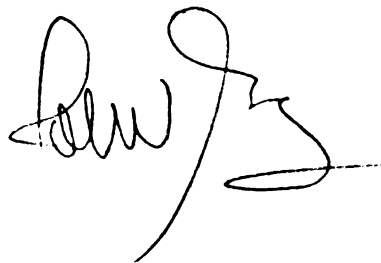
A handwritten signature in black ink, appearing to be 'D. Wang' or similar, with a long horizontal stroke extending to the right.

Table of Contents

Chapter-1	Introduction	3
	Oncogenes and tumor suppressor genes.....	3
	Tools for identifying tumor suppressor genes.....	8
	Deletions of 3p21.3 in malignancy.....	10
	Hyaluronan receptors and signaling pathways.....	14
	Hyaluronidases.....	20
	Hypothesis.....	28
Chapter-2	A Microtiter Based Assay For Hyaluronidase Activity Not Requiring Specialized Reagents.....	41
	Introduction.....	44
	Materials and methods.....	46
	Results.....	52
	Discussion.....	56
	Figures.....	60
	References.....	66
Chapter-3	Purification, Cloning And Expression of Human Plasma Hyaluronidase.....	68
	Introduction.....	71
	Materials and methods.....	72
	Results.....	79
	Discussion.....	83
	Figures.....	84
	References.....	95
Chapter-4	The Hyaluronidase Gene HYAL1 Maps To Chromosome 3p21.2-21.3 in Human And 9F1-F2 In Mouse, A Conserved Candidate Tumor Suppressor Locus.....	97
	Introduction.....	101
	Materials and methods.....	103
	Results.....	109
	Discussion.....	114
	Figures.....	121
	References.....	128

Chapter-5	HYAL1^{LuCa-1}, A Candidate Tumor Suppressor Gene On Chromosome 3p21.3, Is Inactivated In Head And Neck Squamous Cell Carcinomas Through Incomplete Pre-mRNA Splicing	132
	Introduction.....	136
	Results.....	139
	Discussion	147
	Materials and methods	152
	Figures.....	158
	References.....	176
Appendix.....		178
	A. Generation of anti-HYAL1 Monoclonal Antibodies.....	179
	B. Substrate And pH Specificity of HYAL1.....	181
	C. Uptake of Immunoaffinity Purified HYAL1 in Mouse.....	181
	D. Immunoreactivity of HYAL1 in MDCK Cells.....	185

Chapter-1

Introduction

Abbreviations

HA	hyaluronan, hyaluronic acid
bHA	biotinylated HA;
Sulfo-NHS	N-hydroxysulfosuccinimide;
EDAC	1-ethyl-3-(3-dimethylaminopropyl)carbodiimide;
OPD	o-phenylenediamine
rTRU	relative Turbidity Reducing Units
RT-PCR	reverse transcriptase PCR
EST	expressed sequence tag
FISH	fluorescence <i>in-situ</i> hybridization
CGH	comparative genomic hybridization
LOH	loss of heterozygosity
TSG	tumor suppressor gene
UTR	untranslated region

Introduction

The process of carcinogenesis is complex and dynamic. The decision made by an organism to protect the integrity of its genome is essential to maintain homeostasis. Without somatic genomic stability, carcinogenesis is inevitable. It is therefore surprising that the inactivation of a single gene such as p53 is sufficient for the integrity of the genome to eventually break down (1). Fortunately, in the case of such critical tumor suppressor genes, lightning must essentially strike twice in the same place.

Oncogenes

The discovery that carcinogenesis could be initiated in phenotypically normal cells by transformation with certain acute retroviral genomes was an indispensable tool to study malignant transformation (2). More importantly, such experiments defined cancer as a genetic event, something that chemical carcinogenesis had been unable to determine unequivocally. This led to the discovery that the transformed phenotype from these acute retroviruses was a result of viral oncogenes, genes homologous to those already present in the human genome (3). These proto-oncogenes were converted to oncogenes in many tumors and were themselves transforming in the oncogenic state (4).

Conversion of these proto-oncogenes to oncogenes occur in malignancies through genomic amplifications, translocations or mutations (5,6). The diverse signaling pathways that oncogenes utilize to transform cells led to the initial theories of multistep carcinogenesis (7). Although these oncogenes acted in a dominant fashion and were capable of inducing the transformed phenotype in immortalized cells, they were generally unable to transform primary cultures (8).

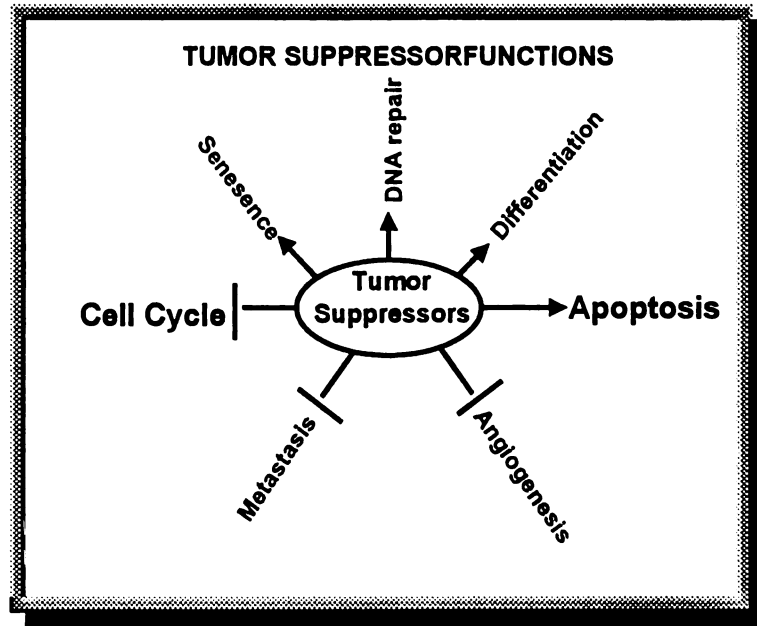
Tumor Suppressors Genes

Somatic cell hybrids of normal cells with malignant cells resulted in an unexpected finding, that malignant transformation was recessive under some conditions (9). While malignant/malignant cell fusions retained their tumorigenic phenotype, normal/malignant cell hybrids were not capable of forming tumors. These studies contradicted the dominant nature of oncogenes. Examination of the genetics of familial cancers such as retinoblastoma, (10,11) led to a revised view that some oncogenes could be recessive rather than dominant. The identification of homozygously deleted regions surrounding the retinoblastoma susceptibility gene suggested that the absence of genetic material could be associated with carcinogenesis, in contrast to the mutated and amplified oncogenes (12,13). Reintroduction of the wild-type retinoblastoma cDNA into

cells demonstrated that the gene was in fact a suppressor of tumor growth, or anti-oncogene (14,15).

Two principal functions ascribed to tumor suppressor genes are either the induction of cell cycle arrest or apoptosis. Both pathways are capable of reverting the malignant phenotype, providing that other elements of these cascades have not been compromised. Although some genes may be preferentially lost or mutated in the process of carcinogenesis, they do not necessarily have the capacity to reverse the tumorigenic phenotype. DNA repair enzymes are examples of genes which play a critical role in protecting the integrity of the genome, but are unable to reverse the malignant phenotype once damage has occurred, and therefore cannot be considered true tumor suppressors (16, 17).

While certain "gate keeper" suppressor genes may play a role early in the development of neoplasia by regulating cell cycle, genomic instability or apoptosis, inactivation of other genes may be essential for the later processes of carcinogenesis, such as metastasis. Such metastasis suppressor genes may play no apparent role in proliferation but prevent the metastatic dissemination of tumors (18). The selective inactivation of gene products that regulate cell-cell



adhesion have been described in a number of malignancies. The E-cadherin adhesion gene is frequently inactivated in carcinomas through hypermethylation, mutations and/or deletions. E-cadherin is generally believed to serve a role as a suppressor of tumor dissemination through the maintenance of cell-cell junctions. Additionally, E-cadherin may regulate cell cycle control, through sequestering β -catenin at the plasma membrane and thereby preventing its mitotic activity in the nucleus. The metastasis suppressor gene KAI1 is another cell surface protein that plays a critical role in the regulation of prostate cancer metastasis, but has no apparent role in the regulation of primary tumor growth (19). DCC (Deleted in Colon Carcinoma) is a neural cell adhesion molecule that deleted in colon

carcinomas. Recent evidence suggests that this gene may also play a role in apoptosis (20).

Known Tumor Suppressor Genes and Their Functions

Gene	Chromosome	Known Functions
Rb	13q.14	G1/S transition
p53	17p.13	Cell Cycle arrest Apoptosis
p16(INK4A)	9p21	G1/S transition
p19ARF	9p21	P53 activation Block MDM2
p21WAF	6p21.2	G1/S transition
BRCA1	17q21	G2/M regulation? DNA repair (RAD52 association)?
BRCA2	13q12.3	DNA repair (RAD52 association)?
APC	5q21-22	Suppression of β -catenin and wnt-signaling pathway
E Cadherin	16q22.1	Metastasis Suppressor Cell cycle (β -catenin-LEF1?)

Multistep Carcinogenesis

In contrast to the *in vitro* transformation assays that use oncogenic retroviruses and immortalized cell lines, carcinogenesis is a multistep process, involving many tumor suppressor genes and oncogenes (21). Epidemiological and molecular genetic studies of both familial and inherited forms of cancer support this model of multistep carcinogenesis, and explains the latency of the disease (22). Some mutations can increase the overall rate of mutation however,

thereby accelerating the process. Aberrant cell cycle progression for example, increases the probability of acquiring new mutations. Loss of apoptosis increases the chance that cells with damaged genomes will survive. The diversity of pathways and cellular compartments where oncogenes and tumor suppressors are found supports the theory that multiple aberrations are required in the process of malignancy.

Tools for Isolating Tumor Suppressor Genes

The tools for isolating individual tumor suppressor genes were only recently developed, and are continuously evolving. The inherent challenge has been to find what is absent, rather than abundant. Several distinct approaches have been used to address this problem.

The observation of cytogenetic abnormalities in a particular cancer was the earliest method to associate specific genetic material with tumor suppression. Such techniques were able to demonstrate a consistent association of retinoblastoma susceptibility to deletions on chromosome 13 (23). Only with the advent of molecular cloning techniques however, could the genetic material within this region be isolated and characterized (24).

More advanced tools have evolved to permit genome wide scanning for candidate tumor suppressor gene loci. Restriction fragment length polymorphism (RFLP) mapping, fluorescence *in situ* hybridization (FISH) (25), and comparative genomic hybridization (CGH) (26), allow potential chromosomal targets frequently deleted in a particular malignancy to be identified with accuracy. Importantly, these methods are efficient enough to allow the screening of multiple samples to find the smallest regions of common overlap as well as the frequency of these chromosomal losses. With these techniques, genes such as WT1 (Wilms Tumor Susceptibility gene) have been isolated using homozygous deletions as a chromosomal "beacon" (27). Such techniques are also applicable to the tumor suppressor gene loci of spontaneous cancers. Deletions identified on chromosome 9p21 for example, were pursued with a massive positional cloning strategy to narrow the locus from overlapping homozygous deletions and identified the p16 tumor suppressor gene (28). In this particular case however, the gene had already been functionally cloned by others (29).

Other tumor suppressor genes have been discovered by serendipity. P53 was for many years thought to be an oncogene, based upon its upregulation following viral transformation of mammalian cells. Studies from reintroducing

P53 into cell lines demonstrated some degree of transforming capacity (30). It was discovered several years later that the transforming P53 cDNA was in fact mutated, and that the wildtype form of P53 had pronounced tumor suppressive properties (31).

There has been a recent shift from the examination of DNA to RNA in the hunt for tumor suppressors by way of differential display techniques (32). By comparing RNA transcripts from normal and malignant tissues, transcripts specifically lost in the process of carcinogenesis can be readily identified. Moreover, such transcripts can be reintroduced back into cells lacking these transcripts to examine for changes in the malignant phenotype. Unfortunately, it is often difficult to rule out whether a silenced gene plays a role in the progression of malignancy, or is simply associated with the malignant process. Therefore, both the functional and expression criteria must be met for any conclusions to be drawn.

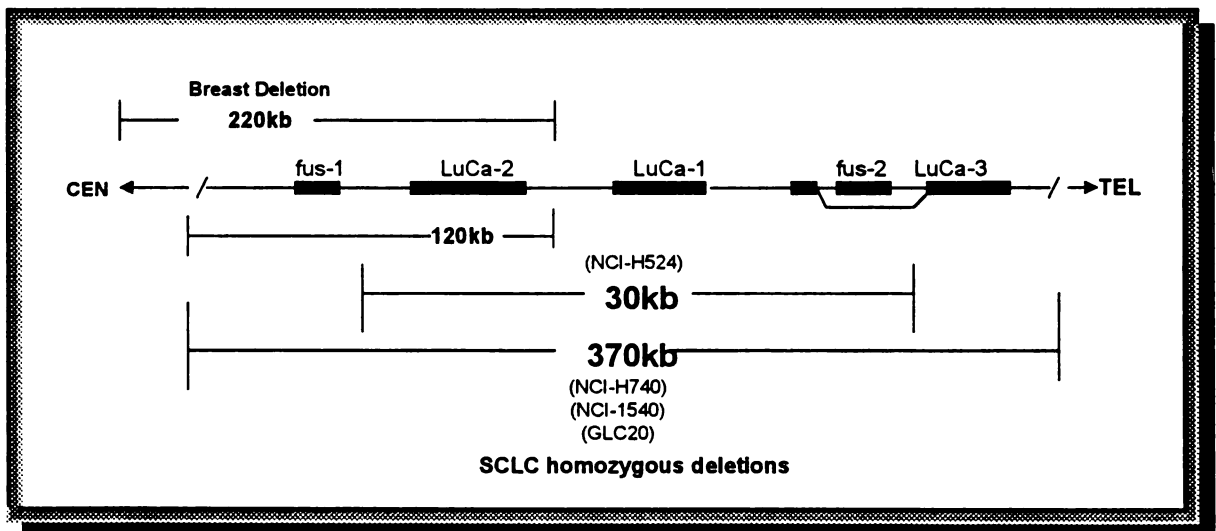
The 3p21.3 Candidate Tumor Suppressor Gene Locus

Chromosomal aberrations of human chromosome 3p21 were first noted in small cell lung carcinomas. Karyotypic analysis of 16 small cell lung carcinoma (SCLC) lines identified deletions over 3p14-23 in all cell lines examined (33).

RFLP mapping of SCLC has identified at least three regions showing loss of heterozygosity over 3p: 3p14-cen, 3p21.3, and 3p25 (34). Candidate tumor suppressor genes within these deleted regions are FHIT at 3p14 (35), the von Hippel-Lindau (VHL) disease region at 3p25 (36), and several candidate genes on 3p21.3 (37). In addition to these hemizygous deletions, homozygous deletions over 3p21.3 are found in approximately 10-15% of small cell lung carcinomas (38). 3p21.3 homozygous deletions have been identified in tumor biopsies as well as in cell lines derived from them, and are absent from normal adjacent tissue or patient matched lymphoblast lines (39). The generation of a transcript map from cosmids covering 600kb of overlapping homozygous deletions in SCLC lines has identified several genes within this region of homozygous deletions over 3p21.3 (40). Although a DNA mismatch repair gene homologue hMSH2, resides on chromosome 3p21.3 and would be considered a strong candidate for such deletions, the gene resides outside the reported homozygous deletions in small cell lung carcinoma. Homozygous deletions over 3p21.3 have also been reported in non-small cell lung carcinomas and in a breast carcinoma cell line (41).

Additional support for the presence of a tumor suppressor gene(s) on 3p21.3 come from reports of functional tumor suppressor activity attributed to this region (42, 43). Chromosome 3p21.3 is deleted non-randomly from chromosome-3 hybrids that regain their tumorigenic potential (44, 45). Furthermore, reintroduction of this region of chromosome 3p21.3 suppresses tumorigenicity *in vivo*, with no apparent changes on *in vitro* growth characteristics, aside from a reduced cloning efficiency in soft agar. Functional tumor suppressor activity coinciding with the reported homozygous deletions of this region has also been identified using a nasopharyngeal carcinoma line (46). This is in agreement with hemizygous deletions of 3p21.3 that are found in head and neck squamous cell carcinomas (HNSCC) (47)

Homozygous Deletions over 3p21.3

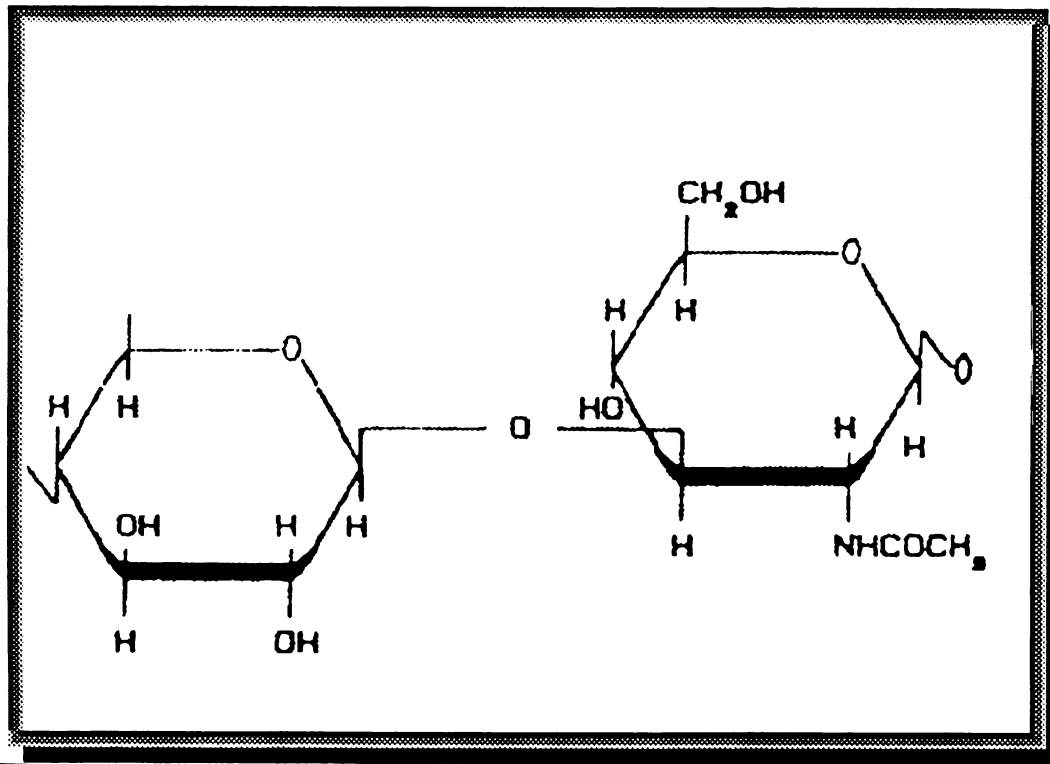


The Relevance of Extracellular Matrix to Malignancy

The *sine qui non*-of malignancy lies in the ability of a carcinoma to invade and colonize surrounding tissues. Carcinomas are presented with multiple barriers that must be overcome in order to escape from their tissues of origin and colonize surrounding tissues. These include disregulated growth, evasion of the immune system, acquisition of neovasculature, and invasion first through basement membrane and then through stroma. In addition to these factors, increasing evidence suggests that epithelial engagement with the extracellular matrix (ECM) is critical to prevent programmed cell death, or apoptosis (48,49,50). Malignant cells, however, frequently become resistant to such apoptotic stimuli, and are no longer dependent on basement membrane-derived signals for survival (51). In many malignancies, hyaluronan (HA), an ECM molecule normally associated with stromal or undifferentiated tissues, is elevated in response to stromal/epithelial or autocrine interactions (52,53). When a carcinoma breaches the basement membrane and enters the stroma, there is a loss of many cell-cell and cell-ECM interactions, and these cells encounter a different class of ECM molecules. Such cells may require new receptors to pass

through such matrices and must evade apoptosis in the presence of a different class of ECM molecules.

Structure of Hyaluronan



Hyaluronan, HA receptors and Related Signaling Pathways

HA, a high molecular weight viscous linear polysaccharide glycosaminoglycan, and major component of the extracellular matrix, consists of repeating disaccharide units [$\text{GlcNAc}\beta$ 1-4 $\text{GlcUA}\beta$ 1-3]. It is also the only non-sulfated glycosaminoglycan. It is prominent in connective tissue, cartilage, synovial fluid (54) and whenever rapid tissue turnover is occurring, such as during embryonic

development (55) and in wound healing (56). It is synthesized by a family of HA synthases (three human synthases to date (57,58,59)), that incorporate UDP-N acetyl glucosamine and UDP-glucuronic acid into the high molecular weight polymer. The cellular location of the three HA synthases have not been established, but it has been suggested that they reside in the plasma membrane (60).

CD44 and Related Signaling Pathways

Several studies implicate a role for HA-cell surface receptor-interactions in signal transduction processes. In thymocytes, engagement of the HA-receptor CD44, through crosslinking antibodies or immobilized HA protected against CD3 or dexamethasone induced apoptosis. This effect appeared to be independent of bcl-2 and p53 modulation and could not rescue radiation-induced apoptosis (61). Function-perturbing antibodies disrupting HA-CD44 interactions also induced apoptosis in lung fibroblasts cultured on a HA-fibrin matrix (62). Overexpression of a soluble CD44 receptor demonstrated that breast carcinoma cells lacking CD44-ligand interactions also underwent apoptosis in response to local HA production at the site of metastasis (63). Alternatively, injection of function-perturbing monoclonal antibodies to CD44 or localized subcutaneous

injection of hyaluronidase was able to block lymph node invasion of lymphoma cells in a murine LB lymphoma tumor model (64). Disruption of HA-receptor interactions is therefore capable of perturbing tumorigenesis under some circumstances by influencing invasion and apoptotic thresholds.

Generation of CD44-null epithelium through use of a keratin-5 driven antisense transgene to CD44 results in epithelium that shows a delayed response to carcinogens and tumor promoters (65). Keratinocytes derived from such mice show a suppressed response to heparin-binding growth factors such as basic FGF and heparin-binding EGF, possibly due to the inability to express the V3 heparan sulfate-containing splice variant. In contrast, the phenotype of CD44 null mice are unexpected, in that SV40 immortalized fibroblasts derived from such mice are highly tumorigenic *in vivo* and display suppressed tumorigenicity following transfection of the standard form of CD44 (CD44s) (66). Indeed, CD44 has been reported to function as a metastasis suppressor gene in prostate carcinomas and localizes to chromosome 11p13, a region believed to harbor a metastasis suppressor gene (67). Furthermore, in colon carcinomas, expression of CD44s is downregulated although CD44 splice variants are upregulated. Restoration of the CD44 standard isoform expression in such cells

results in suppression of tumorigenicity (68). Whether the inherent differences in such models can be reflected in the suppressive effects of the standard form of CD44 versus the tumor promoting effects of CD44 splice variants respectively, is unknown.

CD44 and HA appear to elicit cell-type specific responses. In macrophages, HA fragments (<400kDa) upregulate chemokine expression and nitric oxide synthase through CD44-receptor interactions, without requiring new protein synthesis. This induction of immediate early response genes utilizes an NF-kappa-B pathway independent of CD-14, the LPS receptor (69, 70). Sonication of high molecular weight HA (>6,000kDa) that lacks any signaling capacity to lower molecular weight fragments (<400kDa) is sufficient to induce the HA-CD44 chemokine response. This activation can be blocked with function perturbing anti-CD44 monoclonal antibodies or by the addition of high molecular weight HA.

The role of smaller HA oligosaccharides in neovascularization is another model in which HA-CD44 interactions have been implicated.(71 72, 73). Treatment of bovine aortic endothelial cells with hyaluronidase derived HA fragments (3-10 disaccharides in length) induce endothelial cell proliferation, tube

formation and tyrosine kinase activity (74). This activation results in phosphorylation of the CD44 receptor, and signaling through PKC isoforms leading to activation of ERK-1.

The intracellular signaling cascades initiated by CD44 has not been characterized completely. CD44 can associate with the actin filament system through the ERM (ezrin/radixin/moesin) protein-complex (75) as well as with merlin, the neurofibromatosis tumor suppressor gene product (76). The cytoplasmic domain of CD44 has also been shown to interact directly with the actin-linking protein, ankyrin (77). Phosphorylation of Ser-323/Ser-325 in the cytoplasmic domain of CD44 modulates the association of CD44 with actin. In some cells, interactions of CD44 and HA have also been shown to activate ^{32}P FAK tyrosine kinase activity (78). Despite the amount of information on CD44, the combination of 10 variable exons within the extracellular domain that result in multiple splice variants (79), glycosaminoglycan attachments and other posttranslational modifications (80) have made a generalized understanding of this molecule extraordinarily difficult.

RHAMM, the receptor for HA-mediated motility

In addition to CD44, the receptor for HA mediated motility (RHAMM), has been implicated in a number of other complex HA-mediated signaling processes. RHAMM was discovered initially as an HA binding-protein that is upregulated in response to mutant-ras expression in fibroblasts (81). RHAMM was believed to be a cell surface receptor, but molecular cloning failed to identify a transmembrane domain (82). Overexpression of RHAMM was shown to be transforming in fibroblasts, and a dominant negative form of RHAMM was able to negate H-ras transformation (83). These studies suggested that expression of RHAMM is required in fibroblasts for H-ras transformation. Additionally, HA or anti-RHAMM mAbs against the HA binding domain were capable of stimulating motility in ras-transformed fibroblasts which involves transient focal adhesion turnover, and p^{125} FAK(84) activity. This HA-mediated motility could also be perturbed by inhibition of tyrosine kinase activity.

In addition to effecting cell migration, studies show that suppression of RHAMM with antisense, dominant-negative constructs or soluble RHAMM, modulates Cdc2/Cyclin B levels and leads to G2/M arrest (85). Interestingly, a soluble form of RHAMM was able to suppress lung metastasis. The discovery of

a novel RHAMM variant (RHAMMV4), that exists intracellularly, rather than on the cell surface, led to a study of the role of intracellular RHAMM on signal transduction. A dominant negative form of RHAMMV4 was able to inhibit mutant active ras activation of extracellular regulated kinase (ERK) and coimmunoprecipitated with both mitogen-activated protein kinase kinase and ERK. These results suggest that the intracellular RHAMMV4 acts downstream of ras, possibly at the level of mitogen-activated protein kinase kinase-ERK interactions.

More recent independent studies have drawn serious question as to the assumptions of RHAMM in both ras mediated signaling and carcinogenesis. A novel variant of RHAMM containing the previously overlooked 5' full-length cDNA was isolated that exists as a 95kDa protein and is exclusively intracellular (86). This novel variant of RHAMM was thus termed Intracellular HA Binding Protein (IHABP). This form of RHAMM was shown to be expressed in normal cells, showed no alterations in breast carcinoma lines and was the exclusive form of RHAMM expressed in these cells (87). If RHAMM is exclusively an intracellular protein, its role in motility and carcinogenesis must be reevaluated (88).

Mammalian Hyaluronidases

Until recently, little was known about HA synthases, the enzymes responsible for the synthesis of HA, or about hyaluronidases, the primary enzymes involved in their degradation. Vertebrate hyaluronidases (E.C 3.1.25) are a family of β ,1-4 endoglucosaminidases that degrade HA and chondroitin sulfates (89,90). In vertebrates, these enzymes were initially grouped into two classes, the neutral-active hyaluronidases such as the sperm-associated PH20 (91,92), and those with an acid pH optimum, found in extracts of liver (93), kidney (94), lung (95), brain (96), skin (97), placenta (98), macrophages (99), fibroblasts (100) and in urine (101) and human plasma (102). Attempts to isolate these somatic hyaluronidases have been met with limited success because of difficulties in stabilizing the purified protein and their remarkably high specific activity.

Hyaluronidases are the primary catabolic enzymes involved in the hydrolysis of HA, cleaving internal β -1,4 linkages of this high molecular weight polymer, resulting in smaller oligosaccharides, that can then be further digested by the concerted action of exoenzymes, the β -glucuronidases and N-acetylhexosaminidases (103). These mammalian hyaluronidases differ from

those found in prokaryotic species in that they are non-specific and can also hydrolyze the β (1,4) glucosamidic bonds of the chondroitin sulfates.

The Sperm Hyaluronidase, PH20

PH20 is the most thoroughly characterized of the hyaluronidase enzymes in mammalian species, owing in large part to the high levels of activity found in testes extracts. Though much data has been accrued since the initial observation of testicular hyaluronidase as a "spreading factor" in 1929 (104), it is only recently that information on the structure of this enzyme has been available.

PH20, the predominant sperm hyaluronidase, has been characterized in many species, as a glycosyl phosphatidylinositol-(GPI) anchored enzyme (105) whose sequence and chromosomal location in humans, 7q.31, has been determined (106). PH20 is not normally expressed in tissues other than the testes and can be distinguished by virtue of a broad pH optimum from the other mammalian hyaluronidases which display a sharp optima at pH 3.8-4.0. PH20 shows sequence homology to several venom hyaluronidases (107,108), but was in fact, not discovered by virtue of its enzymatic activity, but rather from its biological role in mediating sperm/egg adhesion. It was not until several years later that researchers sequencing the bee venom hyaluronidase observed a

strong sequence similarity to PH20. This then created the link of PH20 to the sperm hyaluronidase activity.

The sequence homology between the venom hyaluronidases and PH20 family lies within the first 300 amino acids. Site-directed mutagenesis and deletion mapping has refined the catalytic domain of PH20 to the N-terminal domain within the first 300 amino acids (109). PH20 is believed to be involved in penetration of the HA rich cumulus surrounding the egg (110) and in addition, binding to the zona pellucida. It has been proposed that PH20 may have dual function: the N-terminal domain of the protein functioning as a hyaluronidase and the carboxy terminal domain functioning in the adhesion to the zona pellucida (111).

HYAL2, The Lysosomal Hyaluronidase

Following the identification of HYAL1 as the hyaluronidase in human plasma, the examination of several expressed sequence tags (EST's) in the human EST database led to the identification of a second somatic tissue hyaluronidase, termed HYAL2 (112). The HYAL2 gene resides immediately centromeric to HYAL1 on human chromosome 3p21.3. Similar to HYAL1, HYAL2 encodes a hyaluronidase that is active only at acidic pH, but unlike

HYAL1, HYAL2 is localized to lysosomes, does not digest chondroitin sulfates and is only capable of digesting HA to approximately 20kDa oligosacharrides. HYAL2 is expressed in all tissues but the adult brain. The murine homologue of Hyal2, is localized adjacent to murine Hyal1 on mouse chromosome-9 between markers D9Mit183 and D9Mit17, placing HYAL2 between mouse dystroglycan and transferrin (113). Murine Hyal2 is expressed early in the brain, with highest expression at E10 and no expression by P30. This silencing correlates with the hypermethylation of a CpG island upstream of Hyal2.

Alignment of Human Hyaluronidases

HYAL1	1	-----MAAHLLPICALFLTLDMAQGRGRLP---	NRFFTTVGNANTQWCLERHGVDV
HYAL2	1	-----MRAGPGPTVTLALAVAWAMELKPTA	PIFTGRPFVVAADVPTQDGPRLKVPIDL
PH20	1	MGVLKFRKIFFRSFVKSSGVSQIVFTFLIPCC	LTFNFRAPVPIPNVFFLWALNAPSEFLGK
consensus	1	1 L P P F W t C r vDv	
HYAL1	54	SVEDVVANQGTFRGPDITIFYSSQLTTHYYT	PTGEPVGGGLPNASIAELARTFQDILAAP
HYAL2	58	NAEDVQASFNNEGFVNQNITIFYRDRLLYR	RFDSAGRSVHGCVPNVSIWARKMLQKRVE
PH20	71	SLSEFIQSEIRINATGGXTIFYVDRLEVYI	YIDSITGVTVNGGHPKISIQDELDKAKK
consensus	71	F a P RINATGGXTIFY LG YP G V GG	LPQ SL H i i d
HYAL1	123	SLAVIDWEAWKFRVAFNVDTRDHYRQR	RALVQAQHPDWPAQVEAVQDQEQGAARA
HYAL2	127	AGLAVIDWEDWRFVVRNWDQNDVYRRL	SRQLVARRHPDWPPDRIVKQAKQYER
PH20	140	SLAVIDWEVRRFTVARNWPKPKVYKNR	IEIQQQNVQLSLTEATEKAKQSEKAKK
consensus	141	GLAVIDWE WRP W NW KDiy r S LV	A F Aa vm Tl r
HYAL1	193	PKPRGLWCFYGFPCYNYDLS--PNITG	QCPSGIRACNCLGWLWGQSRALYPSIY
HYAL2	197	VRPRHLWCFYLFPCYNHDXVQNWESIT	GRCPDVEVARNDCLAWLWAEESTALP
PH20	210	VRPRHLWCFYLFPCYNHXYK--PGN	SCFNVEIKRNDLSWLVNEESTALP
consensus	211	LRP LWGFY FPCYN f Y G C ND L	WLW S ALyPSiYm
HYAL1	261	VQHRVAEAEFRVAVAAGD-PNLEVL	PVYQIFD-TTNHFLPLDELEHSLGESA
HYAL2	267	VSEFRVCEALRVARTHHANHALPVY	VTRPTYSRCTGLSEMDDLIS-TIGESA
PH20	277	VVRNRVREAIRVSKIPDAKSLPVP	FAKTRIVFTDQVLKFLSQDELVYTF
consensus	281	yV RV EA RV LPV y y D l s	GEs A GA GvvlW
HYAL1	329	PKESQAKKEYMDTTGIFYIRVNSGALL	QALCSGHRCYRRTSHPKALLLN
HYAL2	335	STETCQYKDYLTRLIIVFYVNSWATQY	CSRAQGHGSGYPP--GNPSASTL
PH20	347	PKESQLLDNYMETIINHYKNSVLAAKM	CSQVLEQEQVGRKNWSSDYLH
consensus	351	t sC i Ym L PfiInvt g CS C G	Cv L NPDPNFAIQLEKGGK--
HYAL1	398	---LSLRALSLDQAQMAVEKRCR	PGWQAPWCERKSMW-----
HYAL2	402	EPQLRPELSWADIDHLQTHRCQC	LGWSGEGC-----
PH20	415	---FTVGRKPELDLEQFSEKHYG	SCSTLSCKEKADVKD TDAVDVCI
consensus	421	G s D F C CY ADGVCIDAF LKPPMETEPQIF	
HYAL1		-----	
HYAL2		-----	
PH20	482	YNASPSLSATMFIVSILFLIISVVASL	
consensus	491		

MGEA5, the Caenorhabditis elegans Homologue

Screening of a meningioma library with patient autologous serum led to the identification of a novel gene on human chromosome 10q24.1-q24.3 that was immunoreactive in 22% of patients with meningioma. This protein showed considerable homology to a putative hyaluronidase of *Caenorhabditis elegans* (114). and the nagH gene of *Clostridium perferingens* (115). These endo-beta-N-acetylglucosaminidases are structurally unrelated to the PH20 family of hyaluronidases. The MGEA5 gene product was found to exist with two variants (MGEA5, MGEA5s) resulting in proteins of 92 and 54kDa, respectively. The MGEA5 enzyme is active towards HA at neutral pH and is expressed in both fetal and adult tissues. Given the broad tissue expression of this gene product, the reason for autoreactivity towards this protein is unknown. It was found that one patient developed immunoreactivity towards MGEA5 during the course of disease between the second and third relapse. The higher molecular weight form appears to elicit the predominant immune response in these patients.

Hyaluronidases in Cancer

Contradictory roles for hyaluronidases exist in tumor biology. A secreted hyaluronidase has been described in ovarian (116), prostatic (117), brain, colon

carcinomas, and in malignant melanomas (21). It is entirely absent in normal somatic tissues, suggesting that the enzyme is characteristic of malignant transformation. In the case of melanomas, gliomas and colon carcinomas, this tumor-associated hyaluronidase appears similar or identical to PH20 (118), an enzyme previously assumed to be sperm specific. This hyaluronidase is believed to promote the angiogenesis that accompanies tumor growth. High molecular weight HA has been shown to inhibit vasculogenesis, while hyaluronidase-digested HA fragments are highly angiogenic (119).

On the other hand, enhanced expression of an acid-active hyaluronidase has not been observed to date with any of these malignancies. In contrast to the neutral activity found in these malignancies, levels of a strictly acid-active serum hyaluronidase has been documented to be decreased significantly in the serum of patients with metastatic carcinomas (120), particularly in lung carcinoma (121,122,123). Additionally, glycosaminoglycan degradation is enhanced in low metastatic Lewis lung carcinoma models, compared to their high metastatic counterparts (124). Whether this disparity in hyaluronidase action can be attributed to the difference between neutral-versus acid-active hyaluronidase activities or intracellular versus extracellular degradation of substrate is unclear.

In mice, serum hyaluronidase levels and polymorphisms were shown to reside at a single locus, Hyal-1 (125). The Hyal-1 locus was mapped to mouse chromosome-9, 60 cM from the centromere, a region syntenic to human chromosome 3p21 (126). Transplantable tumors were shown to grow more quickly and animals demonstrated decreased survival in mice carrying the Hyal-1 allele that produces lower levels of serum hyaluronidase (127). Thus in the mouse, the plasma hyaluronidase behaved in a manner consistent with a tumor suppressor. The authors speculated that the Hyal-1 locus might effect tumor growth through the removal of HA pericellular matrices around tumor cells. Such HA-dependent pericellular matrices, or halos were described in various malignancies and their removal was shown to render cells sensitive to cytotoxic lymphocytes (128).

Hypothesis:

Is HYAL1 responsible for the chromosomal aberrations on chromosome 3p21.3 in head and neck squamous cell carcinomas?

Given **i)** the localization of the HYAL1 gene to a region of human chromosome 3p21.3 homozygously deleted in malignancies **ii)** the association of the murine Hyal-1 locus with tumor suppression, **iii)** the potential role of this

enzyme in modifying oncogenic processes such as apoptosis, angiogenesis, immune response or tumor invasion, a functional and molecular genetic examination of the HYAL1 gene in carcinoma lines where 3p21.3 deletions are found would permit the evaluation of whether HYAL1 meets the criterion for a tumor suppressor gene. For the HYAL1 gene to be responsible for the chromosomal aberrations on 3p21.3 it would be expected to be inactivated under Knudson's two hit hypothesis. The loss of heterozygosity of 3p21.3 should be associated with inactivation of the remaining allele by another form of mutation that would distinguish the HYAL1 gene from other candidate tumor suppressor genes on this locus.

References

1. Fukasawa, K., T. Choi, R. Kuriyama, S. Rulong, and G. F. Vande Woude. 1996. Abnormal centrosome amplification in the absence of p53. *Science*. 271:1744-7.
2. Hill, M., and Hillova, J. 1972. Recovery of the temperature sensitive mutant of Rous sarcoma virus from chicken cells exposed to DNA extracted from hamster cells transformed by the mutant. *Virology*. 49:309-313
3. Wong-Staal, F., R. Dalla-Favera, G. Franchini, E. P. Gelmann, and R. C. Gallo. 1981. Three distinct genes in human DNA related to the transforming genes of mammalian sarcoma retroviruses. *Science*. 213:226-8.
4. Der, C. J., T. G. Krontiris, and G. M. Cooper. 1982. Transforming genes of human bladder and lung carcinoma cell lines are homologous to the ras genes of Harvey and Kirsten sarcoma viruses. *Proc Natl Acad Sci U S A*. 79:3637-40.
5. Schwab, M., K. Alitalo, K. H. Klempnauer, H. E. Varmus, J. M. Bishop, F. Gilbert, G. Brodeur, M. Goldstein, and J. Trent. 1983. Amplified DNA with limited homology to myc cellular oncogene is shared by human neuroblastoma cell lines and a neuroblastoma tumour. *Nature*. 305:245-8.
6. Fujita, J., S. K. Srivastava, M. H. Kraus, J. S. Rhim, S. R. Tronick, and S. A. Aaronson. 1985. Frequency of molecular alterations affecting ras protooncogenes in human urinary tract tumors. *Proc Natl Acad Sci U S A*. 82:3849-53.
7. Land, H., L. F. Parada, and R. A. Weinberg. 1983. Cellular oncogenes and multistep carcinogenesis. *Science*. 222:771-8.
8. Newbold, R. F., and R. W. Overell. 1983. Fibroblast immortality is a prerequisite for transformation by EJ c-Ha- ras oncogene. *Nature*. 304:648-51.
9. Stanbridge, E. J. 1976. Suppression of malignancy in human cells. *Nature*. 260:17-20.
10. Knudson, A. G., Jr. 1971. Mutation and cancer: statistical study of retinoblastoma. *Proc Natl Acad Sci U S A*. 68:820-3.
11. Knudson, A. G., Jr., A. T. Meadows, W. W. Nichols, and R. Hill. 1976. Chromosomal deletion and retinoblastoma. *N Engl J Med*. 295:1120-3.

-
12. Dryja, T. P., J. M. Rapaport, J. M. Joyce, and R. A. Petersen. 1986. Molecular detection of deletions involving band q14 of chromosome 13 in retinoblastomas. *Proc Natl Acad Sci U S A*. 83:7391-4.
 13. Lee, W. H., R. Bookstein, F. Hong, L. J. Young, J. Y. Shew, and E. Y. Lee. 1987. Human retinoblastoma susceptibility gene: cloning, identification, and sequence. *Science*. 235:1394-9.
 14. Murphree, A. L., and W. F. Benedict. 1984. Retinoblastoma: clues to human oncogenesis. *Science*. 223:1028-33.
 15. Huang, H. J., J. K. Yee, J. Y. Shew, P. L. Chen, R. Bookstein, T. Friedmann, E. Y. Lee, and W. H. Lee. 1988. Suppression of the neoplastic phenotype by replacement of the RB gene in human cancer cells. *Science*. 242:1563-6.
 16. Bronner, C. E., S. M. Baker, P. T. Morrison, G. Warren, L. G. Smith, M. K. Lescoe, M. Kane, C. Earabino, J. Lipford, A. Lindblom, and et al. 1994. Mutation in the DNA mismatch repair gene homologue hMLH1 is associated with hereditary non-polyposis colon cancer. *Nature*. 368:258-61.
 17. Kok, K., S. L. Naylor, and C. H. Buys. 1997. Deletions of the short arm of chromosome 3 in solid tumors and the search for suppressor genes. *Adv Cancer Res*. 71:27-92.
 18. Petrylak, D. P. 1995. Metastases suppressors and prostate cancer. *Nat Med*. 1:739-40.
 19. Dong, J. T., P. W. Lamb, C. W. Rinker-Schaeffer, J. Vukanovic, T. Ichikawa, J. T. Isaacs, and J. C. Barrett. 1995. KAI1, a metastasis suppressor gene for prostate cancer on human chromosome 11p11.2 [see comments]. *Science*. 268:884-6.
 20. Cho, K. R., and E. R. Fearon. 1995. DCC: linking tumor suppressor genes and altered cell surface interactions in cancer? *Curr Opin Genet Dev*. 5:72-8.
 21. Fearon, E. R., and B. Vogelstein. 1990. A genetic model for colorectal tumorigenesis. *Cell*. 61:759-67.
 22. Weinberg, R. A. 1989. Oncogenes, antioncogenes, and the molecular bases of multistep carcinogenesis. *Cancer Res*. 49:3713-21.

-
23. Orye, E., M. J. Delbeke, and B. Vandenabeele. 1974. Retinoblastoma and long arm deletion of chromosome 13. Attempts to define the deleted segment. *Clin Genet.* 5:457-64.
24. Friend, S. H., R. Bernards, S. Rogelj, R. A. Weinberg, J. M. Rapaport, D. M. Albert, and T. P. Dryja. 1986. A human DNA segment with properties of the gene that predisposes to retinoblastoma and osteosarcoma. *Nature.* 323:643-6.
25. Pinkel, D., T. Straume, and J. W. Gray. 1986. Cytogenetic analysis using quantitative, high-sensitivity, fluorescence hybridization. *Proc Natl Acad Sci U S A.* 83:2934-8.
26. Kallioniemi, A., O. P. Kallioniemi, D. Sudar, D. Rutovitz, J. W. Gray, F. Waldman, and D. Pinkel. 1992. Comparative genomic hybridization for molecular cytogenetic analysis of solid tumors. *Science.* 258:818-21.
27. Ton, C. C., V. Huff, K. M. Call, S. Cohn, L. C. Strong, D. E. Housman, and G. F. Saunders. 1991. Smallest region of overlap in Wilms tumor deletions uniquely implicates an 11p13 zinc finger gene as the disease locus. *Genomics.* 10:293-7.
28. Kamb, A., N. A. Gruis, J. Weaver-Feldhaus, Q. Liu, K. Harshman, S. V. Tavtigian, E. Stockert, R. S. r. Day, B. E. Johnson, and M. H. Skolnick. 1994. A cell cycle regulator potentially involved in genesis of many tumor types [see comments]. *Science.* 264:436-40.
29. Serrano, M., G. J. Hannon, and D. Beach. 1993. A new regulatory motif in cell-cycle control causing specific inhibition of cyclin D/CDK4 [see comments]. *Nature.* 366:704-7.
30. Jenkins, J. R., K. Rudge, P. Chumakov, and G. A. Currie. 1985. The cellular oncogene p53 can be activated by mutagenesis. *Nature.* 317:816-8.
31. Chen, P. L., Y. M. Chen, R. Bookstein, and W. H. Lee. 1990. Genetic mechanisms of tumor suppression by the human p53 gene. *Science.* 250:1576-80.
32. Sager, R. 1997. Expression genetics in cancer: shifting the focus from DNA to RNA. *Proc Natl Acad Sci U S A.* 94:952-5.
33. Whang-Peng, J., P. A. Bunn, Jr., C. S. Kao-Shan, E. C. Lee, D. N. Carney, A. Gazdar, and J. D. Minna. 1982. A nonrandom chromosomal abnormality, del 3p(14-23), in human small cell lung cancer (SCLC). *Cancer Genet Cytogenet.* 6:119-34.

-
34. Hibi, K., T. Takahashi, K. Yamakawa, R. Ueda, Y. Sekido, Y. Ariyoshi, M. Suyama, H. Takagi, Y. Nakamura, and T. Takahashi. 1992. Three distinct regions involved in 3p deletion in human lung cancer. *Oncogene*. 7:445-9.
35. Smith, D. I., H. Huang, and L. Wang. 1998. Common fragile sites and cancer (Review). *Int J Oncol*. 12:187-96.
36. Hibi, K., Takahashi, T., Yamakawa, K., Ueda, R., Sekido, Y., Ariyoshi, Y., Suyama, M., Takagi, H., Nakamura, Y. & Takahashi, T. (1992). *Oncogene*, 7, 445-9.
37. Kok, K., S. L. Naylor, and C. H. Buys. 1997. Deletions of the short arm of chromosome 3 in solid tumors and the search for suppressor genes. *Adv Cancer Res*. 71:27-92.
38. Yamakawa, K., T. Takahashi, Y. Horio, Y. Murata, E. Takahashi, K. Hibi, S. Yokoyama, R. Ueda, T. Takahashi, and Y. Nakamura. 1993. Frequent homozygous deletions in lung cancer cell lines detected by a DNA marker located at 3p21.3-p22. *Oncogene*. 8:327-30.
39. Todd, S., W. A. Franklin, M. Varella-Garcia, T. Kennedy, C. E. Hilliker, Jr., L. Hahner, M. Anderson, J. S. Wiest, H. A. Drabkin, and R. M. Gemmill. 1997. Homozygous deletions of human chromosome 3p in lung tumors. *Cancer Res*. 57:1344-52.
40. Wei, M. H., F. Latif, S. Bader, V. Kashuba, J. Y. Chen, F. M. Duh, Y. Sekido, C. C. Lee, L. Geil, I. Kuzmin, E. Zbarovsky, G. Klein, B. Zbar, J. D. Minna, and M. I. Lerman. 1996. Construction of a 600-kilobase cosmid clone contig and generation of a transcriptional map surrounding the lung cancer tumor suppressor gene (TSG) locus on human chromosome 3p21.3: progress toward the isolation of a lung cancer TSG. *Cancer Res*. 56:1487-92.
41. Sekido, Y., M. Ahmadian, Wistuba, II, F. Latif, S. Bader, M. H. Wei, F. M. Duh, A. F. Gazdar, M. I. Lerman, and J. D. Minna. 1998. Cloning of a breast cancer homozygous deletion junction narrows the region of search for a 3p21.3 tumor suppressor gene. *Oncogene*. 16:3151-7.
42. Killary, A. M., M. E. Wolf, T. A. Giambenedi, and S. L. Naylor. 1992. Definition of a tumor suppressor locus within human chromosome 3p21-p22. *Proc Natl Acad Sci U S A*. 89:10877-81.

-
43. Todd, M. C., R. H. Xiang, D. K. Garcia, K. E. Kerbacher, S. L. Moore, C. H. Hensel, P. Liu, M. J. Siciliano, K. Kok, A. van den Berg, P. Veldhuis, C. H. Buys, A. M. Killary, and S. L. Naylor. 1996. An 80 Kb P1 clone from chromosome 3p21.3 suppresses tumor growth in vivo. *Oncogene*. 13:2387-96.
44. Kholodnyuk, I., M. Kost-Alimova, V. Kashuba, R. Gizatulin, A. Szeles, E. J. Stanbridge, E. R. Zabarovsky, G. Klein, and S. Imreh. 1997. A 3p21.3 region is preferentially eliminated from human chromosome 3/mouse microcell hybrids during tumor growth in SCID mice. *Genes Chromosomes Cancer*. 18:200-11.
45. Imreh, S., I. Kholodnyuk, R. Allikmetts, E. J. Stanbridge, E. R. Zabarovsky, and G. Klein. 1994. Nonrandom loss of human chromosome 3 fragments from mouse-human microcell hybrids following progressive growth in SCID mice. *Genes Chromosomes Cancer*. 11:237-45.
46. Cheng, Y., N. E. Poulos, M. L. Lung, G. Hampton, B. Ou, M. I. Lerman, and E. J. Stanbridge. 1998. Functional evidence for a nasopharyngeal carcinoma tumor suppressor gene that maps at chromosome 3p21.3. *Proc Natl Acad Sci U S A*. 95:3042-7.
47. Maestro, R., D. Gasparotto, T. Vukosavljevic, L. Barzan, S. Sulfaro, and M. Boiocchi. 1993. Three discrete regions of deletion at 3p in head and neck cancers. *Cancer Res*. 53:5775-9.
48. Frisch, S. M. and Francis, H. Disruption of epithelial cell-matrix interactions induces apoptosis, *J Cell Biol*. 124: 619-26, 1994.
49. Boudreau, N., Werb, Z., and Bissell, M. J. Suppression of apoptosis by basement membrane requires three-dimensional tissue organization and withdrawal from the cell cycle, *Proc Natl Acad Sci U S A*. 93: 3509-13, 1996.
50. Boudreau, N., Sympton, C. J., Werb, Z., and Bissell, M. J. Suppression of ICE and apoptosis in mammary epithelial cells by extracellular matrix, *Science*. 267: 891-3, 1995.
51. Howlett, A. R., Bailey, N., Damsky, C., Petersen, O. W., and Bissell, M. J. Cellular growth and survival are mediated by beta 1 integrins in normal human breast epithelium but not in breast carcinoma, *J Cell Sci*. 108: 1945-57, 1995.
52. Knudson, W. Tumor-associated hyaluronan. Providing an extracellular matrix that facilitates invasion [comment], *Am J Pathol*. 148: 1721-6, 1996.
53. Zhang, L., Underhill, C. B., and Chen, L. Hyaluronan on the surface of tumor cells is correlated with metastatic behavior, *Cancer Res*. 55: 428-33, 1995.

-
54. Laurent, T. C., Laurent, U. B., and Fraser, J. R. Functions of hyaluronan, *Ann Rheum Dis.* 54: 429-32, 1995.
55. Toole, B., Munaim, S., Welles, S., and Knudson, C. B. Hyaluronate-cell Interactions and growth factor regulation of hyaluronate synthesis during limb development. *In: Ciba Found. Symp.* pp. 138-149, 1989
56. Ruggiero, S. L., Bertolami, C. N., Bronson, R. E., and Damiani, P. J. Hyaluronidase activity of rabbit skin wound granulation tissue fibroblasts, *J Dent Res.* 66: 1283-7, 1987.
57. Shyjan, A. M., Heldin, P., Butcher, E. C., Yoshino, T., and Briskin, M. J. Functional cloning of the cDNA for a human hyaluronan synthase, *J Biol Chem.* 271: 23395-9, 1996.
58. Itano, N. and Kimata, K. Molecular cloning of human hyaluronan synthase, *Biochem Biophys Res Commun.* 222: 816-20, 1996.
59. Spicer, A. P., Olson, J. S., and McDonald, J. A. Molecular Cloning and Characterization of a cDNA Encoding the Third Putative Mammalian Hyaluronan Synthase, *J Biol Chem.* 272: 8957-61, 1997.
60. Klewes, L., Turley, E. A., and Prehm, P. The hyaluronate synthase from a eukaryotic cell line, *Biochem J.* 290: 791-5, 1993.
61. Ayroldi, E., Cannarile, L., Migliorati, G., Bartoli, A., Nicoletti, I., and Riccardi, C. CD44 (Pgp-1) inhibits CD3 and dexamethasone-induced apoptosis, *Blood.* 86: 2672-8, 1995.
62. Henke, C., Bitterman, P., Roongta, U., Ingbar, D., and Polunovsky, V. Induction of fibroblast apoptosis by anti-CD44 antibody: implications for the treatment of fibroproliferative lung disease, *Am J Pathol.* 149: 1639-50, 1996.
63. Yu, Q., B. P. Toole, and I. Stamenkovic. 1997. Induction of apoptosis of metastatic mammary carcinoma cells in vivo by disruption of tumor cell surface CD44 function. *J Exp Med.* 186:1985-96.
64. Zahalka, M. A., Okon, E., Gossler, U., Holzmann, B., and Naor, D. Lymph node (but not spleen) invasion by murine lymphoma is both CD44- and hyaluronate dependent, *J Immunol.* 154: 5345-55, 1995.
65. Kaya, G., I. Rodriguez, J. L. Jorcano, P. Vassalli, and I. Stamenkovic. 1997. Selective suppression of CD44 in keratinocytes of mice bearing an antisense CD44

transgene driven by a tissue-specific promoter disrupts hyaluronate metabolism in the skin and impairs keratinocyte proliferation. *Genes Dev.* 11:996-1007.

66. Schmits, R., J. Filmus, N. Gerwin, G. Senaldi, F. Kiefer, T. Kundig, A. Wakeham, A. Shahinian, C. Catzavelos, J. Rak, C. Furlonger, A. Zakarian, J. J. Simard, P. S. Ohashi, C. J. Paige, J. C. Gutierrez-Ramos, and T. W. Mak. 1997. CD44 regulates hematopoietic progenitor distribution, granuloma formation, and tumorigenicity. *Blood.* 90:2217-33.

67. Gao, A. C., W. Lou, J. T. Dong, and J. T. Isaacs. 1997. CD44 is a metastasis suppressor gene for prostatic cancer located on human chromosome 11p13. *Cancer Res.* 57:846-9.

68. Takahashi, K., I. Stamenkovic, M. Cutler, H. Saya, and K. K. Tanabe. 1995. CD44 hyaluronate binding influences growth kinetics and tumorigenicity of human colon carcinomas. *Oncogene.* 11:2223-32.

69. Noble, P. W., McKee, C. M., Cowman, M., and Shin, H. S. Hyaluronan fragments activate an NF-kappa B/I-kappa B alpha autoregulatory loop in murine macrophages, *J Exp Med.* 183: 2373-8, 1996.

70. Mckee CM; Penno MB; Cowman M; Burdick MD; Streiter, RM; Noble, P.W. Hyaluronan (HA) Fragments Induce Chemokine Gene Expression In Alveolar Macrophages - The Role Of HA Size And CD44, *J. Clin. Invest.* 98:2403-2413, 1996

71. West, D. C., I. N. Hampson, F. Arnold, and S. Kumar. 1985. Angiogenesis induced by degradation products of hyaluronic acid. *Science.* 228:1324-6.

72. Rooney, P., S. Kumar, J. Ponting, and M. Wang. 1995. The role of hyaluronan in tumour neovascularization (review). *Int J Cancer.* 60:632-6.

73. West, D. C., and S. Kumar. 1991. Tumour-associated hyaluronan: a potential regulator of tumour angiogenesis. *Int J Radiat Biol.* 60:55-60.

74. Slevin, M., J. Krupinski, S. Kumar, and J. Gaffney. 1998. Angiogenic oligosaccharides of hyaluronan induce protein tyrosine kinase activity in endothelial cells and activate a cytoplasmic signal transduction pathway resulting in proliferation. *Lab Invest.* 78:987-1003.

75. Vaheri, A., O. Carpen, L. Heiska, T. S. Helander, J. Jaaskelainen, P. Majander-Nordenswan, M. Sainio, T. Timonen, and O. Turunen. 1997. The ezrin protein family: membrane-cytoskeleton interactions and disease associations. *Curr Opin Cell Biol.* 9:659-66.

-
76. Sainio, M., F. Zhao, L. Heiska, O. Turunen, M. den Bakker, E. Zwarthoff, M. Lutchman, G. A. Rouleau, J. Jaaskelainen, A. Vaheri, and O. Carpen. 1997. Neurofibromatosis 2 tumor suppressor protein colocalizes with ezrin and CD44 and associates with actin-containing cytoskeleton. *J Cell Sci.* 110:2249-60.
77. Lokeshwar, V. B. and Bourguignon, L. Y. Post-translational protein modification and expression of ankyrin-binding site(s) in GP85 (Pgp-1/CD44) and its biosynthetic precursors during T-lymphoma membrane biosynthesis, *J Biol Chem.* 266: 17983-9, 1991.
78. Ohta, S., Yoshida, J., Iwata, H., and Hamaguchi, M. Hyaluronate activates tyrosine phosphorylation of cellular proteins including focal adhesion kinase via CD44 in human glioma cells, *International Journal Of Oncology.* 10: 561-564, 1997.
79. Tanabe, K. K. and Saya, H. The CD44 adhesion molecule and metastasis, *Crit Rev Oncog.* 5: 201-12, 1994.
80. Jackson, D. G., Bell, J. I., Dickinson, R., Timans, J., Shields, J., and Whittle, N. Proteoglycan forms of the lymphocyte homing receptor CD44 are alternatively spliced variants containing the v3 exon, *J Cell Biol.* 128: 673-85, 1995.
81. Turley, E. A., L. Austen, K. Vandelight, and C. Clary. 1991. Hyaluronan and a cell-associated hyaluronan binding protein regulate the locomotion of ras-transformed cells. *J Cell Biol.* 112:1041-7.
82. Hardwick, C., K. Hoare, R. Owens, H. P. Hohn, M. Hook, D. Moore, V. Cripps, L. Austen, D. M. Nance, and E. A. Turley. 1992. Molecular cloning of a novel hyaluronan receptor that mediates tumor cell motility. *J Cell Biol.* 117:1343-50.
83. Hall, C. L., Yang, B., Yang, X., Zhang, S., Turley, M., Samuel, S., Lange, L. A., Wang, C., Curpen, G. D., Savani, R. C., and et al. Overexpression of the hyaluronan receptor RHAMM is transforming and is also required for H-ras transformation, *Cell.* 82: 19- 26, 1995.
84. Hall, C. L., Wang, C., Lange, L. A., and Turley, E. A. Hyaluronan and the hyaluronan receptor RHAMM promote focal adhesion turnover and transient tyrosine kinase activity, *J Cell Biol.* 126: 575-88, 1994.
85. Mohapatra, S., Yang, X., Wright, J. A., Turley, E. A., and Greenberg, A. H. Soluble hyaluronan receptor RHAMM induces mitotic arrest by suppressing Cdc2 and cyclin B1 expression, *J Exp Med.* 183: 1663-8, 1996.

-
- 86 Hofmann, M., C. Fieber, V. Assmann, M. Gottlicher, J. Sleeman, R. Plug, N. Howells, O. von Stein, H. Ponta, and P. Herrlich. 1998. Identification of IHABP, a 95 kDa intracellular hyaluronate binding protein *J Cell Sci.* 111:1673-84.
- 87 Assmann, V., J. F. Marshall, C. Fieber, M. Hofmann, and I. R. Hart. 1998. The human hyaluronan receptor RHAMM is expressed as an intracellular protein in breast cancer cells *J Cell Sci.* 111:1685-94.
- 88 Hofmann, M., V. Assmann, C. Fieber, J. P. Sleeman, J. Moll, H. Ponta, I. R. Hart, and P. Herrlich. 1998. Problems with RHAMM: a new link between surface adhesion and oncogenesis?. *Cell.* 95:591-2; discussion 592-3.
89. Kreil, G. Hyaluronidases--a group of neglected enzymes. *Protein Sci.*, 4: 1666-9, 1995.
90. Frost, G. I., Csoka, T., and Stern, R. Hyaluronidases: A Chemical, Biological and Clinical Overview, *Trends in Glycoscience and Glycotechnology.* 8: 407-421, 1996.
91. Primakoff, P., Hyatt, H., and Myles, D. G. A role for the migrating sperm surface antigen PH-20 in guinea pig sperm binding to the egg zona pellucida, *J Cell Biol.* 101: 2239-44, 1985.
92. Lin, Y., Mahan, K., Lathrop, W. F., Myles, D. G., and Primakoff, P. A hyaluronidase activity of the sperm plasma membrane protein PH-20 enables sperm to penetrate the cumulus cell layer surrounding the egg, *J Cell Biol.* 125: 1157-63, 1994.
93. Fiszer-Szafarz, B., Vannier, P., Litynska, A., Zou, L., Czartoryska, B., and Tytki-Szymanska, A. Hyaluronidase in human somatic tissues and urine: polymorphism and the activity in diseases, *Acta Biochim Pol.* 42: 31-3, 1995.
94. Komender, J., Malczewska, H., and Golaszewska, A. Isolation of hyaluronidase from kidney extract, *Bull Acad Pol Sci [Biol].* 21: 637-41, 1973.
95. Thet, L. A., Howell, A. C., and Han, G. Changes in lung hyaluronidase activity associated with lung growth, injury and repair, *Biochem Biophys Res Commun.* 117: 71-7, 1983.
96. Margolis, R. U., Margolis, R. K., Santella, R., and Atherton, D. M. The hyaluronidase of brain, *J Neurochem.* 19: 2325-32, 1972.
97. Cashman, D. C., Laryea, J. U., and Weissmann, B. The hyaluronidase of rat skin, *Arch Biochem Biophys.* 135: 387-95, 1969.
98. Yamada, M., Hasegawa, E., and Kanamori, M. Purification of hyaluronidase from

human placenta, *J Biochem (Tokyo)*. 81: 485-94, 1977.

99. Goggins, J. F., Lazarus, G. S., and Fullmer, H. M. Hyaluronidase activity of alveolar macrophages, *J Histochem Cytochem*. 16: 688-92, 1968.

100. Longaker, M. T., Chiu, E. S., Adzick, N. S., Stern, M., Harrison, M. R., and Stern, R. Studies in fetal wound healing. V. A prolonged presence of hyaluronic acid characterizes fetal wound fluid, *Ann Surg*. 213: 292-6, 1991.

101. Dicker, S. E. and Franklin, C. S. The isolation of hyaluronic acid and chondroitin sulphate from kidneys and their reaction with urinary hyaluronidase, *J Physiol (Lond)*. 186: 110-20, 1966.

102. De Salegui, M. and Pigman, W. The existence of an acid-active hyaluronidase in serum, *Arch Biochem Biophys*. 120: 60-7, 1967.

103. Roden, L. (1980) In *The Biochemistry of Glycoproteins and Proteoglycans* (W.J. Lennarz, Ed.), pp. 267-371, Plenum Press, New York.

104. Duran-Reynolds, R.F., (1929) *J. Exp. Med.*, 50 327

105. Thaler, C. D. and Cardullo, R. A. Biochemical characterization of a glycosylphosphatidylinositol-linked hyaluronidase on mouse sperm, *Biochemistry* 34: 7788-95, 1995.

106. Jones, M. H., P. M. Davey, H. Aplin, and N. A. Affara. 1995. Expression analysis, genomic structure, and mapping to 7q31 of the human sperm adhesion molecule gene SPAM1. *Genomics*. 29:796-800.

107. Gmachl, M. and Kreil, G. Bee venom hyaluronidase is homologous to a membrane protein of mammalian sperm, *Proc Natl Acad Sci U S A*. 90: 3569-73, 1993.

108. Lu, G., Kochoumian, L., and King, T. P. Sequence identity and antigenic cross-reactivity of white face hornet venom allergen, also a hyaluronidase, with other proteins, *J Biol Chem*. 270: 4457-65, 1995.

109. Arming, S., B. Strobl, C. Wechselberger, and G. Kreil. 1997. In vitro mutagenesis of PH-20 hyaluronidase from human sperm. *Eur J Biochem*. 247:810-4.

110. Lin, Y., Mahan, K., Lathrop, W. F., Myles, D. G., and Primakoff, P. A hyaluronidase activity of the sperm plasma membrane protein PH-20 enables sperm to penetrate the cumulus cell layer surrounding the egg, *J Cell Biol*. 125: 1157-63, 1994.

111. Hunnicutt, G. R., Primakoff, P., and Myles, D. G. Sperm surface protein PH-20 is

bifunctional: one activity is a hyaluronidase and a second, distinct activity is required in secondary sperm-zona binding, *Biol Reprod.* 55: 80-6, 1996.

112. Lepperdinger, G., B. Strobl, and G. Kreil. 1998. HYAL2, a human gene expressed in many cells, encodes a lysosomal hyaluronidase with a novel type of specificity. *J Biol Chem.* 273:22466-70.

113. Strobl, B., C. Wechselberger, D. R. Beier, and G. Lepperdinger. 1998. Structural organization and chromosomal localization of hyal2, a gene encoding a lysosomal hyaluronidase *Genomics.* 53:214-9.

114. Canard, B., T. Garnier, B. Saint-Joanis, and S. T. Cole. 1994. Molecular genetic analysis of the nagH gene encoding a hyaluronidase of *Clostridium perfringens*. *Mol Gen Genet.* 243:215-24.

115. Heckel, D., N. Comtesse, N. Brass, N. Blin, K. D. Zang, and E. Meese. 1998. Novel immunogenic antigen homologous to hyaluronidase in meningioma. *Hum Mol Genet.* 7:1859-72.

116. Miura, R. O., Yamagata, S., Miura, Y., Harada, T., and Yamagata, T. Analysis of glycosaminoglycan-degrading enzymes by substrate gel electrophoresis (zymography), *Anal Biochem.* 225: 333-40, 1995.

117. Lokeshwar, V. B., Lokeshwar, B. L., Pham, H. T., and Block, N. L. Association of elevated levels of hyaluronidase, a matrix-degrading enzyme, with prostate cancer progression, *Cancer Res.* 56: 651-7, 1996.

118. Liu, D., Pearlman, E., Diaconu, E., Guo, K., Mori, H., Haqqi, T., Markowitz, S., Willson, J., and Sy, M. S. Expression of hyaluronidase by tumor cells induces angiogenesis in vivo, *Proc Natl Acad Sci U S A.* 93: 7832-7, 1996.

119. Rooney, P., Kumar, S., Ponting, J., and Wang, M. The role of hyaluronan in tumour neovascularization (review), *Int J Cancer.* 60: 632-6, 1995.

120. Wilkinson, C. R., Bower, L. M., and Warren, C. The relationship between hyaluronidase activity and hyaluronic acid concentration in sera from normal controls and from patients with disseminated neoplasm, *Clin Chim Acta.* 256: 165-73, 1996.

121. Northrup, S. N., Stasiw, R. O., and Brown, H. D. Development of the hyaluronidase activity assay as a cancer screening test, *Clin Biochem.* 6: 220-8, 1973..

122. Kolarova, M., Tobiska, J., and Brada, Z. Host-tumour relationship. XXIX. Hyaluronidase activity and seromuroid concentration in blood serum of patients with cancer, *Neoplasma.* 17: 641-8, 1970.

-
123. Herp, A., DeFilippi, J., and Fabianek, J. The effect of serum hyaluronidase on acidic polysaccharides and its activity in cancer, *Biochim Biophys Acta.* *158*: 150-3, 1968.
124. Pogany, G., Moczar, E., Jeney, A., Timar, J., Timar, F., Ditroi, K., and Lapis, K. Comparative study on Lewis lung tumour lines with 'low' and 'high' metastatic capacity. III. Glycosaminoglycan synthesis, transport and degradation in cell lines, *Clin Exp Metastasis.* *7*: 659-69, 1989.
125. Fiszer-Szafarz, B. and De Maeyer, E. Hyal-1, a locus determining serum hyaluronidase polymorphism, on chromosome 9 in mice, *Somat Cell Mol Genet.* *15*: 79-83, 1989.
126. Dietrich, W. F., Radany, E. H., Smith, J. S., Bishop, J. M., Hanahan, D., and Lander, E. S. Genome-wide search for loss of heterozygosity in transgenic mouse tumors reveals candidate tumor suppressor genes on chromosomes 9 and 16, *Proc Natl Acad Sci U S A.* *91*: 9451-5, 1994.
127. De Maeyer, E. and De Maeyer-Guignard, J. The growth rate of two transplantable murine tumors, 3LL lung carcinoma and B16F10 melanoma, is influenced by Hyal-1, a locus determining hyaluronidase levels and polymorphism, *Int J Cancer.* *51*: 657-60, 1992.
128. McBride, W. H., and J. B. Bard. 1979. Hyaluronidase-sensitive halos around adherent cells. Their role in blocking lymphocyte-mediated cytolysis. *J Exp Med.* *149*:507-15.

Chapter-2

A Microtiter-Based Assay For Hyaluronidase Activity Not Requiring Specialized Reagents

Preface

My contributions to this work included: the concept of covalently modifying hyaluronan with biotin-hydrazide and utilizing this substrate in a microtiter based assay; optimizing the molar ratios of biotin to hyaluronan; comparing the pH profiles and kinetics of different hyaluronidase preparations in this assay; screening plasma samples from normal donors for hyaluronidase activity; the analysis of hyaluronidase activity in normal keratinocytes and the hypothesis that HYAL1 expression was dependent upon the calcium induced differentiation of such cells.

Jackson Hall (department of pathology, UCSF) assisted in screening plasma samples from normal donors and prepared batches of biotinylated hyaluronan for use in routine assays.

Abstract

A sensitive, rapid microtiter-based assay for hyaluronidase activity is described that does not require highly specialized biological reagents, as required heretofore. The free carboxyl groups of hyaluronan are biotinylated in a one-step reaction using biotin-hydrazide. This substrate is then covalently coupled to a 96-well microtiter plate. At the completion of the enzyme reaction, residual substrate is detected with an avidin-peroxidase reaction that can be read in a standard ELISA plate reader. As the substrate is covalently bound to the microtiter plate, artifacts such as pH-dependent displacement of the biotinylated substrate does not occur. The sensitivity permits rapid measurement of hyaluronidase activity from cultured cells and biological samples with an inter-assay variation of less than 5%. Using this new assay, we measured the distribution profile of plasma hyaluronidase levels in normal human sera. A one microliter sample of plasma was sufficient for assays in triplicate. Hyaluronidase activity in human foreskin primary keratinocyte cultures was also quantitated. A twenty-five fold increase in hyaluronidase activity was observed in keratinocyte cultures induced to differentiate in high calcium (1.5mM), compared to levels in low calcium (0.05mM) media. The microtiter-based assay may be used as a routine clinical laboratory procedure.

Introduction

Hyaluronidases are a family of β 1-4 endoglucosaminidases that degrade hyaluronan (HA), and from vertebrate sources, can degrade, to a lesser extent, other glycosaminoglycans (for reviews, see 1,2). These enzymes have been relatively neglected in comparison to other glycosidases, most likely due to the lack of simple yet sensitive assays that measure degradation of substrate. Until recently, the most commonly used hyaluronidase assays were based upon the measurement of the generation of new reducing N-acetylamino groups (3), or loss of viscosity (4) or turbidity (5). These assays are either insensitive or lack specificity. More recently, a new generation of assays have been developed. A microtiter-based assay from this laboratory (6), requires the preparation of a highly specialized reagent, an HA-binding peptide derived from the proteoglycan, aggrecan. It is obtained from tryptic digests of bovine nasal cartilage and isolated by HA-affinity chromatography. This peptide must then be biotinylated (6). Residual substrate in the microtiter plate is then determined as a measure of enzymatic activity. The preparation of such a reagent is not feasible or practical in most laboratories. In addition, the HA substrate binds poorly to standard plastic microtiter plates. This non-covalent immobilization of HA on the microtiter plates is pH sensitive, making comparisons of enzymatic activity at different pH's difficult to interpret.

Hyaluronidases from vertebrate tissues can be separated into two classes; those with maximal activity near neutral pH, such as the enzyme from

the plasma membrane of sperm, PH20 (7,8), and the so-called lysosomal enzymes with maximal activity below pH 4.0 (9,10). These two classes of enzymes are clearly distinct, and appear to have very different biological functions. We have used the present assay to track enzyme activity in the purification and expression of the hyaluronidase from human plasma (11). The assay is as sensitive as the one previously described from this laboratory (5), can be performed using a much shorter incubation period of 15-60 min, and most importantly, does not require preliminary preparation of a complex bioreagent. This assay will facilitate isolation of novel hyaluronidases from other tissues.

The HA substrate for hyaluronidases is becoming increasingly prominent in biology (12,13). Its key role has been recognized in a number of basic biological processes, such as embryogenesis (12,13), carcinogenesis (14,15), wound healing (16), angiogenesis (17) and inflammation (18,19). Clinically, aberrations of HA metabolism are associated with processes such as adult respiratory distress syndrome (20), organ transplant edema and rejection (21,22), and as a marker for cancer remission and relapse (23). An inherited disorder involving serum hyaluronidase deficiency has been described recently (24). The hyaluronidase assay described herein may be used as a routine clinical laboratory procedure.

Materials And Methods

Materials

Human umbilical cord HA from was purchased from ICN (Irvine, CA). COVALINK-NH microtiter plates were obtained from NUNC (Placerville, NJ), and Sulfo-NHS and biotin hydrazide from Pierce (Rockford, IL). Bovine testicular hyaluronidase, Wydase^R, was a gift of the Wyeth-Ayerst Co. (Philadelphia, PA). Human plasma samples were obtained from the UCSF blood donor facility. DMSO and Guanidine hydrochloride were products of Fisher Scientific (Pittsburgh, PA). O-phenylene-diamine was purchased from Calbiochem (La Jolla, CA). All other reagents were from Sigma Chem. Co. (St. Louis, MO).

Preparation of biotinylated HA

One hundred mg of human umbilical cord HA was dissolved in 0.1M MES, pH 5.0 to a final concentration of 1mg/ml and allowed to dissolve for at least 24 hours at 4°C prior to the coupling of biotin. Sulfo- NHS was added to the hyaluronate MES solution to a final concentration of 0.184mg/ml. Biotin hydrazide was dissolved in DMSO as a stock solution of 100mM and added to the HA solution to a final concentration of 1 mM. A stock solution of 1-ethyl -3-(3-dimethylaminopropyl) carbodiimide (EDAC) was prepared as a 100 mM stock solution in dH2O and added to the HA biotin solution at a final concentration of 30mM. This solution was left stirring overnight at 4°C.

Unlinked biotin and EDAC were removed by dialysis against dH₂O with 3 changes of 1000x volumes of dH₂O. The dialyzed, biotinylated HA (bHA) was aliquoted and stored at -20°C for up to several months.

Immobilization of bHA onto ELISA plates.

Sulfo-NHS was diluted to 0.184 mg/ml in dH₂O with the bHA at a concentration of 0.2mg/ml and pipetted into 96 well Covalink-NH plates at 50µl per well. EDAC was diluted to 0.123 mg/ml in dH₂O and pipetted into the Covalink plates with the HA solution resulting in a final concentration of 10µg/well hyaluronate and 6.15 µg/well EDAC. The plates were incubated overnight at 4°C or for 2 hours at 23°C, which gave comparable results. After covalent immobilization of bHA on the microtiter plates, the coupling solution was removed by shaking and the plates were washed 3 times in PBS containing 2M NaCl and 50mM MgSO₄ (Buffer A). The plates could be stored at 4°C for up to one week.

Assay for hyaluronidase activity

The Covalink plates with immobilized bHA were equilibrated with 100µl/well assay buffer (0.1M formate, pH 3.7, 0.1M NaCl, 1% Triton X-100, 5mM saccharolactone for lysosomal hyaluronidase; 0.1M formate pH 4.5, 0.15M NaCl, 1% Triton X-100, 5mM saccharolactone for neutral-active enzymes). A set of standards for the calibration of enzyme activity against relative Turbidity Reducing Units (rTRU's) was generated by diluting Wydase^R in neutral enzyme

buffer from 1.0 to 1×10^{-6} TRU/well and assaying 100 μ l/well in triplicate. Samples of acid-active hyaluronidase were diluted in lysosomal assay buffer from 1:10 to 1:130,000 in immunoaffinity-purified preparations of recombinant human plasma hyaluronidase (11) and were pipetted in triplicate at 100 μ l/well. For most assays of tissue extracts and human plasma, a 30 min incubation at 37°C was sufficient. Positive and negative control wells (no enzyme or no ABC, respectively) were also included in triplicate.

The reaction was terminated by the addition of 200 μ l/well of 6M Guanidine HCl followed by three washes of 300 μ l/well with PBS, 2M NaCl, 50mM MgSO₄, 0.05% Tween 20 (Buffer B). An avidin biotin complex (ABC) kit (Vector Labs, Burlingame Ca) was prepared in 10ml of PBS containing 0.1% Tween 20, which was preincubated for 30 min at room temperature during the hyaluronidase incubation.

The ABC solution was then added 100 μ l/well, for 30 min at room temperature. For the negative control wells, ABC was not included. The plate was then washed five times with Buffer B and an o-phenylenediamine (OPD) substrate was added at 100 μ l/well by dissolving one 10 mg tablet of OPD in 10ml of 0.1M citrate-PO₄ buffer, pH 5.3 and adding 7.5 μ l of 30% H₂O₂. The plate was incubated in the dark for 10-15 min and was then read using a 492nm filter in an ELISA plate reader (Titertek Multiskan PLUS, ICN) monitored by computer using the Delta Soft II plate reader software from Biometallics (Princeton, NJ). A standard curve using the bovine testicular hyaluronidase was generated by a four parameter curve fit of the commercial hyaluronidase

preparation and unknowns were interpolated through their absorbance at 492nm.

Measurement of Kinetics of different hyaluronidases

Three different hyaluronidases were used for the analysis of time dependence of HA degradation. Using 0.01 rTRU of immunoaffinity purified recombinant human plasma hyaluronidase (600,000 rTRU/mg), bovine testicular hyaluronidase (Sigma Type VI-s 3,000 TRU/mg) , or *Streptomyces* hyaluronidase (Calbiochem) samples were placed into a microtiter bHA plate at 0, 5, 10, 15 and 30 min in a 37°C water bath. Samples were then processed as usual and bHA degradation measured at 492nm.

Analaysis of pH dependence of hyaluronidase activitiy

To analyze pH dependence of hyaluronidases, immunoaffinity purified recombinant human plasma hyaluronidase and bovine testicular hyaluronidase were used. The pH dependence of enzyme activity was measured by diluting purified plasma hyaluronidase or partially purified bovine testicular hyaluronidase to 0.1 rTRU in the following buffers: 50mM formate pH 3-4.5, 50mM Acetate pH 5-6, 50mM MES pH 6-7, 50 mM HEPES pH 7-8. Samples were assayed for 30 min at 37°C and activity expressed as a percent of maximal activity. NaCl was not used in buffers, as this has been reported to alter the pH optima of testicular hyaluronidase preparations (25, 26). We have verified this phenomenon. Physiological salt concentrations (0.15 M),

decreased the apparent pH optimum. This was more pronounced in purified preparations of the testicular enzyme than in the original crude sample.

Establishment of normal distribution of hyaluronidase activity in human plasma

Levels of hyaluronidase in human plasma were established from 40 normal human plasma samples obtained from the UCSF Blood Bank. All plasma samples had been collected in EDTA. Residual cellular material was removed by centrifugation. Plasma samples were then assayed after a 30 min incubation using 1:200 dilutions in the formate assay buffer.

Preparation of hyaluronidase extracts from keratinocyte cultures

Hyaluronidase activity was characterized in normal keratinocytes. Primary foreskin keratinocyte cultures were generated from circumcision tissue from the Newborn Nursery at UCSF. Briefly, tissue was washed 5x in PBS with penicillin, streptomycin, and fungizone followed by digestion overnight at 4°C in dispase. Epithelium was then stripped from mesenchymal tissue with forceps and digested in trypsin followed by plating on collagen-coated plates in KGM (keratinocyte growth medium) with 0.05mM calcium (Clonetics, San Diego, CA). Cells were used between the first and fourth passage. To test the effects of induction of differentiation on hyaluronidase activity, cells were plated into 6-well plates and at confluence the media was changed to either KGM with 1.5 mM calcium or left at 0.05mM calcium. Cell layers and conditioned media were harvested after 72 hours in culture. Cell layers were harvested with 60mM

octylglucoside with 50 U/ml DNA'ase I (Boehringer Mannheim, Indianapolis, IN) and Complete™ protease inhibitor cocktail (Boehringer Mannheim) in PBS. Cells were extracted for 30 min on ice followed by centrifugation at 10,000 x g for 10min. Conditioned media from each sample was treated with octylglucoside and protease inhibitors. Cell extracts were normalized on the basis of total cellular protein using the Biorad Protein Assay kit (Biorad, Richmond CA). Extracts were then assayed at 1:10 dilutions in the described formate assay buffer at 37°C for 60 min. Activity was expressed as rTRU/mg cellular protein.

Results

Covalent Biotinylation of HA

Hyaluronan from human umbilical cord was biotinylated in a one step reaction using biotin-hydrazide and EDAC, resulting in a reaction product as depicted in Fig.1. By limiting the EDAC, which couples the free carboxyl groups on HA with biotin hydrazide, only a small fraction of the total glucuronic acid residues on HA are labeled. This amount of EDAC ($3 \times 10^{-5}\text{M}$) added to HA ($2.8 \times 10^{-3}\text{M}$), would result in a maximum of one molecule of biotin hydrazide coupled per 93 disaccharide units of HA .

Incorporation of bHA Into a Microtiter Based Assay for Hyaluronidase

The bHA reagent was used to generate a microtiter-based hyaluronidase assay. The bHA was coupled to NH-bearing microtiter plates at a final concentration of $10\mu\text{g}/\text{well}$ using EDAC. The amount of HA bound to the plates through this procedure was assayed with the HABP hyaluronan assay. Based upon the HABP hyaluronan assay, approximately $7.5\mu\text{g}$ of the $10\mu\text{g}$ added per well bound to the plate.

A four parameter curve fit of bovine testicular hyaluronidase standard reactions measured at pH 3.7, and diluted from 1.0 to 1×10^{-6} TRU/well is presented in Fig. 2. Four parameter curve fits were established from the equation $y = \frac{(A-D)}{1 + (\text{conc}/C)^B} + D$ where $\text{logit } y = \ln(y'/1-y')$, $y' = (y-D)/(A-D)$, $B = -b/\text{Ln}10$ and $C = \text{EXP}(a/B)$. The four parameters (A,B,C,D) were

calculated with a software program that utilized the 2+2 algorithm with linear regression (27). This curve fit incorporates the sigmoidal aspects the standard curve seen in Fig.2. Optimal accuracy for measurement of a sample occurs from 0.001 to 0.01 at TRU/well. During a 30 min incubation, 1/1000th of a TRU is clearly detectable. A standard logarithmic curve may also be utilized over a shorter range of values to establish a standard curve fit.

To establish linearity of the assay over time, samples of plasma, *Streptomyces* and testicular hyaluronidase were assayed as a function of time (Fig.3a). Linearity over a 30 min incubation of enzyme was clearly present over this time period for recombinant human plasma hyaluronidase, whereas preparations of testicular hyaluronidase and streptomyces hyaluronidase deviated slightly. Log dilutions of human plasma hyaluronidase (Fig.3b) revealed that linearity was observed in more dilute preparations, presumably where substrate had not become limiting.

The pH dependence of a neutral- and an acid-active hyaluronidase were examined. In Fig.4, recombinant human plasma hyaluronidase was compared to a commercial preparation of bovine testicular hyaluronidase (Sigma, Type VI-S). The plasma enzyme had an acid optimum at pH 3.8, with no detectable activity above pH 4.5, whereas the bovine testicular hyaluronidase had a bimodal distribution of activity with optima at pH 4.5 and pH 7.5.

Analysis of hyaluronidase levels in human plasma

Hyaluronidase activity from the plasma of normal donors were assayed to establish the distribution of hyaluronidase levels in the human circulation. The histogram in Fig.5 represents the distribution of hyaluronidase activity assayed at pH 3.7 from 40 healthy male and female subjects from ages 20-70 years. The mean plasma hyaluronidase level was 5.9 rTRU/ml. The standard deviation was 1.2 rTRU. The inter- and intra-assay variations established from repeated sampling of a single plasma sample were less than 5 and 10%, respectively, thus establishing the reproducibility of this procedure. The inter-assay variation was calculated from comparing the standard deviation of the interpolated values of a serum sample assayed in 10 different wells in a single plate to the mean interpolated value of those ten wells against a standard curve. The intra-assay variation was obtained from comparing the standard deviation of interpolated values from the serum sample assayed in six different plates with different standard curves to the mean interpolated value of those six samples.

Effects of Calcium on Hyaluronidase Levels In Keratinocyte Cultures

Primary cultures of keratinocytes can be induced to stratify and express several markers for differentiation in a defined culture medium when calcium levels are elevated from 0.05mM to 1.5mM (28). The effects of calcium-induced differentiation on levels of hyaluronidase activity in keratinocyte cultures (Fig.6) resulted in an approximately 25-fold increase in hyaluronidase activity in both conditioned media and cell layer, compared to cultures in 0.05mM calcium.

EDTA was included with protease inhibitors in the extraction buffer, making it unlikely that calcium was directly effecting enzymatic activity. In purified preparations of human plasma hyaluronidase, EDTA had no inhibitory effect on enzyme activity, nor did added calcium have a stimulatory effect. All of the hyaluronidase activity secreted into the media of the keratinocyte cultures was immunoprecipitated in its entirety with monoclonal antibodies against the plasma enzyme (data not shown).

Discussion

This new assay for hyaluronidase activity was developed to provide a faster and less labor intensive procedure, compared to assays previously described. In addition, covalent coupling of the HA substrate to the microtiter plate made the assay more resistant to pH variations during the generation of pH optima curves and when different enzymes with different pH optima were being compared. This became particularly important after we realized that HA adherence to the standard plastic microtiter plates was pH-dependent, using the assay previously described (6).

As HA does not contain free amines (Fig.1), biotinylation of HA using NHS-biotin results in a very low level of biotinylation. This previously described method (29) using NHS-biotin may actually be a result of biotinylation of free amine groups from contaminating HA-binding proteins rather than the substrate itself. The use of EDAC as the limiting reagent to couple free carboxyl groups on HA, that are present at one site per disaccharide, with biotin hydrazide, can be used to overcome this difficulty. This EDAC coupling procedure has been used successfully in our laboratory to link HA to Sepharose beads in the preparation of HA-Sepharose affinity resins.

We initially attempted to link biotin to HA with photoactivatable biotin, as has been described for DNA labeling. However, this resulted in a very low signal and in addition, was very expensive in comparison to other biotin preparations. Biotin hydrazide with EDAC as a coupling reagent was then tested as a method for linking biotin to HA. This procedure permitted the control

of biotinylation through by using the EDAC as the limiting reagent and was very easy to utilize. Through initial studies it was found that coupling the biotin at a ratio of 1 molecule of biotin per approximately 80 disaccharide units provided a strong signal in the avidin-peroxidase system and did not interfere with the ability of the enzyme to degrade substrate. Higher levels of biotinylation resulted in inhibition of enzyme activity and was beyond the range of sensitivity of the system. Both long and short chain biotin hydrazide was analyzed, and short chain biotin had the least interference with enzymatic activity.

This HA-biotinylation procedure was simple to perform, requiring only a one step biotinylation procedure rather than the multistep modification of HA with pendant amine groups described previously (30). Excess biotin could easily be removed by dialysis. The Guanidine HCl was added to the preparation before dialysis to aid in the removal of any non-covalent interactions between biotin and HA.

Coupling the bHA to NH-microtiter plates was shown to be very efficient at a concentration of 10 μ g/well. Approximately 75% of the added HA was bound to the microtiter plate, as determined by measuring the residual HA in solution using the HA-binding peptide competition assay for hyaluronate (31). Thus, approximately 7.5 μ g of HA was coupled to each well of the microtiter plate. The amount of EDAC used to couple the HA to the plate was optimized as well, and it was demonstrated that a 10-fold increase in EDAC resulted in a significant loss of sensitivity to enzymatic degradation. This was presumably due to excessive crosslinking of the biotinylated substrate to the microtiter plate, as

most endoglucosaminidases digest the substrate to the tetrasaccharide level as the smallest digestion product (32).

The present assay was very sensitive over short incubation periods and was approximately 1,000 times more sensitive than the commonly used assays under identical incubation times. Increased sensitivity for detecting enzyme in cell cultures that produce very low levels of activity could be obtained by using a longer incubation time of 2-12 hours. However, relative activities of these enzymes are difficult to evaluate over the longer incubations because of variations in enzyme stability, and loss of the kinetic nature of the reaction. As seen in Fig. 2, the use of a four parameter curve fit has a semi-logarithmic relationship over a three log range between absorbance and activity, from 0.6 to 0.006 relative TRU/ml during a 30 min incubation. If the incubation is extended to two hours, this curve shifts from 0.06 to 0.00006 TRU/ml, resulting in a more sensitive measurement of activity. We routinely used the one hour incubation for cell culture extracts and the 30 min assay for tissue extracts.

The utility of the assay for the measurement of pH optima of various enzymes was also evident. As seen in Fig. 3a, immunoaffinity purified plasma hyaluronidase had the characteristic acid pH optimum of 3.8, whereas the commercial semi-purified preparation of bovine testicular hyaluronidase, contained two distinct peaks of activity, one at neutrality and one at pH 4.0. The pH profile of immunoaffinity-purified recombinant human plasma hyaluronidase was identical to that of unprocessed human plasma (11), with no activity detected at neutral pH. This is the only enzyme detectable in plasma using this

assay based upon immunological and amino acid sequencing criteria (11). The bimodal pH optima for preparations of sperm hyaluronidase have been described using substrate gel zymography (33), and are not likely due to an artifact of the assay, as two disparate methods give the same result. It has been postulated that two hyaluronidase enzymes are present in these testicular preparations (30, 31).

Legends to the Figures

Fig.1. Structure of the biotinylated disaccharide repeating subunits of HA resulting from a reaction between HA, biotin-hydrazide and EDAC.

Fig.2. A four parameter curve fit of bovine testicular hyaluronidase assays as standard reactions performed at pH 3.7, diluted from 1.0 to 1×10^{-6} TRU/well.

Fig.3.a Linearity of the enzyme reaction over a 30 min incubation period, comparing three different hyaluronidases. 0.01 rTRU/well was utilized at each time, and assayed in triplicate.

Fig 3b. Kinetic analysis of log dilutions of immunoaffinity-purified recombinant human plasma hyaluronidase. Human plasma hyaluronidase, from 1 to 0.0001 rTRU/well, was assayed from 0-30 minutes.

Fig.4. Comparison of the pH profiles of recombinant human plasma hyaluronidase and a partially purified bovine testicular hyaluronidase preparation, Sigma, Type VI-S.

Fig.5. Distribution of hyaluronidase levels in normal human plasma. Samples were from freshly collected specimens obtained from the UCSF Blood Bank. The forty normal healthy donors ranged in age from 20 to 70 years. Samples were assayed at pH 3.7 as described in the Materials and Methods.

Fig.6. Levels of hyaluronidase activity in human keratinocytes in primary culture, grown in low (0.05mM) and high (1.5mM) calcium. High calcium-containing medium induces differentiation and stratification in such cells, and enhances levels of hyaluronidase activity in both the medium and in the cell layer.

FIGURE-1

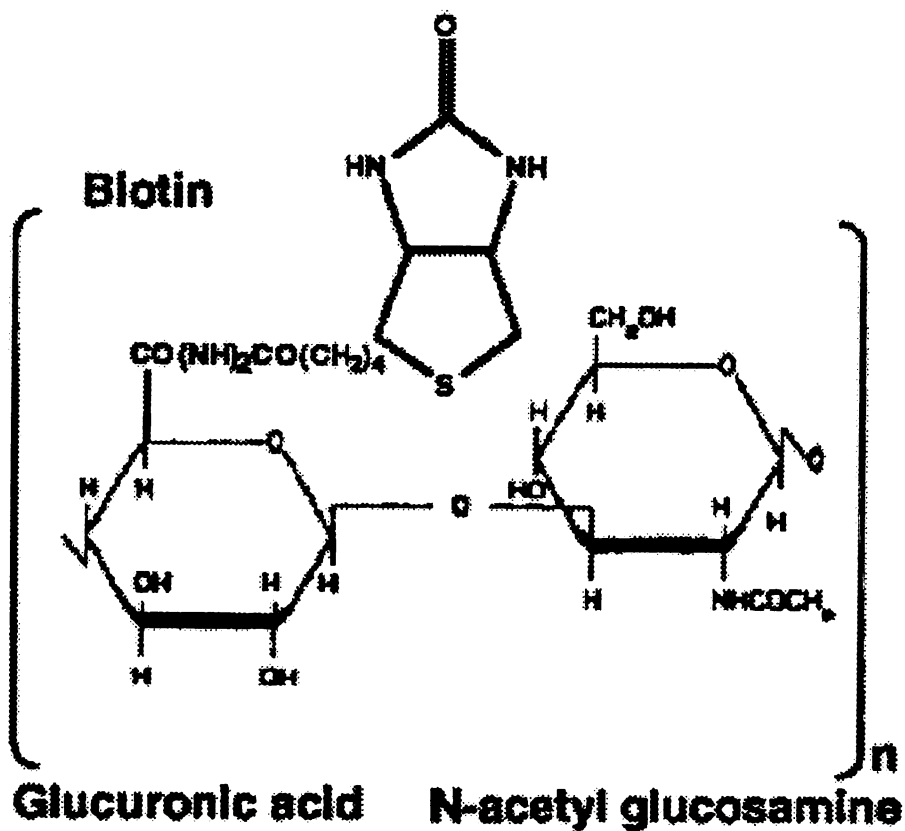


FIGURE-2

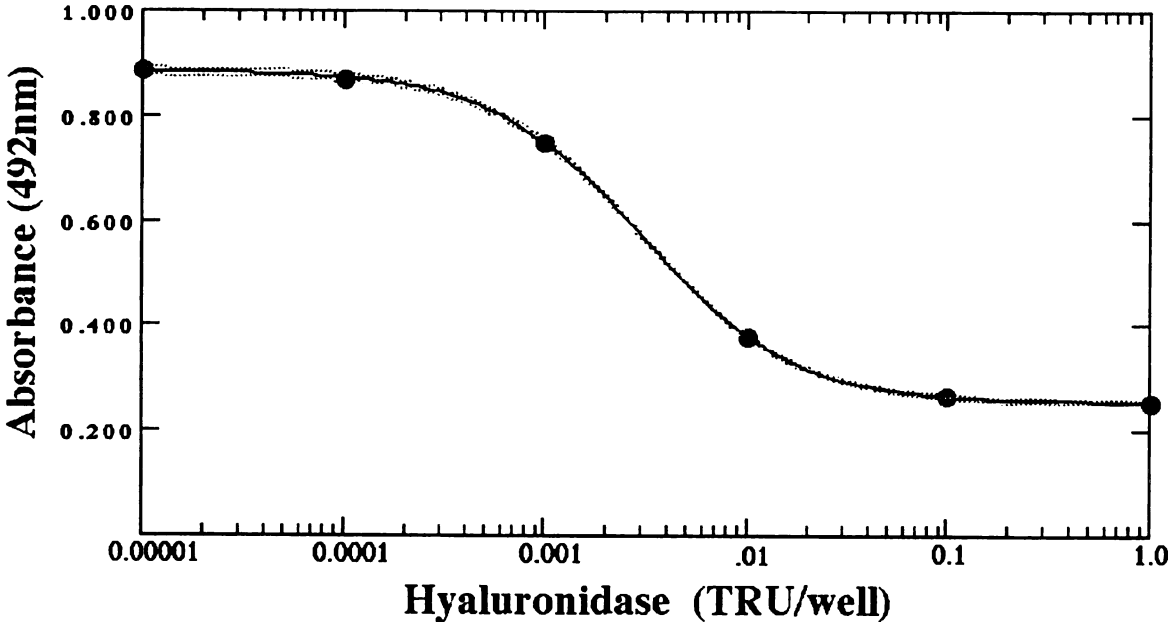


FIGURE-3

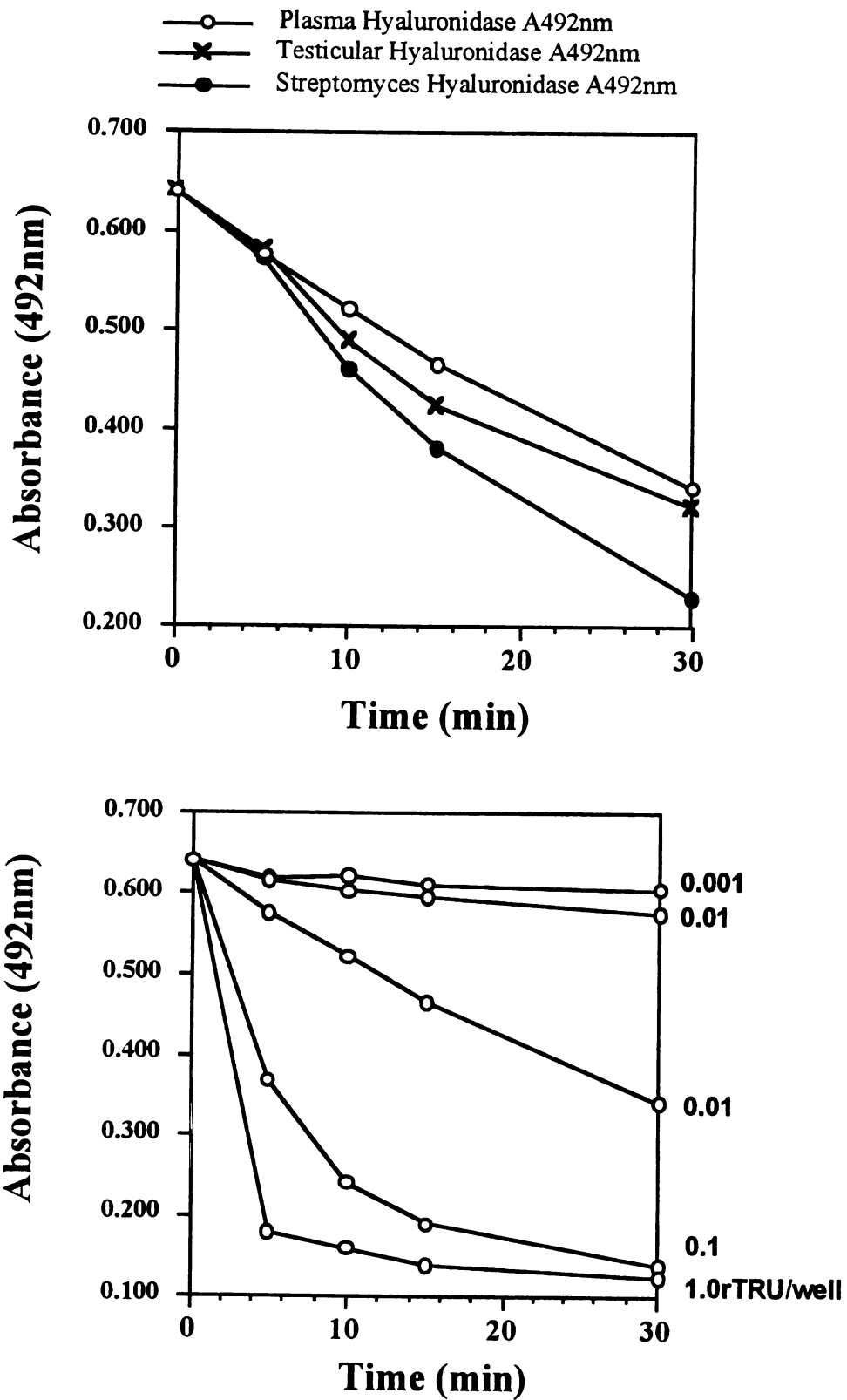


FIGURE-4

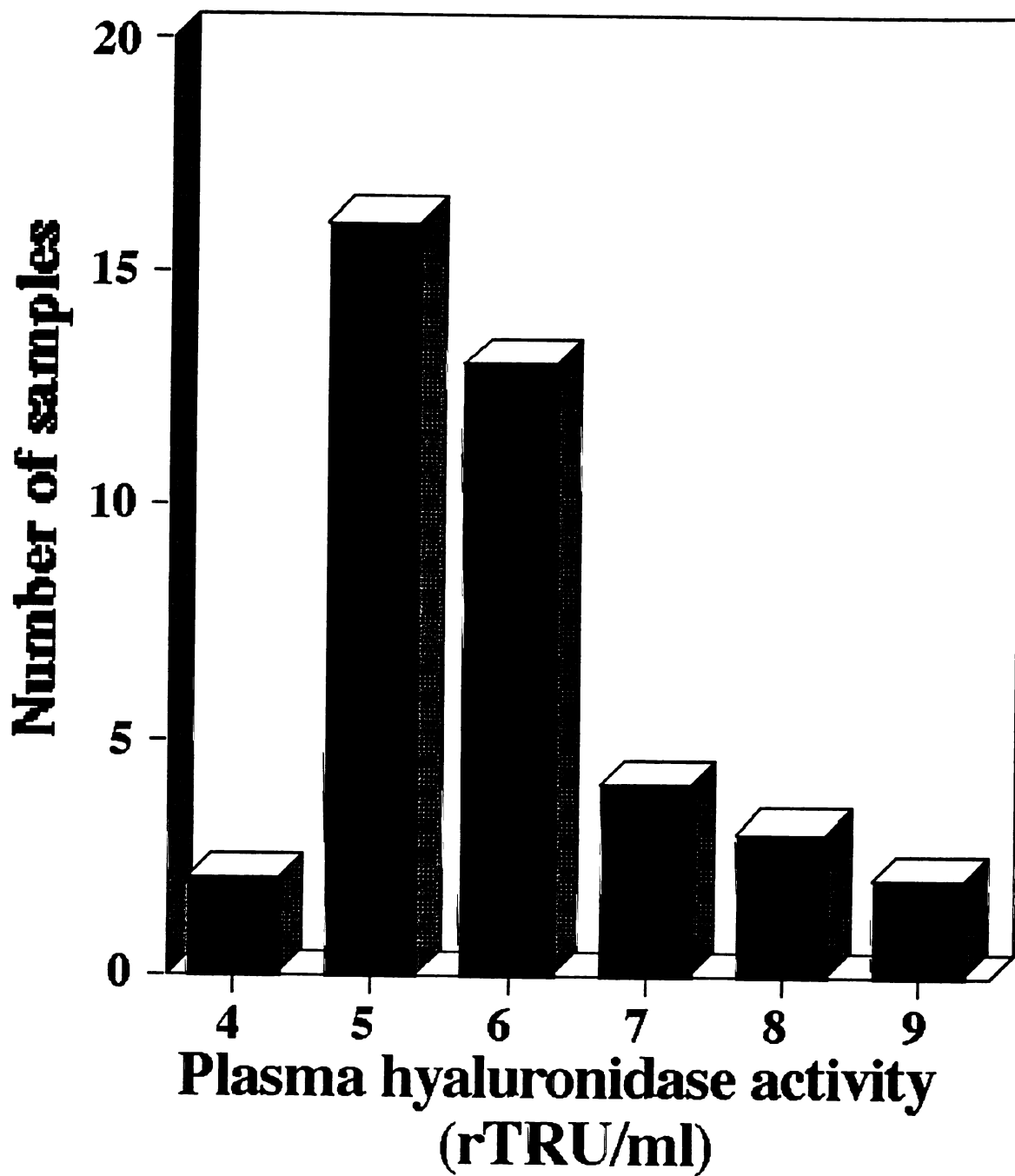
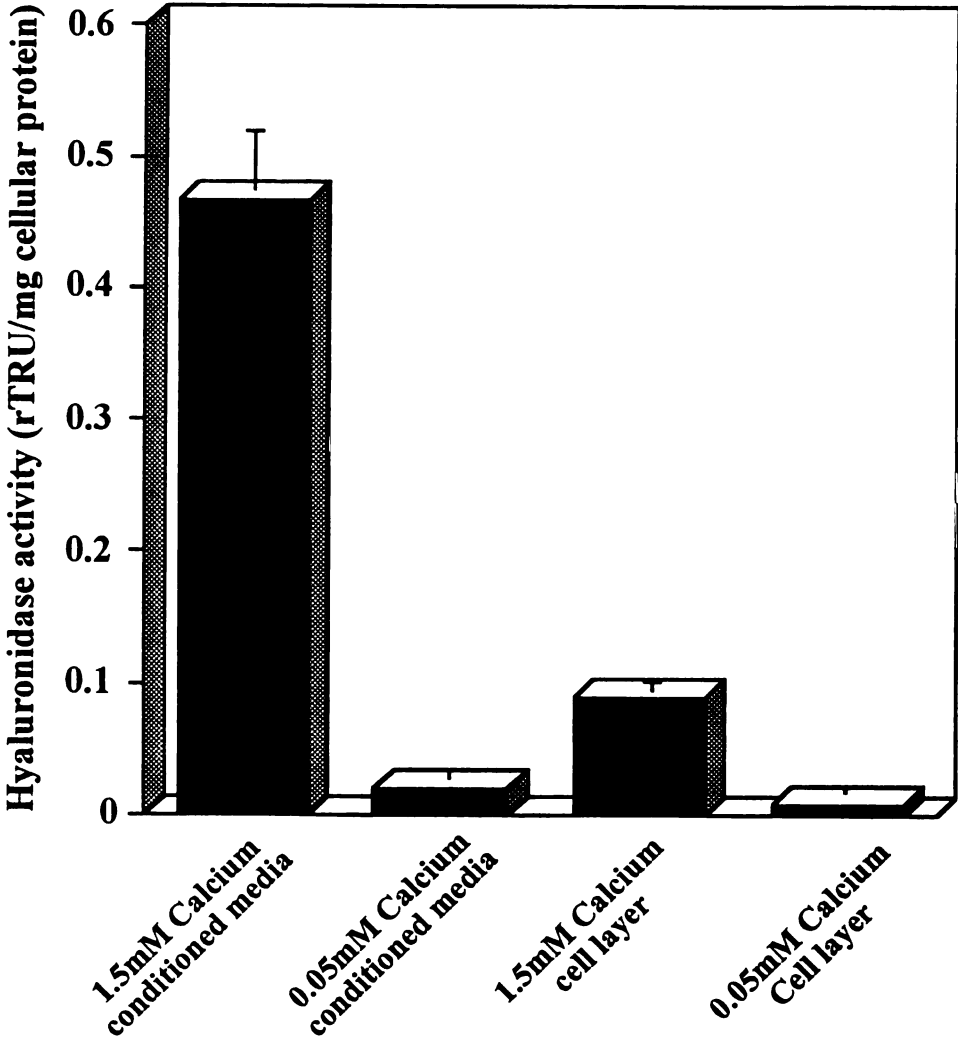


FIGURE-5



References

- 1) Frost, G. I., Csoka, T., and Stern, R. (1996) *Trends in Glycoscience and Glycotechnology* **8**, 419-434.
- 2) Kreil, G. (1995) *Protein Sci* **4**, 1666-9.
- 3) Bonner, W. M., Jr., and Cantey, E. Y. (1966) *Clin Chim Acta* **13**, 746-52.
- 4) De Salegui, M., Plonska, H., and Pigman, W. (1967) *Arch Biochem Biophys* **121**, 548-54.
- 5) Dorfman, A., and Ott, M.L., (1948) *J. Biol. Chem.*, **172**, 367.
- 6) Stern, M., and Stern, R. (1992) *Matrix* **12**, 397-403.
- 7) Primakoff, P., Hyatt, H., and Myles, D. G. (1985) *J Cell Biol* **101**, 2239-44.
- 8) Gmachl, M., Sagan, S., Ketter, S., and Kreil, G. (1993) *FEBS Lett* **336**, 545-8.
- 9) Aronson, N. N., Jr., and Davidson, E. A. (1967) *J Biol Chem* **242**, 437-40.
- 10) De Salegui, M., and Pigman, W. (1967) *Arch Biochem Biophys* **120**, 60-7.
- 11) Frost, G.I., Csóka, T.B., Wong, T., and Stern, R. (1997) *Biochem Biophys Res Commun*, in press.
- 12) Brown, J. J., and Papaioannou, V. E. (1993) *Development* **117**, 483-92.
- 13) Meyer, M. F., and Kreil, G. (1996) *Proc Natl Acad Sci U S A* **93**, 4543-7.
- 14) Knudson, W. (1996) *Am J Pathol* **148**, 1721-6.
- 15) Sherman, L., Sleeman, J., Herrlich, P., and Ponta, H. (1994) *Curr Opin Cell Biol* **6**, 726-33.
- 16) Estes, J. M., Adzick, N. S., Harrison, M. R., Longaker, M. T., and Stern, R. (1993) *J Pediatr Surg* **28**, 1227-31.
- 17) West, D. C., and Kumar, S. (1989) *Ciba Found Symp* **143**, 187-201; discussion 201-7, 281-5.
- 18) Edelstam, G. A., Laurent, U. B., Lundkvist, O. E., Fraser, J. R., and Laurent, T. C. (1992) *Inflammation* **16**, 459-69.

-
- 19) Noble, P. W., McKee, C. M., Cowman, M., and Shin, H. S. (1996) *J Exp Med* **183**, 2373-8.
- 20) Kropf, J., Grobe, E., Knoch, M., Lammers, M., Gressner, A. M., and Lennartz, H. (1991) *Eur J Clin Chem Clin Biochem* **29**, 805-12.
- 21) Rao, P. N., Bronsther, O. L., Pinna, A. D., Demetris, A., Snyder, J., Fung, J., and Starzl, T. E. (1993) *Transplant Proc* **25**, 2141-2.
- 22) Itasaka, H., Suehiro, T., Wakiyama, S., Yanaga, K., Shimada, M., and Sugimachi, K. (1995) *J Surg Res* **59**, 589-95.
- 23) Hernandez Hernandez, J. R., Garcia Garcia, J. M., Martinez Muniz, M. A., Allende Monclus, M. T., and Ruibal Morell, A. (1995) *Int J Biol Markers* **10**, 149-55.
- 24) Natowicz, M. R., Short, M. P., Wang, Y., Dickersin, G. R., Gebhardt, M. C., Rosenthal, D. I., Sims, K. B., and Rosenberg, A. E. (1996) *N Engl J Med* **335**, 1029-33.
- 25) Gold, E. W. (1982) *Biochem J* **205**, 69-74.
- 26) Gacesa, P., Savitsky, M. J., Dodgson, K. S., and Olavesen, A. H. (1979) *Biochem Soc Trans* **7**, 1287-9.
- 27) Rodbard, D., Lenox, R.H., Wray, H.L., and Ramseth, D. (1976) *Clin. Chem.* **22**, 350
- 28) Hennings, H., and Holbrook, K. A. (1983) *Exp Cell Res* **143**, 127-42.
- 29) Hoare, K., Savani, R. C., Wang, C., Yang, B., and Turley, E. A. (1993) *Connect Tissue Res* **30**, 117-26.
- 30) Pouyani, T., and Prestwich, G. D. (1994) *Bioconjug Chem* **5**, 370-2.
- 31) Fosang, A. J., Hey, N. J., Carney, S. L., and Hardingham, T. E. (1990) *Matrix* **10**, 306-313.
- 32) Aronson, N. N., Jr., and Davidson, E. A. (1967) *J Biol Chem* **242**, 441-4.
- 33) Cherr, G. N., Meyers, S. A., Yudin, A. I., VandeVoort, C. A., Myles, D. G., Primakoff, P., and Overstreet, J. W. (1996) *Dev Biol* **175**, 142-53.
- 31) Hunnicutt, G. R., Mahan, K., Lathrop, W. F., Ramarao, C. S., Myles, D. G., and Primakoff, P. (1996) *Biol Reprod* **54**, 1343-9.

Chapter-3

Purification, Cloning, and Expression of Human Plasma Hyaluronidase.

Preface

My contributions to this work included: developing the biochemical protocols to purify HYAL1 from human plasma; amino acid sequencing of HYAL1; generation of monoclonal antibodies and hybridoma screening strategies; generation of immunoaffinity columns and reagents; transfection, screening and biochemical characterization of recombinant HYAL1 in HEK cells.

Collaborators in this work included Tony B. Csóka (Department of Gerontology, University Medical School of Debrecen, Hungary) for the PCR strategies, generation of expression constructs for HYAL1 and PCR organ surveys.

Tim M. Wong (Department of Pathology, UCSF) assisted in the purification of HYAL1 from human plasma, screening extracts for hyaluronidase activity and substrate gel zymography.

Jane Yao (Department of Stomatology, UCSF) contributed her protocols on hybridoma techniques.

Abstract

Human plasma hyaluronidase, an acid-active endoglucosaminidase, was purified to homogeneity using sequential Triton X-114 phase extractions and ion-exchange chromatography. Monoclonal antibodies generated against this purified protein were used to obtain sufficient amounts of protein for N-terminal and internal amino acid sequences. These sequences were used in a homology search of the Expressed Sequence Tag Database (dbEST). A single EST was identified, and in combination with 5' RACE, was used to clone the full length plasma hyaluronidase gene. The predicted amino acid sequence of human plasma hyaluronidase shares over 40% identity with PH-20, a sperm-specific hyaluronidase. Unlike PH-20, which is only expressed in the testis, transcripts of human plasma hyaluronidase were found in heart, kidney, liver, lung, skeletal muscle and placenta. Human embryonic kidney cells stably transfected with the cDNA encoding plasma hyaluronidase secreted a hyaluronidase activity, that when immunoaffinity purified, was biochemically indistinguishable from the plasma enzyme. We conclude that human plasma hyaluronidase is a member of a conserved family of sperm and venom hyaluronidases but distinct from other members of this family in being strictly acid active.

Introduction

Hyaluronic acid (HA) is a high molecular weight linear glycosaminoglycan (GAG), and a major component of the extracellular matrix. It is composed of repeating disaccharide units [GlcNAc β 1-4GlcUA β 1-3] and is the only non-sulfated GAG. It is prominent in connective tissue, skin, cartilage, synovial fluid (1) and whenever rapid tissue turnover is occurring, such as during embryonic development (2) and wound healing (3). Elevated levels of HA correlate with tumor aggressiveness in many human malignancies (4, 5). The enzymes that catabolize HA, the hyaluronidases (E.C 3.1.25), are a family of β ,1-4 endoglucosaminidases that depolymerize HA and to a lesser extent chondroitin sulfate (for review, see 6,7). In vertebrates, these enzymes are grouped into two classes, the neutral-active hyaluronidases such as sperm-associated PH-20 (8,9), and those with an acid pH optimum, found in extracts of liver (10), kidney (11), placenta (12) and plasma (13). None of the human somatic hyaluronidases have ever been purified to homogeneity, nor have their genes been identified. Attempts to isolate the hyaluronidase from human plasma have met with limited success because of a high specific activity and very low abundance. In order to purify plasma hyaluronidase to homogeneity in sufficient quantity for amino acid sequencing, we generated monoclonal antibodies specific to the purified enzyme using an enzyme-capture screening assay. This enabled us to clone the gene that codes for plasma hyaluronidase.

Materials and Methods

Assays for hyaluronidase activity. Hyaluronidase activity was measured throughout the purification as described previously (14). For pH optima analysis, 0.1M buffers were used: formate, pH 3-4.5, Acetate pH 5.0-6.0, Mes pH 6.0-7.0, and Hepes pH 7.0-8.0. Bovine testicular hyaluronidase (Sigma Type VI-S, 3,000 TRU/mg solid) was used for pH optima comparisons. HA substrate gel zymography using 10% SDS-polyacrylamide gels were performed as described previously (15). Gels were incubated at pH 3.7 overnight followed by staining sequentially with Alcian blue followed by Coomassie blue R250 counterstaining.

Purification of human plasma hyaluronidase. To two liters of human plasma from Irwin Memorial Blood Bank (San Francisco, CA), 0.02% Na Azide, 50 mM NaCl, 5% sucrose and 7.5% Triton X-114 (Boehringer Mannheim, Indianapolis, IN) were dissolved at 4°C with stirring for 90 min followed by centrifugation at 10,000 x g for 30 min. The plasma was then subjected to temperature-induced phase extraction at 37°C. The extract was centrifuged at 10,000 x g for 30 min at 37°C to clarify the two phases. The detergent-rich phase was removed and diluted to 2 L with ice cold 50 mM Hepes, pH 7.5, 0.15M NaCl, followed by repartitioning at 37°C with centrifugation. This washing procedure was repeated three times. The final detergent phase was diluted six-fold with 25 mM Mes, pH 6.0, and 20 mL of equilibrated SP-Sepharose cation

exchange resin was added (Pharmacia, Piscataway NJ) and stirred overnight at 4°C. The beads were collected by centrifugation and washed with 25 mM Mes, pH 6.0, containing 46 mM octylglucoside (Boehringer Mannheim). Hyaluronidase was eluted from the beads by the addition of 0.3 M NaCl in Mes buffer pH 6.0 with several washes. The SP-Sepharose eluant was concentrated on a YM3 membrane (Amicon, Beverly, MA) and desalted into 10 mM PO₄ pH 7.4 with 25 mM NaCl, 46 mM octylglucoside on a F.P.L.C. Fast-Desalting column (Pharmacia). The hyaluronidase preparation was then combined with 10 mL of hydroxylapatite resin (Biorad, Richmond, CA) equilibrated in the same buffer, and left on a rocker overnight at 4°C. Plasma hyaluronidase did not adsorb to the resin and was recovered in the supernatant. The supernatant was concentrated to 0.5 mL on a Centriplus YM3 concentrator (Amicon, Beverly, MA), applied to a 12.5% polyacrylamide gel on a Phast Gel System (Pharmacia), and stained with silver according to the manufacturer's instructions. Protein determinations were measured throughout the purification using the Lowry (Pierce) and Bradford (Biorad) assays with BSA as a standard.

Generation of anti-hyaluronidase monoclonal antibodies. Six week-old female BALB/c mice were immunized using purified antigen from the post hydroxyapatite step using established procedures (16). Hybridomas secreting anti-hyaluronidase antibodies were screened by a modified enzyme capture assay. The bHA was coated onto Covalink plates under the same conditions as those described for the microtiter based enzyme assay except that 1.25 µg/well

of goat anti-mouse IgG (Jackson Immunolabs, West Grove, PA) was included with the bHA so that both bHA and goat anti-mouse IgG were covalently coupled to the plates. Hybridoma supernatants were incubated with diluted human plasma for 60 min at 37°C followed by incubation in the bHA/anti-mouse-IgG plates for 60 min at 37°C. Plates were washed 5x with PBS containing 1% Triton X-100, and 10 mg/ml BSA followed by the addition of formate assay buffer and incubation at 37°C for 60 min. Digested bHA as a result of immunoprecipitated hyaluronidase was detected as in the standard assay. IgG2a from ascites of single-cell cloned hybridoma lines were generated in BALB/c mice and was purified through Protein-A affinity chromatography.

Immunoprecipitation and immunoaffinity purifications. Purified IgG2a from the 17E9 anti-hyaluronidase hybridoma clone was used for routine immunoprecipitation and purifications. For the immunoprecipitation of hyaluronidase from plasma, serial dilutions of purified 17E9 IgG or control mouse IgG2a was mixed with plasma diluted in RIPA buffer (1% NP40, 1% deoxycholate, 1% Triton X-100, 5 mM EDTA in PBS) followed by immunoprecipitation with protein-A beads. Residual hyaluronidase activity in the supernatant was then measured in the microtiter assay. For the immunoaffinity purification of hyaluronidase, 3 mg of purified IgG from the 17E9 hybridoma clone was coupled to a 1 mL Hi-Trap-NHS activated column (Pharmacia). Plasma or HEK-293 human embryonic kidney cell recombinant

hyaluronidase conditioned media was diluted 1:2 with RIPA buffer, and passed over the anti-hyaluronidase IgG column. The column was first washed with PBS containing 2M NaCl, 100 mM octylglucoside followed by washing with 100 mM citrate pH 4.0, 0.15M NaCl and octylglucoside, and then eluted with the same buffer adjusted to pH 3.0.

Amino acid sequencing of hyaluronidase. For N-terminal amino acid sequencing, the immunoaffinity purified protein was electroblotted from an SDS gel to a PVDF membrane (ABI, Foster City, CA) and submitted to the UCSF Biomolecular Resource Center for Edman sequencing. Internal peptides of immunoaffinity purified plasma hyaluronidase were obtained through digestion with CnBr followed by fragment separation on a Vydac C-18 column.

Cloning the complementary DNA (cDNA) of plasma hyaluronidase. A TBLASTN (18) homology search (compares a protein sequence against a nucleotide sequence database translated in all reading frames) of the Expressed Sequence Tag database (19) revealed a single I.M.A.G.E. Consortium clone (19) (GenBank accession no. AA223264) with 100% identity to the N-terminal amino acid sequence of plasma hyaluronidase. We obtained this EST from Genome Systems (St. Louis,MI) and sequenced the insert, which was 2 kb including the poly-A tail at the 3' end. To obtain the 5' end of the hyaluronidase cDNA, 5' RACE (20) was performed on a Marathon Ready™ human heart cDNA library (Clontech Laboratories, Inc., Palo Alto, California,

USA) according to the manufacturer's instructions, with some modifications. Briefly, for the first PCR reaction the following primers were used: HPHRACE1 (5'-ATCGAAGACACTGACATCCACGTCCACACC-3') and the Adapter Primer 2 (AP2) from Clontech; annealing/extension was at 73°C for 40 cycles. Advantage™ KlenTaq polymerase mix (Clontech Laboratories, Inc., Palo Alto, California, USA) was used to provide a "hot start". A diffuse band of 800 bp was observed on agarose gel electrophoresis. The band was excised using a QIAquick gel extraction kit (Qiagen Inc. Chatsworth, CA, USA) according to the manufacturer's instructions. The excised DNA was used as a template for a second nested PCR using primer HPHRACE2 (5'-TGCCTCTCCAGGCACCACTGGGTGTTTGC-3') with the AP2 primer; annealing/extension was at 72°C for 15 cycles. A "hot start" was employed, as before. A single sharp band of 800 bp was observed on agarose gel electrophoresis. 120 ng of the PCR product was ligated into the TA cloning vector pCR2.1 (Invitrogen, San Diego, CA) and used to transform One Shot TOP10F' competent cells according to the manufacturer's instructions. Positive colonies were sequenced as above. As expected, the 800bp product overlapped 100% with the 5' end of the EST by 300 bp.

Expression of recombinant plasma hyaluronidase in human embryonic kidney cells. For generation of the hyaluronidase cDNA coding sequence, a PCR reaction was performed with the EST as template with the following primers: HPHF1 5'-GTGCCATGGCAGCCCACC-3' and HPHR1 5'-

ATCACCATGCTCTTCCGC-3' with annealing at 58°C for 35 cycles. 120 ng of the PCR product was cloned into the TA expression vector pCR3.1-Uni (Invitrogen, San Diego, CA) and used to transform One Shot TOP10F' competent cells according to the manufacturer's instructions. Plasma hyaluronidase in the pCR3.1-Uni expression vector was purified from positive colonies, verified by restriction mapping with *Pst* I and *Dra* III, and transfected into 75% confluent T75 flasks of HEK-293 cells for five h. serum free using 9 µg of purified plasmid with 60 µl of Lipofectin (Gibco BRL) in 20 mL of DME/F12 50/50. The transfected cells were then grown for an additional 48 h in DME/F12 50/50 mix containing 10%FBS. After 48 h, cells were plated out using limiting dilution method into 24 well plates with 500µg/ml G418. After 14 days, the conditioned media of resistant colonies was assayed for hyaluronidase activity using the described protocol. Colonies with high level expression were then expanded and used for further characterization. For the analysis of the recombinant hyaluronidase and comparison with plasma hyaluronidase, a recombinant overexpressing hyaluronidase 293-line was grown for 48 h serum free and conditioned media passed over a 17E9 anti-plasma hyaluronidase immunoaffinity column. Recombinant enzyme was eluted using the same protocol as for human plasma. Purified recombinant hyaluronidase was then blotted to PVDF and subjected to N-terminal amino acid sequencing to ensure authenticity.

Organ survey of hyaluronidase transcripts. Nested PCR primers amplifying the 1.3 kb coding region of the plasma hyaluronidase cDNA were used to analyze the tissue distribution of transcripts in λ gt10cDNA libraries. For the first round of PCR the following primers were used: HPHF2 (5'-AGGTTGTCCTCGACCAGTC-3') and HPHR2 (5'-ATGTGCAACTCAGTGTGTGGC-3') at an annealing temp. of 58°C. The second PCR reaction consisted of 15 cycles at an annealing temp. of 58°C with primers HPHF1 and HPHR1 (see above).

Results

Purification of hyaluronidase

The enzyme partitioned into the temperature-induced Triton X-114 detergent phase and gave a 60 fold enrichment. The enzyme was very stable at 37°C in the presence of non-ionic detergents. Removal of Triton X-114 was performed by batch absorption onto a SP-Sepharose cation exchanger resin. The post SP-Sepharose preparation of hyaluronidase could be purified to homogeneity as determined by silver staining (Fig. 1a). Batch adsorption using hydroxyapatite resin, resulted in an overall purification of 1.5-million fold (Table-1). The specific activity of the enzyme (600,000 rTRU/mg) was approximately 6-fold that of the reported values for the sperm hyaluronidase, PH-20 (17). The protein migrated on SDS-PAGE with a relative molecular mass of 57 kDa (Fig. 1a).

Generation of monoclonal antibodies against plasma hyaluronidase.

The post-hydroxyapatite step in the preparation was used to generate monoclonal antibodies. An enzyme capture assay was developed for screening hybridomas that exploited the lack of activity of hyaluronidase at neutral pH and the fact that the enzyme had no binding affinity for HA above pH 4.5, as determined by HA-Sepharose affinity chromatography (data not shown). The hybridoma supernatants were incubated with crude plasma at neutral pH in the bHA/anti-mouse IgG microtiter plates to immunoprecipitate the antibody-

antigen complex. Eight clones were identified from twenty hybridoma fusion plates using this screening procedure. One clone of the IgG2a class, 17E9, was used to generate ascites. Addition of serial dilutions of the 17E9 antibody to human plasma followed by immunoprecipitation with Protein-A resulted in precipitation of all detectable acid-active hyaluronidase activity (Fig. 2).

Immunoaffinity purification and amino acid sequencing.

Hyaluronidase could be purified to homogeneity in a single step from human plasma by immunoaffinity chromatography using the 17E9 antibodies. After washing the column under stringent conditions, the enzyme eluted at pH 4.0 and was purified to homogeneity as determined by SDS-PAGE and amino acid sequencing. Three sequences were obtained from CnBr digests of immunopurified protein (Figure-2 overlined sequences).

Cloning the cDNA of plasma hyaluronidase.

The N-terminal and internal amino acid sequences (underlined in Fig.3a) of plasma hyaluronidase were 100% identical to the conceptual translation of the cDNA. This strongly suggests that we cloned the gene that codes for plasma hyaluronidase. Alignment (21) of the predicted translation of plasma hyaluronidase and human PH-20 indicated 40% sequence identity and 60% homology at the amino acid level (Fig. 3a). PH-20 is a sperm specific neutral-active hyaluronidase. The homology between a strictly acid-active

hyaluronidase and PH-20 suggests that all mammalian β ,1-4 hyaluronidases may be members of a conserved family.

Expression of recombinant plasma hyaluronidase.

To substantiate the identity of plasma hyaluronidase with the cloned gene, the cDNA was stably transfected into HEK-293 cells. The cDNA was amplified from the EST and then subcloned into a unidirectional expression vector. This vector was used to generate HEK-293 clones overexpressing hyaluronidase. The parental HEK-293 cell line produced undetectable levels of hyaluronidase in the conditioned media and cell layer whereas the stably transfected clones secreted approximately 15 rTRU/ml, a 3,000 fold increase (*Fig. 4*). To ensure that the hyaluronidase activity found in the recombinant HEK-293 cell clones was the product of the transfected cDNA, we immunoaffinity purified the hyaluronidase from serum free conditioned medium of the HEK-293 overexpressing clone and sequenced the eluent from the 17E9 column. This yielded the same processed N-terminus (FRGPLLV) found in human plasma and a migrated as a single band on SDS-PAGE (*Fig 5a*). This band aligned with the purified plasma using both silver stain and substrate gel zymography (*Fig 5b*). A commercial preparation of testicular hyaluronidase (3,000 TRU/mg solid) was run for comparison of the specific activity. The pH activity curve of recombinant plasma hyaluronidase (*Fig. 6*) has the same profile as the immunoaffinity-purified plasma enzyme, with no activity *in vitro* above pH 4.5, in contrast to bovine testicular hyaluronidase, which has maximal activity above pH 7.

Organ survey of hyaluronidase transcripts.

Nested amplimers amplifying the 1.3 kb coding region of the plasma hyaluronidase cDNA were used to analyze the tissue distribution of transcripts in λ gt10 cDNA libraries. As illustrated in *Fig.7*, PCR products were found in heart, kidney, liver, lung, placenta, and skeletal muscle, but were not detected in brain. Whether plasma hyaluronidase is the predominant acid-active hyaluronidase described in other tissues awaits further studies. However, it is the only hyaluronidase we have detected in human plasma.

Discussion

An acid-active HA-degrading activity was first described in human plasma in 1967 (13). We now report the successful isolation of this hyaluronidase. The enzyme is present at exceedingly low levels, approximately 50 ng/mL and has a very high specific activity, 6.0×10^5 rTRU/mg protein, approximately 6-fold that of PH-20. A 1.5 million-fold purification was required to achieve homogeneity. Generation of monoclonal antibodies was essential to purify enough enzyme for sequence analysis.

Few serum proteins partition into the detergent rich phase as did hyaluronidase. Phospholipase treatment however, did not expose a GPI-anchor, as has been described for PH-20 (44,45). Analysis of the hyaluronidase amino acid sequence failed to reveal a potential transmembrane domain that would explain the partitioning properties (not shown). Nevertheless, recombinant hyaluronidase from the HEK-293 overexpressing clones had similar phospholipase-resistant detergent phase partitioning characteristics. We assume that either the lipid modification was resistant to cleavage, as has been demonstrated for other GPI-linked proteins (42), or another lipid modification is responsible for the hydrophobic character of the enzyme.

Legends to the Figures

Fig.1. Analyses of hyaluronidase throughout the purification procedure. 4 μ l samples at each step were electrophoresed on 12.5% acrylamide gels and silver stained. Hyaluronidase migrated with an apparent molecular mass of 57 kDa in the post hydroxylapatite concentrate step.

Fig.2. Immunoprecipitation of hyaluronidase from human plasma with monoclonal antibodies. Serial dilutions of purified 17E9 anti plasma hyaluronidase IgG2a or corresponding amounts of mouse control IgG2a were combined with human plasma diluted with RIPA buffer followed by immunoprecipitation with Protein-A Sepharose beads. Supernates were then assayed using the microtiter based bHA assay as described. All detectable hyaluronidase activity from human plasma was immunoreactive with the monoclonal antibodies generated against the purified protein.

Fig.3. Alignment of plasma hyaluronidase to human PH-20. Identical amino acids are boxed, similar amino acids are shaded. Plasma hyaluronidase has 40% amino acid identity with human PH-20, a sperm-specific hyaluronidase.

Fig.4. HEK-293 cells stably transfected with coding cDNA secrete hyaluronidase activity not present in the parental line. Cells were transfected

with a CMV driven pCR3.1-Uni vector containing hyaluronidase gene from nucleotides X to Y. Cells from a hyaluronidase secreting G418-resistant HEK-293 clone and the parental cell line control were grown for 48 h in the absence of serum. Conditioned media and cell layer were harvested and assayed for hyaluronidase activity using the described microtiter assay. Error bars indicate the standard error of three samples.

Fig 5a. Immunoaffinity-purified recombinant hyaluronidase migrated with a relative molecular mass indistinguishable from biochemically purified plasma hyaluronidase. For comparison of specific activities, bovine testicular hyaluronidase, corresponding to an equal level of activity, was electrophoresed with plasma hyaluronidase and recombinant hyaluronidase.

Fig.5b. Substrate gel zymography of testicular, plasma and recombinant hyaluronidase. Samples were electrophoresed on a 10% SDS PAGE gel impregnated with 50 μ g/ml HA. After substituting SDS with Triton X-100, the gel was incubated in formate buffer, pH 3.7, overnight. The gel was then stained for HA with Alcian blue and counterstained with Coomassie blue R-250.

Fig.6. Secreted recombinant hyaluronidase in HEK-293 cells has the same pH activity profile as plasma hyaluronidase. Immunopurified plasma hyaluronidase, immunopurified recombinant hyaluronidase or bovine testicular

hyaluronidase were assayed in the microtiter assay from pH 3.0-8.0. Activity at given pH intervals were plotted as a percent of maximum activity.

Fig.7. A PCR organ survey of plasma hyaluronidase reveals transcripts in heart, kidney, liver, lung, placenta, and skeletal muscle, but not in brain. gt10 human cDNA organ libraries were analyzed for plasma hyaluronidase transcripts using a nested PCR reaction that amplified the same 1.3 kb open reading frame that was used for sequencing and expression.

Table 1. Purification Scheme For Human Plasma Hyaluronidase

Purification step	Volume (ml)	Activity (rTRU/ml)	Protein (mg/ml)	Specific Activity (rTRU/mg)	X-Fold purification
Starting material	2,100	5	86	0.058	1.0
Final detergent phase	650	4.71	1.3	3.62	63
SP-sepharose	60	42.5	0.85	50	875
Hydroxyapatite	1.0	1943	0.0225	86,355	1.5 x 10⁶

FIGURE-1

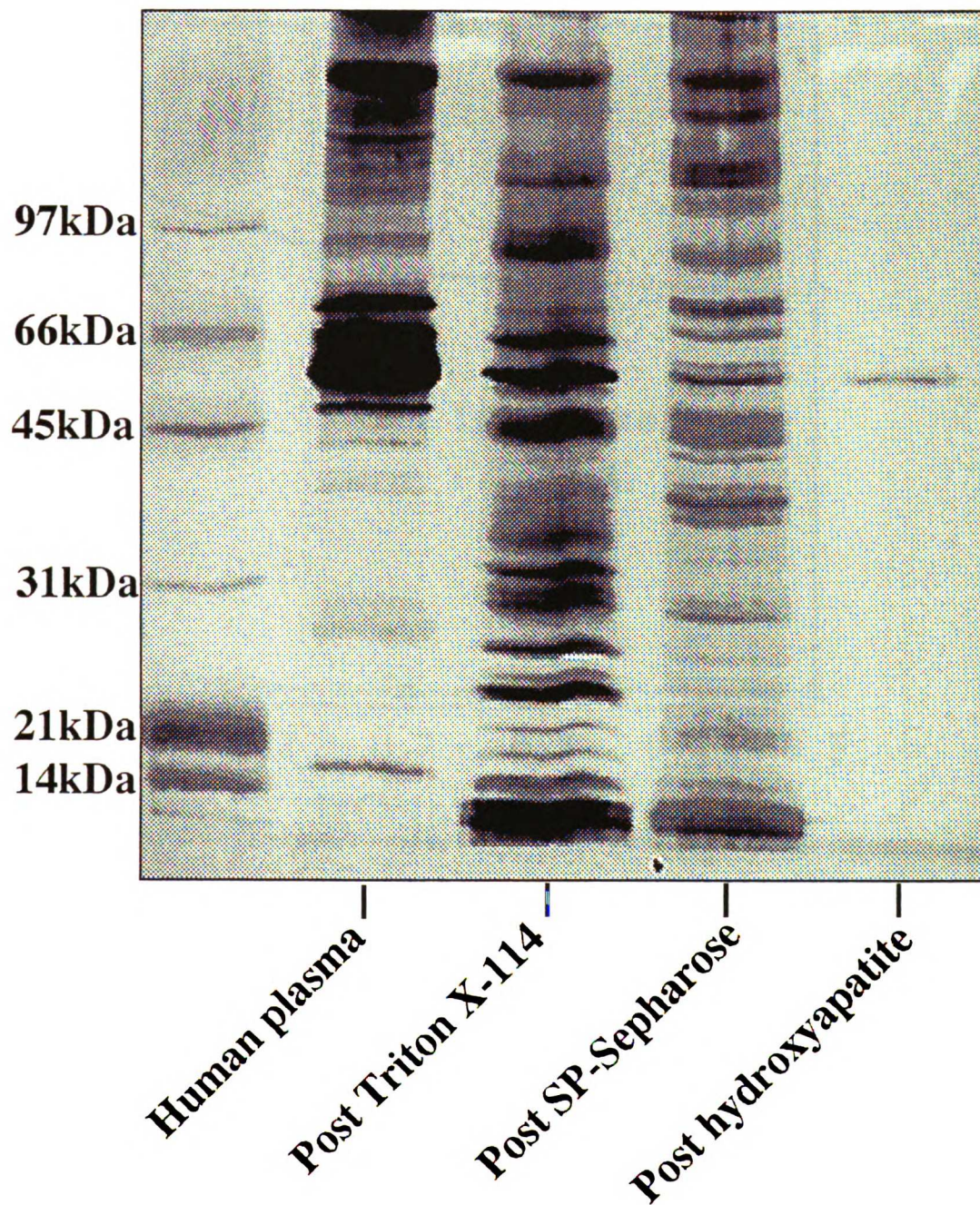


FIGURE-2

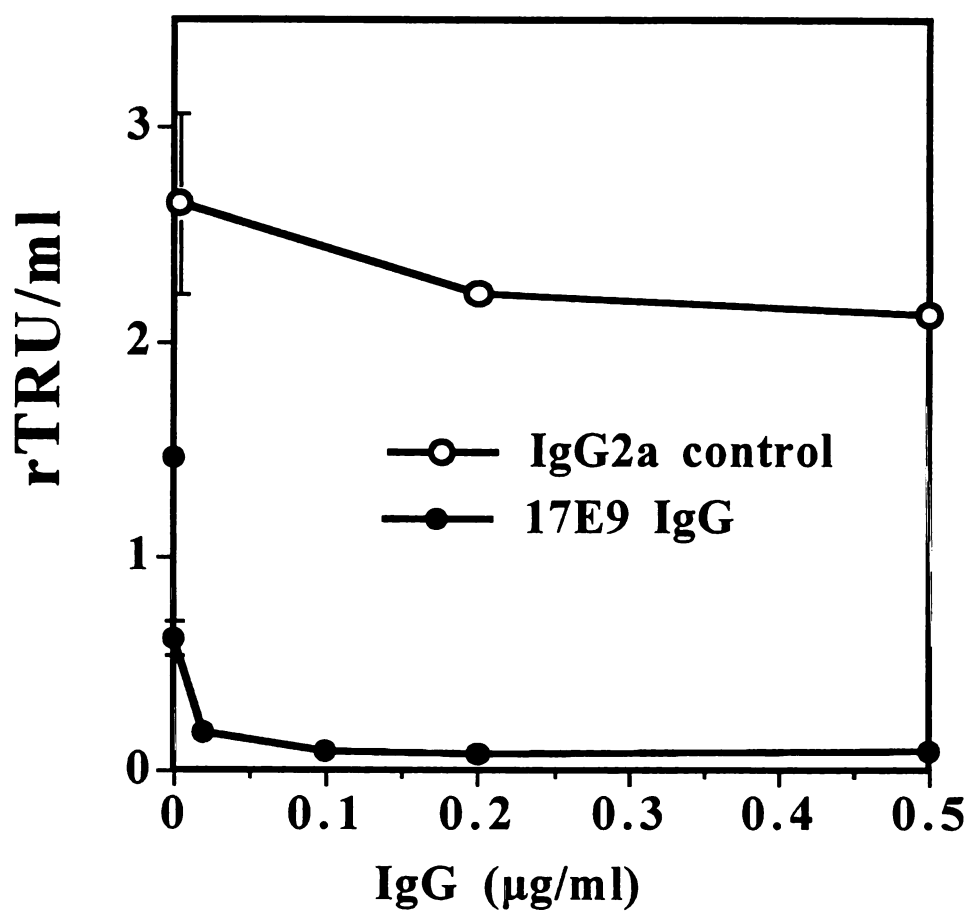


FIGURE-3

1
 Hyd-1 PH-20 Bee Ve no m
 1WA AH P I C I L F I L E D B A O G H G : P I L I N R P T V M N A N T O W S E R H G V D V : D V S T V I D V Y A N P G O T F
 1 M G V L K F K H F F R S F V K S S G V S O I F T F I L E P C C I L E N E B A P V I P N V A S W A N A P B E C L G X D E P L D M S L L E S F I G S P R I N A
 M S R P L V I T E G M I G V T E M L P I N A E L G F V O S . P D N N K T V R E A V V M N V P T C H X Y G R F E S Y S E K Y G I O W M D K E

2
 Hyd-1 PH-20 Bee Ve no m
 67 R G P O N I E V S S O G T V P Y T P I G E P V . F G G I P O N A S I A I I A R T F O D I E A A P A P D S S E L A V I D V E A W P R W A E A W D T I K O T V R C H S R A I N V O A
 84 P O G V I E N V D R E G Y P Y D S I . I G V T V . I G G I P O K I E D D I O K A K K D I T E Y A P V D H E G A V I D V E E W R P T W A R W M K P K O V M K P S E W O D
 7 9 I G E E I A I A D P G M P A L L K D P N G N V A R I G G V P O I G R I K I L O V F R D H I N O P D K S P S Y G V I D E S W R P P R O N W A S L O P M K A L S Y E V W R R

3
 Hyd-1 PH-20 Bee Ve no m
 158 O H P D M P A P Q V E A V A D O D O G G A R A M A G I E D E G R A E R P R G W I G E V G I P D C V N K D E L S A N M T G O G P S G I R A O N D T O S M L W Q Q S T A L V F S I M V P A V L
 175 O N V O L S L T E A T E K A K D E E K A K D I F C V E L P X L G K L R P A H L W G Y A P P D C V N H Y K K S G M N S O F N V E K R N D D S M L W N E S T A L V P S I M I N T . O
 172 # H P W D D O R M E D E A N F R E K Y S O L I M E T E K A A R I R P A A N W G Y A Y G V N I T P N Q E S A G G E A T T M D E N D K M S M E F E S E D V L P S N V L R W . K

4
 Hyd-1 PH-20 Bee Ve no m
 253 E G I S K S Q M V V C H R V A E A T R V A V A A G D P H E P V L P V Q I V I J T T N H I E P L D E L E H S G E S A A N O G A A G V E W M S M E N T A I K V S C O A L K E V I D I T I G I
 260 Q S P V A A T E A V R M V E A R V S K P D A K S P E P V A V R V E T D D V L K F L S O D E L V A I F G E V A L G A S G I W G F L S I M F S M K S C L L O H V M E T I N
 264 L T S S E R V G L V G G V K E A L R A T . Q M T T S R K K V L P Y W Y K V D R R D T D L S R A D I E A L E R K I T O L G A D G F W G S S D D I N U K A K C L O F R E V I N H E L G

Hyd-1 PH-20 Bee Ve no m
 346 P E I N V I S G A L C S O A C S G H S R O V R T S H P K A L E N P A S S O L T P G G S P L S L I G A L S I E D D A O M A V E K R C V F Q W O A P W C E R K S M W
 364 P A N V I E A K M C S O L C O E O S C E K N W N S S D Y I N P O N A O L E . K G G F X Y I G T P I E D . E O F S E K Y S S V S T L S O K E K A D V K D T D A
 368 P A N I A E N I N A N D R I V D V S D O V

Hyd-1 PH-20 Bee Ve no m
 455 V D V C I A D G V C I D A F L K P P M E T E E P Q

FIGURE-4

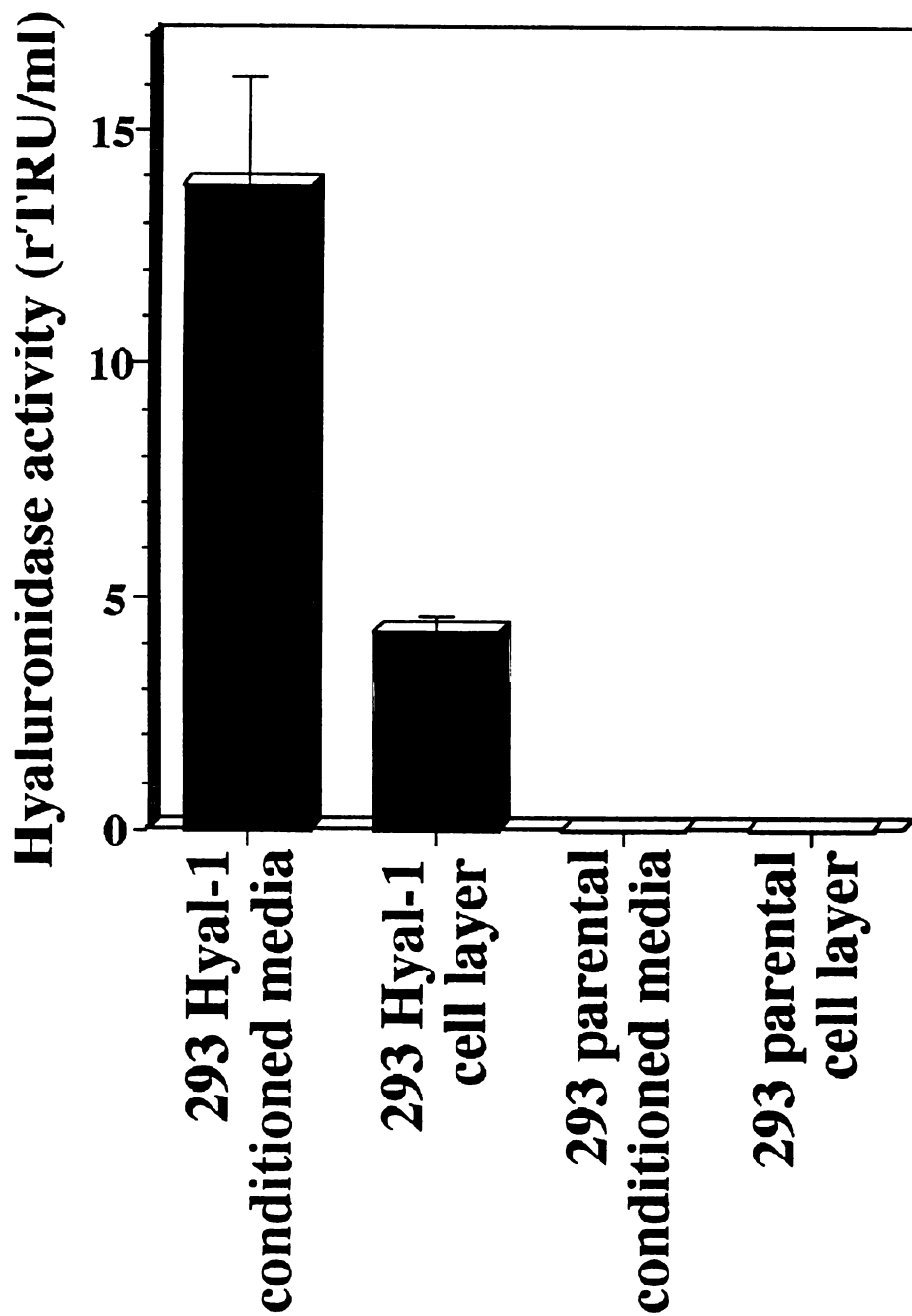


FIGURE 5

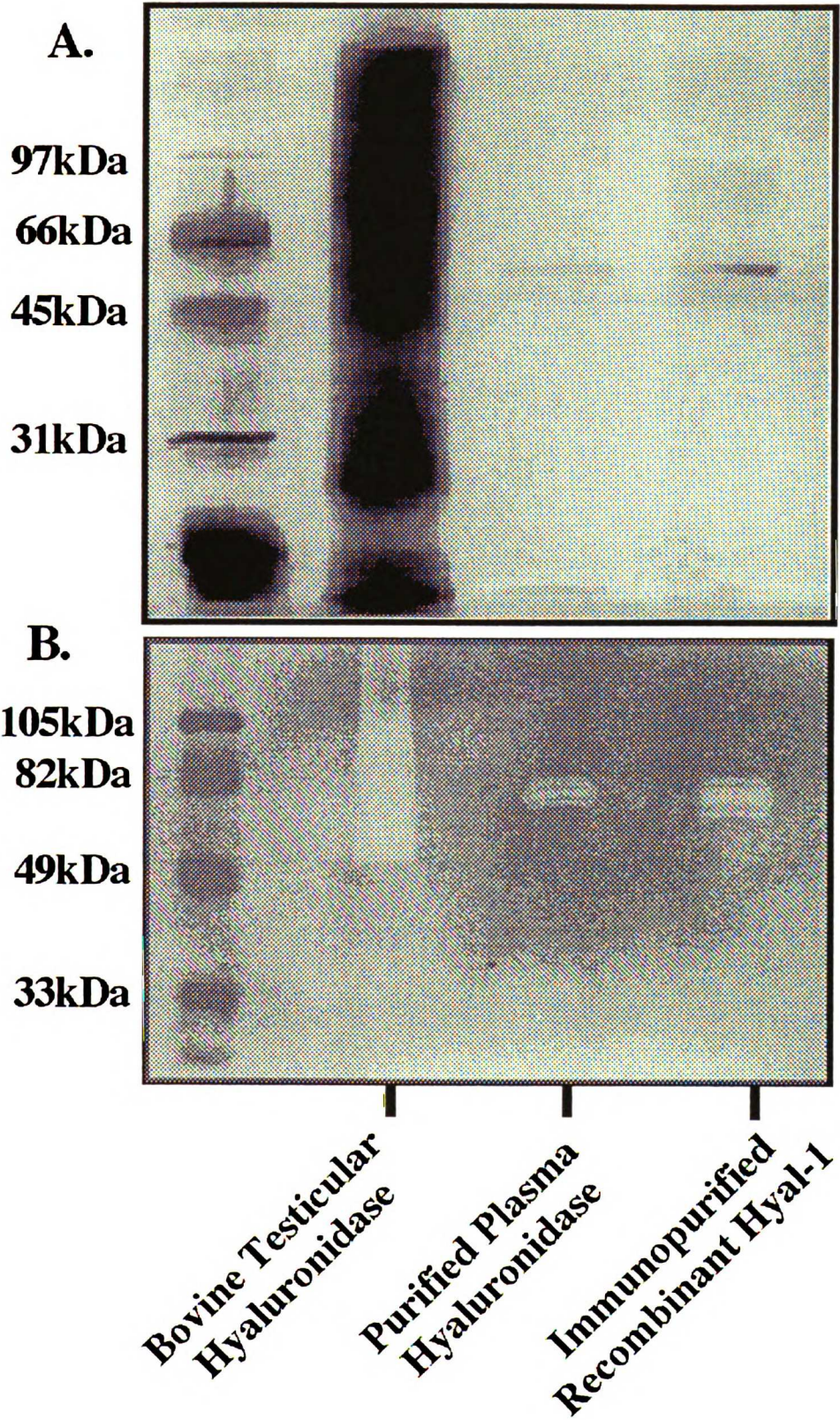


FIGURE-6

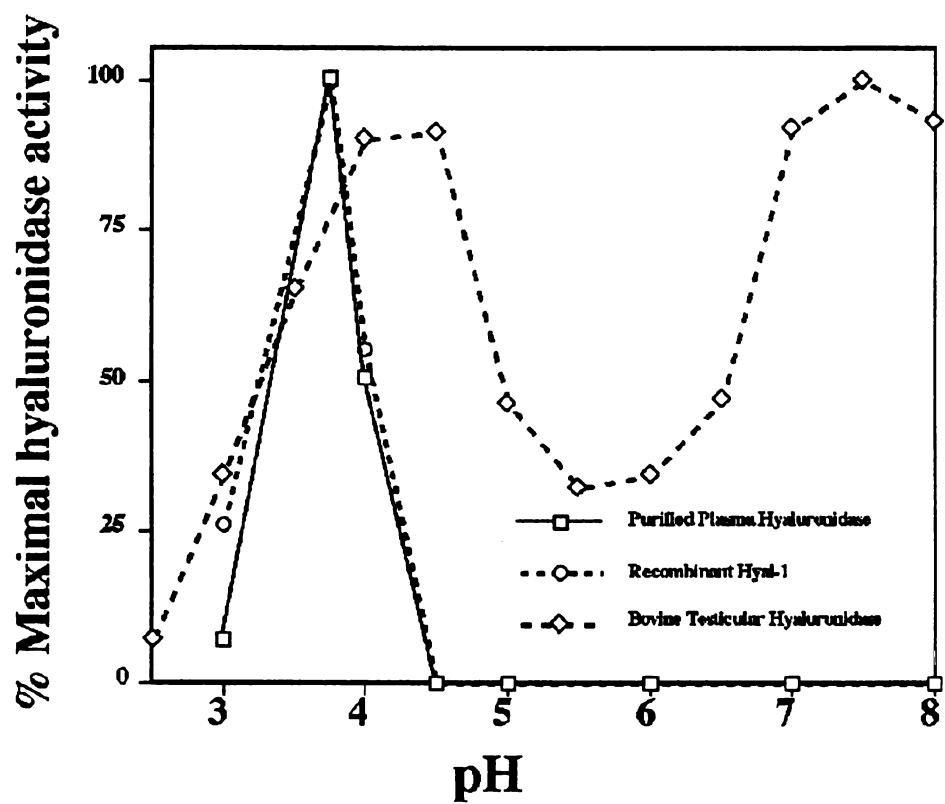
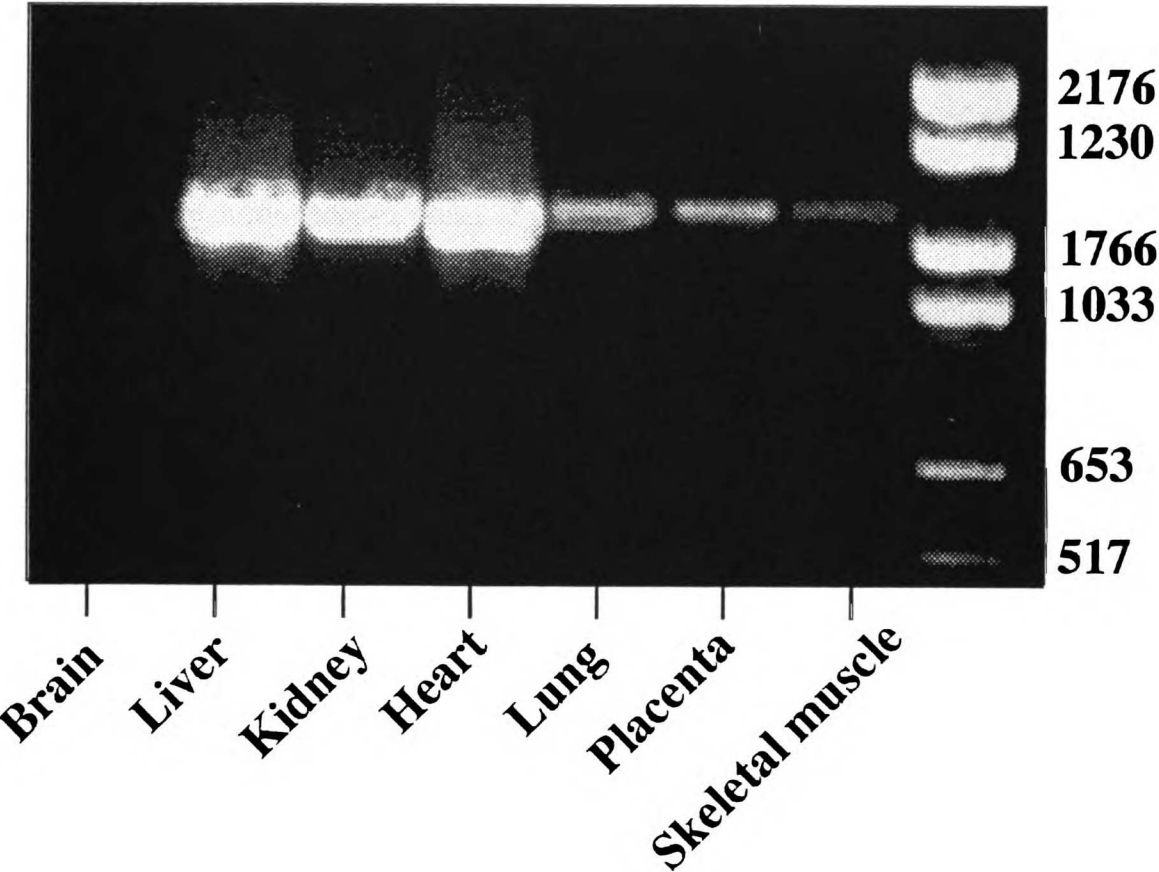


FIGURE-7



References

1. Laurent, T. C., Laurent, U. B., and Fraser, J. R. Functions of hyaluronan, *Ann Rheum Dis.* 54: 429-32, 1995.
2. Toole, B., Munaim, S., Welles, S., and Knudson, C. B. Hyaluronate-cell Interactions and growth factor regulation of hyaluronate synthesis during limb development. *In: Ciba Found. Symp.* pp. 138-149, 1989
3. Longaker, M. T., Chiu, E. S., Adzick, N. S., Stern, M., Harrison, M. R., and Stern, R. Studies in fetal wound healing. V. A prolonged presence of hyaluronic acid characterizes fetal wound fluid, *Ann Surg.* 213: 292-6, 1991.
4. Knudson, W. Tumor-associated hyaluronan. Providing an extracellular matrix that facilitates invasion [comment], *Am J Pathol.* 148: 1721-6, 1996.
5. Zhang, L., Underhill, C. B., and Chen, L. Hyaluronan on the surface of tumor cells is correlated with metastatic behavior, *Cancer Res.* 55: 428-33, 1995.
6. Kreil, G. Hyaluronidases--a group of neglected enzymes. *Protein Sci.*, 4: 1666-9, 1995.
7. Frost, G. I., Csoka, T., and Stern, R. Hyaluronidases: A Chemical, Biological and Clinical Overview, *Trends in Glycoscience and Glycotechnology.* 8: 407-421, 1996.
8. Primakoff, P., Hyatt, H., and Myles, D. G. A role for the migrating sperm surface antigen PH-20 in guinea pig sperm binding to the egg zona pellucida, *J Cell Biol.* 101: 2239-44, 1985.
9. Lin, Y., Mahan, K., Lathrop, W. F., Myles, D. G., and Primakoff, P. A hyaluronidase activity of the sperm plasma membrane protein PH-20 enables sperm to penetrate the cumulus cell layer surrounding the egg, *J Cell Biol.* 125: 1157-63, 1994.
10. Fiszer-Szafarz, B., Vannier, P., Litynska, A., Zou, L., Czartoryska, B., and Tytki-Szymanska, A. Hyaluronidase in human somatic tissues and urine: polymorphism and the activity in diseases, *Acta Biochim Pol.* 42: 31-3, 1995.
11. Komender, J., Malczewska, H., and Golaszewska, A. Isolation of hyaluronidase from kidney extract, *Bull Acad Pol Sci [Biol].* 21: 637-41, 1973.
12. Yamada, M., Hasegawa, E., and Kanamori, M. Purification of hyaluronidase from human placenta, *J Biochem (Tokyo).* 81: 485-94, 1977.
13. De Salegui, M. and Pigman, W. The existence of an acid-active hyaluronidase in serum, *Arch Biochem Biophys.* 120: 60-7, 1967.
14. Stern, M., and Stern, R. (1992) *Matrix* 12, 397-403.
15. Guntenhoner, M. W., Pogrel, M. A., and Stern, R. A substrate-gel assay for hyaluronidase activity, *Matrix.* 12: 388-96, 1992.
16. Ed Harlow, D. L. *Antibodies : a laboratory manual* Cold Spring

Harbor Laboratory, Cold Spring Harbor, NY. 1988

17. Harrison, R. A. Hyaluronidase in ram semen. Quantitative determination, and isolation of multiple forms, *Biochem J.* 252: 865-74, 1988.
18. Altschul SF; Gish W; Miller W; Myers EW; Lipman DJ. Basic local alignment search tool. *Journal of Molecular Biology*, 1990 Oct 5, 215(3):403-10.
19. Lennon G; Auffray C; Polymeropoulos M; Soares MB. The I.M.A.G.E. Consortium: an integrated molecular analysis of genomes and their expression. *Genomics*, 1996 Apr 1, 33(1):151-2.
20. Boguski MS; Lowe TM; Tolstoshev CM. dbEST--database for "expressed sequence tags". *Nature Genetics*, 1993 Aug, 4(4):332-3.
21. Frohman MA; Dush MK; Martin GR. Rapid production of full-length cDNAs from rare transcripts: amplification using a single gene-specific oligonucleotide primer. *Proc Natl Acad USA*, 1988 Dec, 85(23):8998-9002.

Chapter-4

**The Hyaluronidase Gene HYAL1 Maps To Chromosome
3p21.2-21.3 In Human And 9F1-F2 In Mouse, A
Conserved Candidate Tumor Suppressor Locus.**

Preface

My contribution to this work involved:

Transfection of murine Hyal1 into HEK-293 cells and the generation of Hyal1 overexpressing clones; biochemical characterization of recombinant mouse Hyal1 and comparison with human HYAL1 and bovine PH20.

My initial observation that the isoelectric point of human HYAL1 was identical to the predicted isoelectric point of LuCa-1 initiated my hypothesis to examine the inactivation of HYAL1 in head and neck squamous cell carcinomas.

The hyaluronidase gene HYAL1 maps to chromosome 3p21.2-21.3 in human and 9F1-F2 in mouse, a conserved candidate tumor suppressor locus.

Tony B. Csóka, Gregory I. Frost*, Henry H.Q. Heng*, Stephen W. Scherer*, Gayatri Mohapatra†, and Robert Stern*¹

Department of Gerontology, University Medical School of Debrecen, H-4012, Hungary, *Department of Pathology, School of Medicine, University of California, San Francisco, CA 94143, USA, †Department of Genetics, The Hospital For Sick Children, Toronto, Ontario, M5G1XB, Canada, and † Cancer Genetics Program, UCSF Cancer Center, University of California, San Francisco, CA 94115, USA.

Abstract

We recently cloned and expressed the major hyaluronidase activity from human plasma, HYAL1, and found that the protein is 40% identical to the testicular hyaluronidase, PH-20. The HYAL1 mRNA sequence was used in a homology search of the mouse database of Expressed Sequence Tags (dbEST). Two EST's were obtained, and in combination with 5'RACE-PCR, were used to clone the mouse HYAL1 ortholog (Hyal1). Hyal1 codes for a protein of 462 amino acids that is 73% identical to the human sequence. Hyal1 stably expressed in human embryonic kidney cells resulted in a 20,000-fold increase of hyaluronidase activity. Sequence-tagged sites derived from the HYAL1 gene from both species were used to isolate P1 genomic clones which were used as probes for fluorescence *in-situ* hybridization. The human gene was localized to chromosome 3p21 and the mouse gene to a syntenic region on chromosome 9F1-F2. In mouse, serum hyaluronidase polymorphism has previously been mapped by an interspecific backcross to 60 cM from the centromere of chromosome 9, which corresponds to a cytogenetic location of 9F1-F2. The

mouse Hyal1 gene is therefore very likely to be responsible for the hyaluronidase polymorphism linked to this locus. We also present evidence that human HYAL1 is identical to an uncharacterized gene positionally cloned by others from chromosome 3p21.3 that is homozygously deleted in several small cell lung carcinoma cell lines.

Introduction

Hyaluronic acid (HA), a high molecular weight glycosaminoglycan, is ubiquitously present in the extracellular space of higher animals (Laurent and Fraser, 1992). The biological roles of HA include maintenance of matrix structure and water balance, and also cellular functions such as control of cell proliferation, differentiation, and locomotion (Laurent and Fraser, 1992). The hyaluronidases, a group of enzymes that catabolize HA, are widely distributed in the animal kingdom, but until recently have defied characterization (Kreil, 1995 ; Frost *et al.*, 1997a). Mammalian hyaluronidases have been partially purified from sources such as liver (Gold, 1982), plasma (Cobbin and Dicker 1962), serum (Affify *et al.*, 1993), and urine (Dicker and Franklin, 1966).

Recently two genes encoding mammalian hyaluronidases have been cloned. The first, termed PH-20 (also known as SPAM-1), had earlier been detected with monoclonal antibodies (Primakoff *et al.*, 1985). PH-20 enables the sperm to penetrate a layer of HA-rich cumulus cells that surround the ovum. Using Northern blot analysis, the PH-20 mRNA could only be detected in testis (Lin *et al.*, 1993). It was assumed that PH-20 homologs do not exist in somatic tissues. However, recently we showed that human plasma hyaluronidase, which we termed HYAL1, is 40% identical to PH-20 at the amino acid level, and widely expressed in somatic tissues (Frost *et al.*, 1997b).

We identified two EST's in the mouse Expressed Sequence Tag database (dbEST) (Boguski *et al.*, 1993) that were highly homologous to the human sequence at the nucleotide level. In combination with 5'RACE-PCR, an

open reading frame was identified that codes for a protein with strong homology to human plasma hyaluronidase. Here we report full sequence of the gene, termed Hyal1, Northern expression analysis, and recombinant protein characterization. Sequence tagged sites derived from the hyaluronidase gene from both species were used to isolate P1 genomic clones that were used as probes to map the genes by fluorescence *in-situ* hybridization to metaphase chromosomes.

Materials and Methods.

Assays for hyaluronidase activity.

Hyaluronidase activity was measured using a classical colorimetric assay (Reissig *et al.*, 1955), a new microtiter-based assay (Frost and Stern, 1997) and HA substrate-gel zymography (Guntenhöner *et al.*, 1992). All of the assays were standardized to the Turbidity Reducing Unit (TRU) with commercial hyaluronidase (Sigma Type VI-S hyaluronidase) as a standard. One TRU of hyaluronidase is defined as the amount of enzyme that will decrease the turbidity-producing capacity of 0.2 mg HA to that of 0.1 mg HA in 30 minutes at 37°C (Tolksdorf *et al.*, 1949)

Sequencing and contig assembly.

All sequencing reactions were performed on double stranded DNA with the *Taq* dye deoxy terminator cycle sequencing kit (Applied Biosystems) according to the manufacturers instructions, and run on an ABI Prism™ automated sequencer (Applied Biosystems). The EST and 5'RACE sequences were assembled into a contig with the Sequencher™ program (Gene Codes corp.). The sequences of mouse and human HYAL1 have been deposited in GenBank (accession numbers: AF011567 and U96078 respectively).

Cloning and expression of human HYAL1.

The cloning and expression of HYAL1, and the production of anti-HYAL1 monoclonal antibodies, have been described previously (Frost *et al.*, 1997b).

Cloning of mouse Hyal1.

Two overlapping EST's (GenBank accession nos. AA072684 and AA444812) were obtained by a BLASTN (Altschul *et al.*, 1990) homology search of the mouse dbEST that were highly homologous to the human HYAL1 sequence. Both EST's were sequenced as described above. To obtain the 5' end of the Hyal1 cDNA, 5' RACE (Frohman *et al.*, 1988) was performed on a Marathon Ready™ Mouse Liver cDNA library (Clontech). The following primers were used: Hyal1RACE1 (5-TGTTAGAGCCTTGGAACTCTGCTCC-3') and the AP2 primer from Clontech. Reaction conditions were a 1 min. denaturation at 95°C, and a 2 min. annealing/extension at 71°C for 40 cycles. The product of this reaction was used as a template for a second PCR using AP2 and Hyal1RACE2 (5'-TGTTGGCAACCACATCGAAGACACTG-3') primers with conditions as before, for 10 cycles. The product, which was 350 nucleotides, was ligated into the pCR2.1 vector (Invitrogen), and sequenced.

Expression of recombinant Hyal1 in HEK-293 cells.

For generation of the Hyal1 cDNA coding sequence, PCR was performed with a mouse liver Marathon Ready™ cDNA library (Clontech) as template. Primers used were: Hyal1FE1 (5'-ACATGCTTGGGCTTACACAGC-3'), and Hyal1RE1 (5'-TGCAGCTAATCATCACATACCC-3') which amplify nucleotides 52 to 1455 of the cDNA. Reaction conditions were a 1 min. denaturation at 95°C, 1 min. annealing at 60°C, and a 2.5 min. extension at 72°C for 38 cycles, followed by a final 7 min. extension at 72°C. A "hot start" was used to increase specificity. The PCR product was cloned into the pCR3.1-Uni vector

(Invitrogen), transfected into HEK-293 cells using lipofectin (Gibco BRL), and single-cell colonies were selected by the limiting dilution method with 500 µg/ml Geneticin (Gibco BRL) according to the manufacturer's instructions. After 10 days, resistant colonies with high level expression were expanded for further analysis. Empty pCR3.1-Uni vector was used as a control.

Northern analysis of mouse Hyal1 expression.

The cDNA from EST AA072684 was subcloned from the pBluescript SK-vector (Stratagene) into the pCR3.1-Uni vector (Invitrogen) in reverse orientation using the primers subHyal1F (5'-GAGAATGAAGCCCTTCAGTCC-3') and Hyal1RE1 (see above). The vector was then linearized with *Eco* RI and an antisense RNA probe was labeled with [α^{32} P] dCTP as previously described (Melton *et al.*, 1984). A mouse multiple-tissue poly-A⁺ Northern blot (Clontech) was prehybridized according to the manufacturer's instructions and hybridized with 10 ml of 1x10⁶ cpm/ml of the probe at 65°C in 0.5% SDS, 6 x SSC, 2 x Denhardt's reagent, 0.1 mg/ml salmon sperm DNA, and 60% formamide for 12 hr. The filter was washed twice at 65°C in 1.0xSSC, 0.1% SDS for 20 min., twice at 65°C in 0.1xSSC + 0.1% SDS + 60% formamide for 30 min., and once at 80°C in 0.1xSSC + 0.1% SDS + 60% formamide for 30 min. The filter was then exposed to Kodak XOMAT AR film for 20 hr. After stripping by boiling in 0.1% SDS for 15 min. the filter was reprobbed with a human β -actin cDNA probe (Clontech) labelled with [α^{32} P] dCTP by random priming (Feinberg and Vogelstein, 1983). Following a 2 hr. prehybridization, 10 ml of 1x10⁶ cpm/ml probe was added at 42°C in 0.5% SDS, 6xSSPE, 5 x Denhardt's reagent, 0.1

mg/ml salmon sperm DNA, and 50% formamide for 18 hr. The filter was then washed three times in 1xSSC, 0.1% SDS at 45°C for 30 min., twice in 0.1xSSC and 0.1%SDS at 65°C, and then exposed to film for 6 hr.

PCR screening of a human P1 artificial chromosome (PAC) library.

PCR primers were designed that amplify a 192 bp fragment from the 3' untranslated region (UTR) of the HYAL1 mRNA: HYAL1STSF (5'-CATATTGAGAACCTAATGCACTCTG-3') and HYAL1STSR (5'-GGAATGAATGGTGTCTGCTGTGG-5'). The primers produced a single band from total human genomic DNA that was confirmed to be HYAL1 by sequencing. These primers were used to screen a complete human PAC library (Genome Systems). Reaction conditions were a denaturation at 95°C for 1 min., an annealing at 65°C for 1 min. and an extension at 72°C for 1 min. for 35 cycles.

PCR screening of a mouse P1 library.

PCR primers were designed that amplify a 186 bp fragment from the 5' region of the Hyal1 mRNA: Hyal1STSF (5'-TACTCTCTTCCTGACTTTGCTCGAG-3') and Hyal1STSR (5'-CATGTTAGAGCCTTGAAACTCTGC-3'). The primers produced a single band from total mouse genomic DNA that was confirmed to be Hyal1 by sequencing. These primers were used to screen a complete mouse P1 library (Genome Systems). Reaction conditions were a denaturation at 95°C for 1 min., an annealing at 63°C for 1 min. and an extension at 72°C for 1 min. for 35 cycles.

Homozygous deletion analysis of HYAL1 in lung carcinoma cell lines.

The human HYAL1 cDNA was found to be very homologous (identical size and greater than 99% nucleotide identity, including UTR's) to an uncharacterized gene positionally cloned by others from chromosome 3p21.3 called LuCa-1 (Wei *et al.*, 1996; GenBank acc. no. U03056). This gene has also been localized between STS markers D3S3582-D3S1578 by Radiation Hybrid mapping (Schuler *et al.*, 1996). In order to test the possibility that HYAL1 and LuCa-1 are identical, we examined the small cell carcinoma cell lines NCI-H740 and NCI-H524 that contain homozygous deletions of LuCa-1 (Wei *et al.*, 1996 ; Latif *et al.*, 1997), to see if HYAL1 could be amplified by genomic PCR. Four small cell carcinoma lines that do not have a homozygous deletion of 3p21.3 (NCI-H209, NCI-H1436, NCI-H1184, DMS-153) (Buchhagen, 1996) and human HS27 fibroblasts, were used as controls. Lung cancer lines were grown in RPMI, and the fibroblasts in DME H-21, using standard techniques. Genomic DNA was extracted from 1×10^7 cells with the QIAamp Tissue Kit (Qiagen Inc.). The PCR primers and conditions used were identical to those used for the P1 screen. Primers amplifying a 200 bp fragment of the 3' UTR of PH-20, which maps to chromosome 7q31 (Jones *et al.*, 1995), were used as controls: PH20STS_F (5'-GAGTTGTAAGGAGAAAGCTGAT-3') and PH20STS_R (5'-TCGCTACAGAAGAAATGATAAGAAACA-3') with annealing at 60°C.

Fluorescence *in-situ* hybridization.

Human. A PAC clone obtained from the PCR screen was biotinylated with dATP using the BRL BioNick labeling kit (Gibco) and used for FISH on synchronized human lymphocytes as previously described (Heng *et al.* , 1992 ; Heng and Tsui, 1993).

Mouse. P1 clones obtained from the PCR screen were labeled by nick translation (as above) with dig-11-dUTP. Clone 5734, that maps near the centromere of chromosome 9 (Shi *et al.*, 1997a), was labelled with biotin-11-dUTP by nick translation and used to confirm the mapping result. FISH was performed as described (Shi *et al.*, 1997a).

Results.

Cloning of mouse Hyal1.

The two EST's identified contained the 3' end of the Hyal1 gene as evidenced by the presence of a poly-A tail. EST AA072684 was longer than AA444812 by 478 nucleotides. The 5'RACE product was identical to EST AA072684 with the exception of an additional 88 nucleotides of upstream sequence. These sequences were assembled into a contig. The mouse Hyal1 cDNA was calculated to be 2125 nucleotides in length and contained an open reading frame of 1386 nucleotides with an AUG translation initiation codon at nucleotides 54-56 in good context for expression (Kozak, 1987). The protein is predicted to consist of 462 amino acids (Figure 1) with a calculated (unprocessed) molecular weight of 52 kDa and an isoelectric point of 6.1. Overall the mouse Hyal1 cDNA coding sequence was 80% identical to the human sequence. Amino acid identity to human HYAL1 is 73 % (Figure 1), with 45% identity to mouse PH-20 (not shown). The gene we have cloned is very likely to be the mouse ortholog of human HYAL1. The conceptual translation of the mouse protein suggests the presence of a hydrophobic signal sequence at the N-terminus. This signal sequence is 28 amino acids longer in mouse than in human, but the biological significance of this difference is unclear.

Expression of recombinant Hyal1 in HEK-293 cells.

The conditioned media of six clones stably transfected with the mouse Hyal1 cDNA, contained an average of 100 TRU/ml as determined by three independent assays of hyaluronidase activity (Reissig *et al.* 1955 ; Guntenhöner

et al., 1992 ; Frost and Stern, 1997). A commercial preparation of testicular hyaluronidase (Sigma, type VI-S) was used for comparison. Hyaluronidase activity in untransfected HEK-293 cells, and in controls transfected with empty vector, was 5 mTRU/ml. This represents a 20,000-fold increase in activity. The molecular weight of Hyal1 determined by substrate gel zymography (Guntenhöner *et al.*, 1992) was 70 kDa. The recombinant enzyme aligned precisely with the hyaluronidase of mouse serum (Figure 2). Since the predicted molecular weight of the protein is 52 kDa, this indicates that Hyal1 is post-translationally processed. Hyal1 has an optimum pH of 3.5–4.0 (Figure 3), which is identical to that of mouse and human plasma (Cobbin and Dicker, 1966; Fiszler-Szafarz *et al.*, 1990; Frost *et al.* 1997) and characteristic of lysosomal hyaluronidases. No activity was detected at neutral pH, unlike testicular hyaluronidase which is maximally active at pH 7.5 (Figure 3).

Northern analysis of mouse Hyal1 expression.

Mouse Hyal1 had a complex expression profile. Under high stringency conditions, transcripts were detected in most tissues with strongest expression in liver, kidney, and lung (Figure 4). This expression profile is similar to that obtained from human HYAL1 by RT-PCR (Frost *et al.*, 1997b). The strong Hyal1 signals in liver and kidney are in agreement with previous experiments that have indicated that these organs are the major sites of HA degradation (Roden *et al.*, 1989 ; Engstrom-Laurent and Hellstrom, 1990). No Hyal1 mRNA was detected in spleen, and very little in skeletal muscle. However, we could not conclude that Hyal1 is not expressed in spleen because the signal from the β -

actin cDNA control probe was very weak from this organ, indicating that the spleen mRNA on this blot was degraded. The major Hyal1 hybridization signals were at 7.5- and 3.8 kb, with a weaker signal at 2.1 kb. Since the Hyal1 cDNA is 2.1 kb, the larger transcripts may contain pre-spliced polyadenylated sequences. Also, there were some other tissue-specific transcripts such as a 1.4 kb signal in liver, and a 2.6 kb signal in testis. We have confirmed by nested RT-PCR and sequencing of EST's, that both human and mouse Hyal1 have numerous alternatively-spliced isoforms (Csoka *et al.*, manuscript in preparation). Some of these transcripts have untranscribed exons, or retained introns. For example human EST 650884 (GenBank acc. # AA223264) does not contain 486 bp of 5' UTR present in the HYAL1 gene, which might imply the existence of a second promoter site, and EST49651 (GenBank acc. # AA343666) has a large deletion of 1389 bp of central coding sequence, which would theoretically produce a much smaller protein.

PCR screening of a human P1 artificial chromosome (PAC) library.

A single PAC was obtained that was confirmed to contain the genomic sequence of HYAL1 by partial sequencing and long-range PCR (data not shown).

PCR screening of a mouse P1 library.

Four P1 clones were obtained, which were shown to be overlapping by restriction fingerprint mapping with *Eco* R1 and *Hind* III endonucleases, and to

contain the genomic sequence of Hyal1 by partial sequencing and long-range PCR (data not shown).

Fluorescence in-situ hybridization

Human: Among 100 checked mitotic figures, all showed specific signals on one pair of chromosomes. DAPI banding (Figure 5B), (Heng and Tsui, 1993), was used to assign the signal to the short arm of chromosome 3. The detailed position was determined based on the summary from 10 different metaphases (Figure 5A). No additional loci were detected with the conditions used. HYAL1 was therefore assigned to chromosome 3p21.2-21.3 (figure 7).

Mouse: The initial FISH experiment with the four P1 clones resulted in specific labeling of what was believed to be chromosome 9 on the basis of DAPI banding pattern (Figure 6B). A second experiment was conducted in which a biotin-labeled P1 probe (clone 5734, known to map near the centromere of chromosome 9), was co-hybridized separately with all four Hyal1 P1 clones. This resulted in a specific signal in red near the centromere for clone 5734, and in green near the distal long arm of chromosome 9 for the Hyal1 clones (Figure 6A). All four Hyal1 clones mapped to the same location, which was determined as 9F1-F2 (Figure 7) based on the summary from 20 different metaphases.

Homozygous deletion analysis of lung carcinoma cell lines.

The HYAL1 primers failed to amplify the expected 192 bp fragment in the NCI-H740 and NCI-H524 small cell lung carcinoma cell lines, but did amplify the fragment in all the control lines (Figure 8A). The H740 and H524 lines both have homozygous deletions that contain an uncharacterized gene called LuCa-

1 that is highly similar to HYAL1. The deletion in the H740 line covers approximately 1 megabase (Wei *et al.*, 1996), but the deletion in H524 is much smaller, covering only 30 kb (Latif *et al.*, 1997). Because the HYAL1 primers did not amplify in either of these cell lines, this strongly suggests that HYAL1 is identical to LuCa-1. This result also demonstrates that HYAL1 is a single copy gene in the human genome. The PH-20 control primers produced the expected band of 200 bp in all seven cell lines. (Figure 8B)

Discussion.

Humans and mice carry a circulating lysosomal-like hyaluronidase activity in their serum (De Salegui and Pigman, 1967 ; Fiszer-Szafarz *et al.*, 1990 ; Afify *et al.*, 1993). Recently we purified and cloned the major hyaluronidase activity in human plasma and found the enzyme to be 40% identical in amino acid sequence to PH-20 (Frost *et al.*, 1997b). We have now cloned the mouse ortholog of human plasma hyaluronidase and determined the chromosomal location of the gene in human and mouse. The gene maps to chromosome 3p21 in human and a syntenic region (Nadeau, 1986 ; Imai, 1997) on chromosome 9F1-F2 in mouse. Both of these regions have been described as candidate tumor suppressor regions (Kok *et al.*, 1987 ; Killary *et al.*, 1992 ; Dietrich *et al.*, 1994 ; Shi *et al.*, 1997b).

In mouse, segregation analysis by an interspecific backcross of BALB/c x C57BL/6 strains has shown that serum hyaluronidase level polymorphism is linked to a single locus on chromosome 9, which was designated *Hyal-1* (Fiszer-Szafarz and De Maeyer, 1989). This locus was subsequently refined to 60 cM from the centromere of chromosome 9 (De Maeyer-Guignard *et al.*, 1991), which corresponds to a cytogenetic location of 9F1-F2 (Imai, 1997). Therefore the mouse *Hyal1* gene we have cloned is very likely to be the gene responsible for the hyaluronidase polymorphism mapped to this locus. Congenic mouse strains differing only at the *Hyal-1* locus have been used to investigate the effect of serum hyaluronidase levels on transplanted tumor growth (De Maeyer and De Maeyer-Guignard, 1992). Mice with the allele

producing higher levels of circulating hyaluronidase have greater resistance to tumor growth than mice possessing alleles that produce lower levels of hyaluronidase (De Maeyer and De Maeyer-Guignard, 1992). The proposed mechanism for this effect is that removal of the pericellular coats of HA that surround tumor cells by hyaluronidase renders the tumor more accessible to cytolytic cells (McBride and Bard, 1979 ; Dick *et al.*, 1983). HA is frequently present in elevated amounts around tumor cells, and it is presumed to facilitate tumor-cell migration and proliferation (Knudson *et al.*, 1989 ; Zhang *et al.*, 1995 ; Knudson, 1996). There is evidence for a direct relationship between levels of HA and malignancy and invasiveness. This was first noted by Ozzello (Ozello *et al.*, 1959), who observed the growth-promoting effect of glycosaminoglycans on mammary carcinomas. Subsequently Toole and coworkers observed that the HA content of invasive V2 rabbit carcinoma was 3 to 4 times greater than that of the same tumor when grown under non-invasive conditions (Toole *et al.*, 1979).

Intravenous injection of hyaluronidase has been shown to decrease the carcinogenic activity of dimethylbenzanthracene in BALB/c mice (Pawlowski *et al.*, 1979). Also, significant aberrations in the localization of hyaluronidase have been reported in various carcinomas (Fischer-Szafarz and Gullino, 1969 ; Fischer-Szafarz and Szafarz, 1973), and human serum hyaluronidase levels drop markedly in neoplasia (Wilkinson *et al.*, 1996). However, since mutations or other aberrations in *HYAL1*^(LuCa-1) have not yet been reported in small cell or other carcinomas, the evidence that hyaluronidase may be involved in

suppression of tumor growth is indirect. Furthermore, the experiments of Fiszler-Szafarz and others may only indicate linkage disequilibrium between an allele producing elevated levels of hyaluronidase, and another closely-linked gene that has tumor suppressor function. There are several other candidate genes at this locus (Wei *et al.*, 1996), and we are currently investigating these possibilities.

Figure Legends

Figure 1.

Alignment of the amino acid sequences of the conceptual translations of human and mouse plasma hyaluronidase reveals 73% identity. Identical amino acids are boxed and similar amino acids are shaded. The mouse hyaluronidase differs from the human enzyme by having an additional 28 amino acids at the N-terminal signal sequence. The alignment was generated using the ClustalW 6.1 program.

Figure 2.

Analysis of the molecular weight of native and recombinant mouse hyaluronidase by substrate gel zymography. Hyaluronidase activity is visualized as a clearing against a darker background. Both the native and recombinant hyaluronidase migrate with a molecular weight of approximately 70 kDa. A commercial preparation of testicular hyaluronidase (Sigma, type VI-S) contains two hyaluronidase isozymes of 70 kDa and 55 kDa. Prestained molecular weight markers (Bio-Rad broad range) are shown on the left.

Figure 3.

Comparison of the pH optima of recombinant Hyal1, mouse plasma, and testicular hyaluronidase. Recombinant Hyal1 from the conditioned media of a positive HEK-293 clone, mouse plasma, and a commercial preparation of testicular hyaluronidase (Sigma, type VI-S, 500 TRU/ml) were diluted 1:40 in

0.1M citrate-phosphate buffer at the indicated pH and assayed for hyaluronidase activity. Recombinant Hyal1 and mouse plasma have maximum activity at pH 3.5-4.0, with no activity above pH 5.0. Testicular hyaluronidase has maximum activity at pH 7.5.

Figure 4.

Northern analysis of mouse Hyal1 expression. Strongest expression was detected in liver, kidney, and lung, in which hybridization signals at 7.5-, 3.8-, and 2.1 kb can be seen. Tissue-specific signals were also detected. A northern blot of the same filter with a β -actin probe was used to control for loading of mRNA. Molecular weight markers are shown on the left in kilobases. (Sk. muscle = Skeletal muscle).

Figure 5.

FISH of the human HYAL1 PAC to metaphase chromosomes. The right image (B) shows the DAPI stain used for identification and the left image (A) shows the location of the orange hybridization signal from the PAC, which was shown by the DAPI banding to be hybridized to chromosome 3p21.2-21.3. The identity of the chromosome is shown, and the location of the PAC signal is indicated by the arrow.

Figure 6.

FISH of the mouse Hyal11 P1's to metaphase chromosomes. The right image (B) shows the DAPI stain in gray scale used for identification and the left image (A) shows the locations of FITC and Texas Red hybridization signals. The P1 clones (green) map to 9F1-F2, and clone 5734, which maps near the centromere of chromosome 9 is shown in red on a blue background representing the DAPI staining. The identity of the chromosome is shown, and the locations of the two P1 signals are indicated by the arrows.

Figure 7.

Idiograms of the results shown in Figures 5 and 6. Based on ten metaphase spreads, the human HYAL1 gene was shown to localize to chromosome 3p21.2-21.3, indicated by the solid bar to the right of the chromosome. Based on twenty metaphase spreads, the mouse Hyal1 gene was shown to localize to a syntenic region on chromosome 9F1-F2, indicated by the solid bar to the left of the chromosome. The images are not to scale.

Figure 8.

A. PCR primers specific for HYAL1 (see text) were used to investigate the possibility that HYAL1 is identical to an uncharacterized gene at 3p21.3 called LuCa-1. The HYAL1 primers failed to amplify the 192 bp fragment of HYAL1 in cell lines NCI H-524 and NCI H-740. Since these cell lines have a homozygous deletion at 3p21.3 (see text), this result suggests that HYAL1 and LuCa-1 are likely to be identical. **B.** Primers amplifying a fragment of PH-20, which is on

chromosome 7q31, worked in all cell lines, demonstrating the integrity of the DNA. Boehringer Mannheim molecular weight markers VI are shown on the left.

FIGURE-1

Human 1 -----
 Mouse 1 MLQLTQNAQGVWWRKSRFSFVVRPQESDAT-----P-CA-----A-OF-----P-SP-----

Human 33 T-----N-----R-----K-----Y-----P-----L-----S-----D-----G-----E-----R-----G-----R-----
 Mouse 61 I-----D-----H-----T-----E-----Y-----S-----D-----V-----S-----V-----L-----A-----A-----K-----H-----H-----C-----S-----H-----E-----L-----R-----E-----R-----E-----

Human 93 F-----Q-----G-----H-----A-----L-----A-----T-----D-----L-----L-----R-----K-----I-----A-----D-----E-----S-----C-----L-----A-----V-----E-----N-----S-----A-----N-----K-----W-----A-----D-----D-----E-----D-----I-----E-----R-----E-----
 Mouse 121 R-----D-----E-----D-----D-----S-----L-----T-----E-----A-----T-----F-----D-----I-----K-----A-----K-----N-----E-----I-----P-----S-----C-----L-----A-----V-----E-----N-----S-----W-----L-----R-----W-----A-----P-----H-----M-----K-----L-----I-----R-----K-----E-----

Human 153 A-----V-----S-----Q-----H-----O-----K-----A-----P-----Q-----V-----R-----Y-----D-----D-----D-----P-----C-----A-----R-----K-----H-----N-----T-----E-----C-----G-----H-----A-----R-----R-----I-----R-----C-----L-----M-----C-----Y-----C-----F-----L-----C-----Y-----T-----E-----L-----
 Mouse 181 H-----V-----G-----H-----I-----D-----D-----V-----H-----I-----T-----L-----P-----A-----K-----H-----S-----P-----O-----R-----A-----N-----A-----N-----N-----A-----T-----H-----O-----R-----G-----V-----H-----P-----D-----L-----W-----Y-----P-----F-----I-----Y-----N-----D-----

Human 213 D-----P-----V-----D-----C-----E-----C-----L-----A-----N-----D-----L-----C-----D-----L-----C-----H-----R-----E-----K-----S-----E-----Q-----T-----I-----N-----Y-----E-----S-----O-----S-----O-----N-----Y-----V-----K-----K-----A-----B-----P-----L-----
 Mouse 241 L-----N-----Y-----A-----G-----S-----V-----T-----D-----D-----D-----D-----L-----G-----A-----L-----M-----T-----H-----Y-----S-----L-----E-----L-----E-----A-----A-----M-----E-----E-----R-----C-----K-----Y-----G-----R-----H-----U-----O-----L-----S-----

Human 273 K-----A-----A-----G-----M-----E-----E-----L-----P-----C-----L-----P-----E-----K-----N-----K-----F-----R-----I-----Q-----C-----E-----R-----S-----G-----D-----A-----C-----A-----A-----V-----V-----L-----K-----W-----E-----N-----H-----E-----I-----K-----E-----
 Mouse 301 K-----E-----V-----E-----K-----W-----Y-----D-----U-----N-----Y-----V-----O-----L-----V-----K-----M-----D-----Y-----L-----N-----I-----L-----P-----E-----Y-----N-----E-----R-----G-----C-----A-----A-----Q-----V-----A-----V-----M-----L-----C-----S-----K-----K-----S-----T-----F-----E-----

Human 333 Q-----A-----I-----E-----C-----D-----G-----P-----A-----V-----L-----P-----L-----A-----I-----C-----Q-----A-----C-----G-----H-----C-----H-----T-----H-----K-----L-----L-----L-----D-----F-----A-----L-----G-----H-----L-----
 Mouse 361 C-----E-----K-----A-----L-----I-----E-----P-----C-----I-----N-----T-----F-----A-----L-----L-----C-----N-----A-----N-----E-----R-----R-----V-----P-----T-----H-----E-----S-----A-----I-----T-----L-----K-----D-----A-----L-----G-----H-----

Human 393 P-----C-----L-----L-----H-----K-----A-----S-----L-----E-----Q-----A-----M-----L-----K-----S-----R-----P-----I-----N-----Q-----Y-----P-----K-----K-----S-----W-----
 Mouse 421 H-----D-----R-----P-----H-----E-----P-----L-----E-----N-----E-----R-----L-----C-----M-----A-----K-----L-----K-----S-----R-----H-----R-----S-----R-----N-----G-----O-----

FIGURE-2

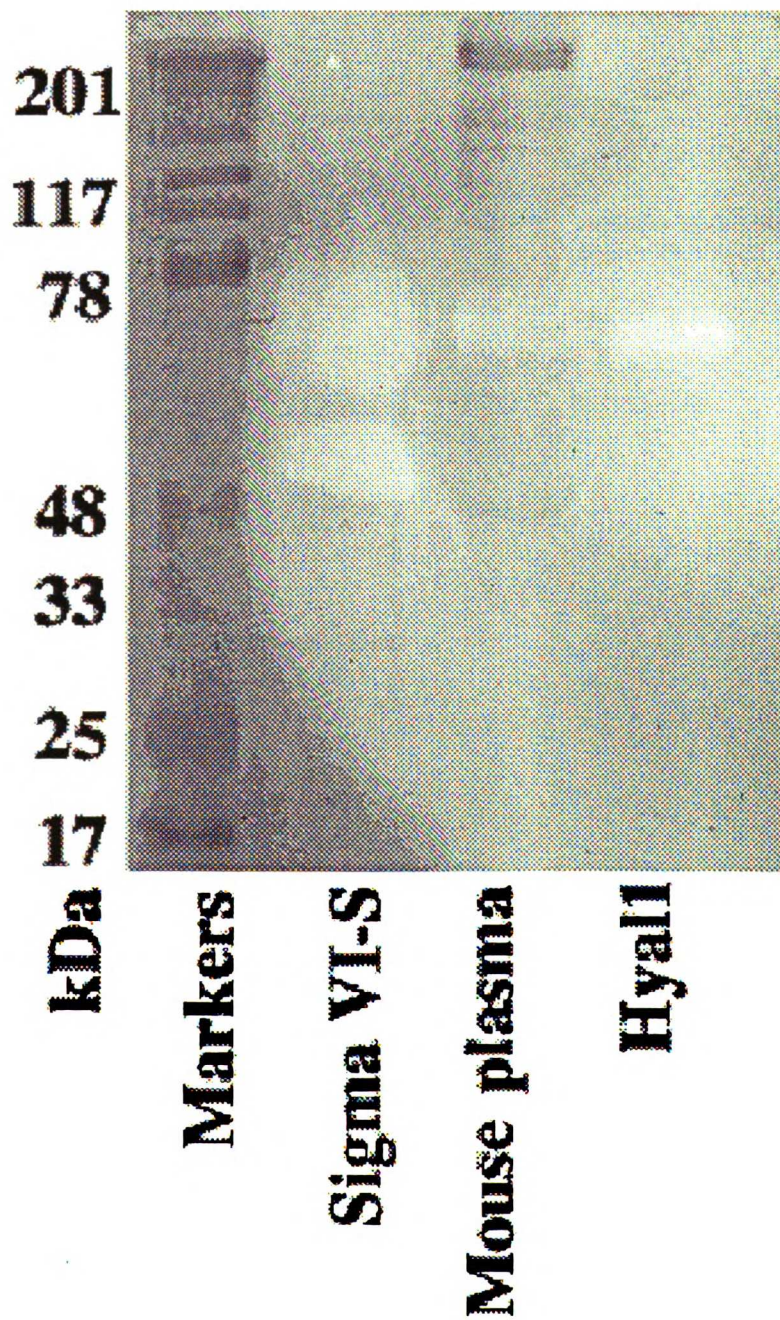


FIGURE-3

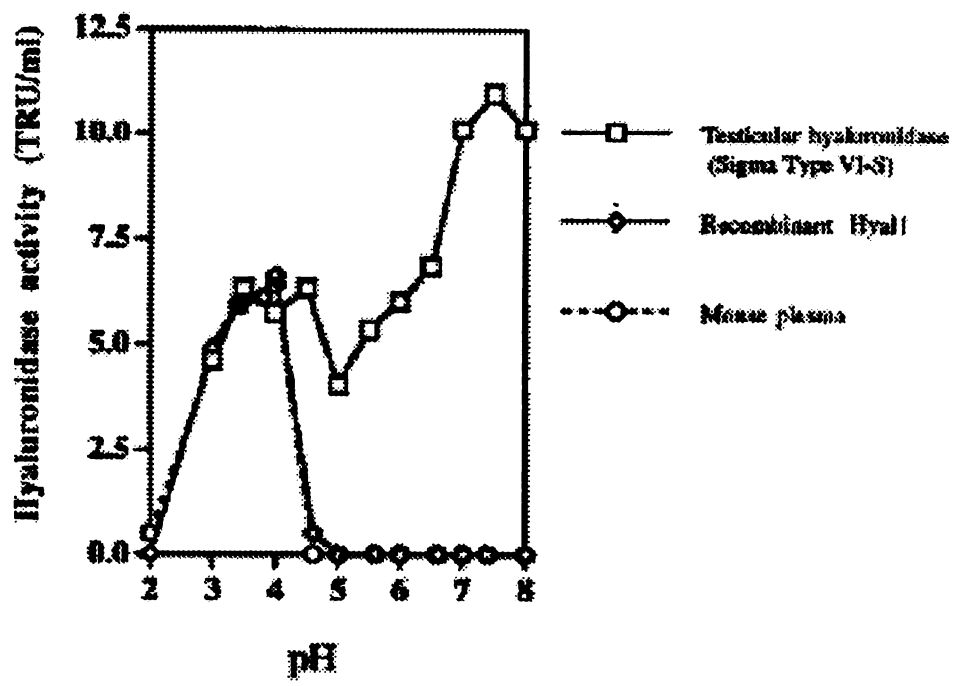


FIGURE-4

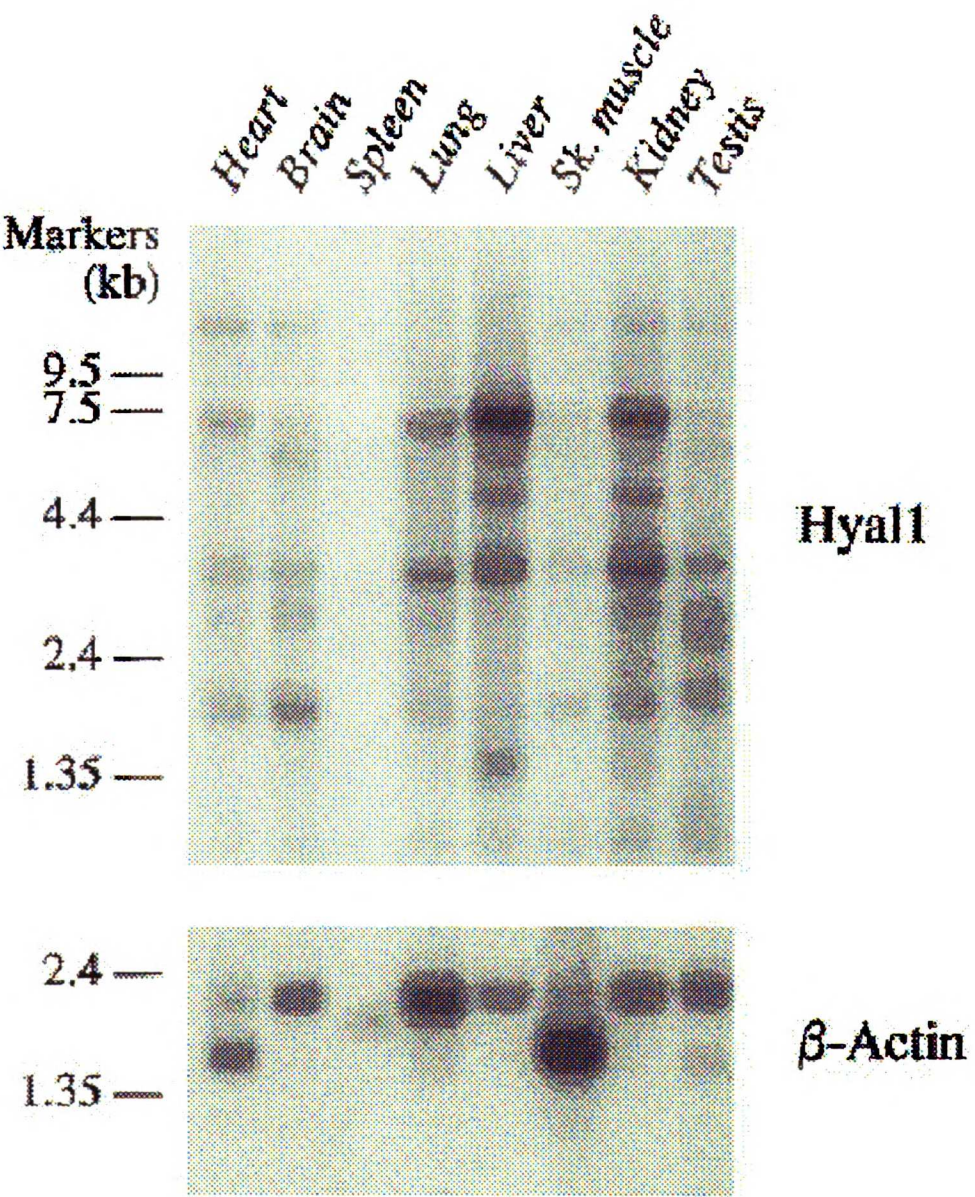


FIGURE-5

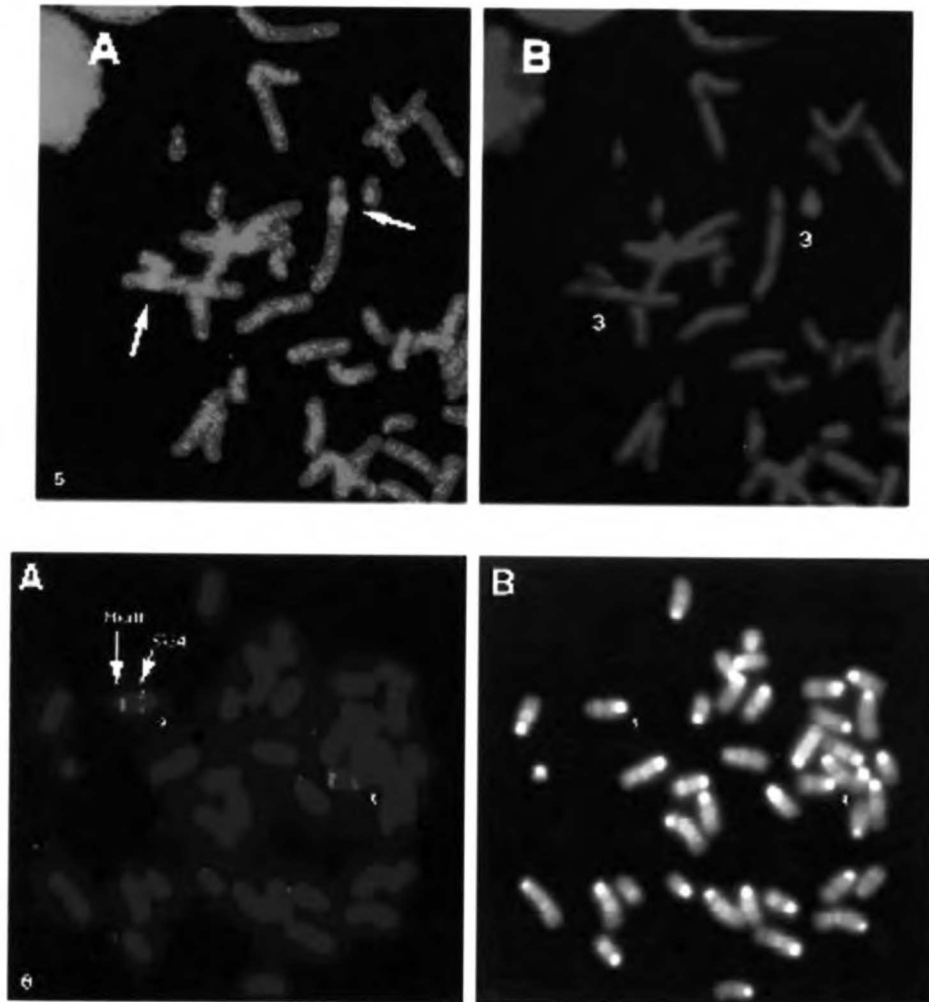


FIGURE-6

Human Chromosome 3



Mouse Chromosome 9

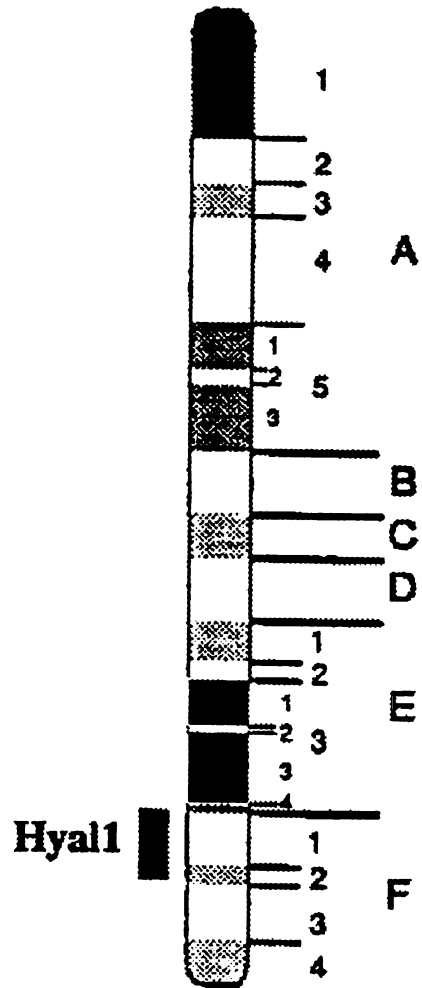
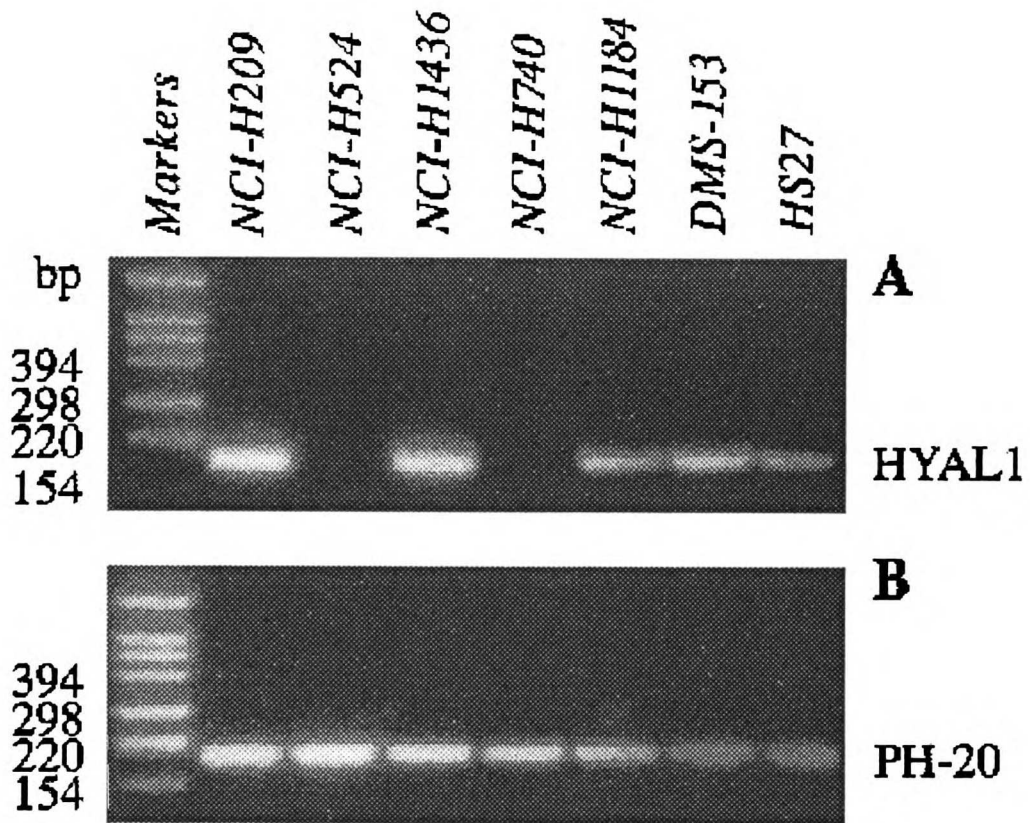


FIGURE-7



References

- Afify AM, Stern M, Guntenhoner M, Stern R. (1993) Purification and characterization of human serum hyaluronidase. *Arch Biochem Biophys* **305**: 434-441.
- Altschul SF, Gish W, Miller W, Myers EW, Lipman DJ. (1990) Basic local alignment search tool. *J. Mol. Biol.* **215**: 403-410.
- Boguski MS, Lowe TM, Tolstoshev CM. (1993) dbEST - database for "expressed sequence tags". *Nature Genet.* **4**: 332-333.
- Buchhagen DL. (1996) Frequent involvement of chromosome 3p alterations in lung carcinogenesis: allelotypes of 215 established cell lines at six chromosome 3p loci. *J Cell Biochem.* **24**: S198-S209.
- Cobbin LB, Dicker SE. (1966) Some characteristics of plasma and urine hyaluronidase. *J. Physiol. (London)* **163**: 110-120.
- De Maeyer-Guignard J, Cachard-Thomas A, De Maeyer E. (1991) Linkage analysis of the murine *Hyal-1* locus on chromosome 9. *Exp. Zool.* **258**: 246-248.
- De Maeyer E, De Maeyer-Guignard J. (1992) The growth rate of two transplantable murine tumors, 3LL lung carcinoma and B16F10 melanoma, is influenced by *Hyal-1*, a locus determining hyaluronidase levels and polymorphism. *Int. J. Cancer* **19**: 657-660.
- De Saegui M, Pigman W. (1967) The existence of an acid-active hyaluronidase in serum. *Arch. Biochem. Biophys.* **120**: 60-67.
- Dick SJ, Macchi B, Papazoglou S, Oldfield EH, Kornblith PL, Smith BH, Gately MK. (1983) Lymphoid cell-glioma cell interaction enhances cell coat production by human gliomas: novel suppressor mechanism. *Science* **220**: 739-742.
- Dicker SE, Franklin CS. (1966) The isolation of hyaluronic acid and chondroitin sulfate from kidneys and their reaction with urinary hyaluronidase. *J. Physiol. (London)*. **186**: 110-120.
- Dietrich WF, Radany EH, Smith JS, Bishop JM, Hanahan D, Lander ES. (1994) Genome-wide search for loss of heterozygosity in transgenic mouse tumors reveals candidate tumor suppressor genes on chromosomes 9 and 16. *Proc. Nat. Acad. Sci. USA* **27**: 9451-9455.
- Engstrom-Laurent A, Hellstrom S. (1990) The role of liver and kidneys in the removal of circulating hyaluronan. An experimental study in the rat. *Connect. Tissue. Res.* **24**: 219-224.
- Feinberg AP; Vogelstein B. (1983) A technique for radiolabeling DNA restriction endonuclease fragments to high specific activity. *Anal Biochem.* **132**: 6-13.
- Fischer-Szafarz B, Gullino PM. (1970) Hyaluronidase activity of normal and neoplastic interstitial fluid. *Proc. Soc. Exp. Biol. Med.* **133**: 805-807.
- Fischer-Szafarz B, Szafarz D. (1973) Lysozomal hyaluronidase activity in normal rat liver and in chemically induced hepatomas. *Cancer Res.* **33**: 1104-1108.

- Fischer-Szafarz B, De Maeyer E. (1989) *Hyal-1*, a locus determining serum hyaluronidase polymorphism, on chromosome 9 in mice. *Somat. Cell. Mol. Genet.* **15**: 79-83.
- Fischer-Szafarz B, Szafarz D, Vannier P. (1990) Polymorphism of hyaluronidase in serum from man, various mouse strains, and other vertebrate species revealed by electrophoresis. *Biol. Cell.* **68**: 95-100.
- Frohman MA, Dush MK, Martin GR. (1988) Rapid production of full-length cDNAs from rare transcripts: amplification using a single gene-specific oligonucleotide primer. *Proc. Nat. Acad. Sci. USA* **85**: 8998-9002.
- Frost GI, Csóka TB, Stern R. (1997a) The hyaluronidases: a chemical, biological, and clinical overview. *Trends Glycosci. Glycotech.* **8**: 419-434.
- Frost GI, Csóka TB, Wong T, Stern R. (1997b) Purification, cloning, and expression of human plasma hyaluronidase. *Biochem. Biophys. Res. Commun.* **236**: 10-15.
- Frost G.I., Stern R. (1997) A microtiter based assay for hyaluronidase activity not requiring specialized reagents. *Anal. Biochem.* **251**: 263-269.
- Gold EW. (1982) Purification and properties of hyaluronidase from human liver. Differences from and similarities to the testicular enzyme. *Biochem. J.* **205**: 69-74.
- Guntenhöner MW, Pogrel MA, Stern R. (1992) A substrate-gel assay for hyaluronidase activity. *Matrix* **12**: 388-396.
- Heng HH, Tsui LC. (1993) Modes of DAPI banding and simultaneous *in-situ* hybridization. *Chromosoma* **102**: 325-332.
- Heng HH, Squire J, Tsui LC. (1992) High-resolution mapping of mammalian genes by *in-situ* hybridization to free chromatin *Proc. Nat. Acad. Sci. USA* **89**: 9509-9513.
- Imai K. (1997) Mouse chromosome 9. *Mamm. Genome* **7**: S159-S175.
- Jones MH, Davey PM, Aplin H, Affara NA. (1995) Expression analysis, genomic structure, and mapping to 7q31 of the human sperm adhesion molecule gene SPAM1. *Genomics* **29**: 796-800.
- Killary AM, Wolf ME, Giambernardi TA, Naylor SL. (1992) Definition of a tumor suppressor locus within human chromosome 3p21-p22. *Proc. Nat. Acad. Sci. USA* **15**: 10877-10881.
- Kozak M. (1987) An analysis of 5'-noncoding sequences from 699 vertebrate messenger RNAs. *Nucleic Acids Res.* **15**: 8125-8148.
- Knudson W, Biswas C, Li XQ, Nemecek RE, Toole BP. (1989) The role and regulation of tumor-associated hyaluronan. *Ciba Found. Symp.* **143**: 150-159.
- Knudson W. (1996) Tumor-associated hyaluronan. Providing an extracellular matrix that facilitates invasion. *Am. J. Pathol.* **148**: 1721-1726.
- Kok K, Osinga J, Carritt B, Davis MB, van der Hout AH, van der Veen AY, Landsvater RM, de Leij LF, Berendsen HH, Postmus PE, *et al.* (1987) Deletion of a DNA sequence at the chromosomal region 3p21 in all major types of lung cancer. *Nature* **330**: 578-581.

- Kreil G. (1995) Hyaluronidases - a group of neglected enzymes. *Protein Sci.* **4**: 1666-1669.
- Latif F, Duh FM, Bader S, Sekido Y, Li H, Geil L, Zbar B, Minna JD, Lerman MI. (1997) The human homolog of the rodent immediate early response genes, PC4 and TIS7, resides in the lung cancer tumor suppressor gene region on chromosome 3p21. *Hum. Genet.* **99**: 334-341.
- Laurent TC, Fraser JR. (1992) Hyaluronan. *FASEB J.* **6**: 2397-2404.
- Lin Y, Kimmel LH, Myles DG, Primakoff P. (1993) Molecular cloning of the human and monkey sperm surface protein PH-20. *Proc. Nat. Acad. Sci. USA* **90**: 10071-10075.
- McBride WH, Bard JB. (1979) Hyaluronidase-sensitive halos around adherent cells. Their role in blocking lymphocyte-mediated cytotoxicity. *J. Exp. Med.* **149**: 507-515.
- Melton DA, Krieg PA, Rebagliati MR, Maniatis T, Zinn K, Green MR. (1984) Efficient in vitro synthesis of biologically active RNA and RNA hybridization probes from plasmids containing a bacteriophage SP6 promoter. *Nucleic Acids Res.* **12**: 7035-7056.
- Nadeau JH. (1986) A chromosomal segment conserved since divergence of lineages leading to man and mouse: the gene order of aminoacylase-1, transferrin, and beta-galactosidase on mouse chromosome 9. *Genet. Res.* **48**: 175-178.
- Ozzello L, Lasfargues, EY, Murray MR. (1959) Growth-promoting activity of acid mucopolysaccharides on a strain of human mammary carcinoma cells. *Cancer Res.* **20**: 600-604.
- Pawlowski A, Haberman HF, Menon IA. (1979) The effects of hyaluronidase upon tumor formation in BALB/c mice painted with 7,12-dimethylbenz(a)anthracene. *Int. J. Cancer*: **23**: 105-109.
- Primakoff P, Hyatt H, Myles DG. (1985) A role for the migrating sperm surface antigen PH-20 in guinea pig sperm binding to the egg zona pellucida. *Cell. Biol.* **101**: 2239-2244.
- Reissig JL, Strominger JL, Leloir LF. (1955) A modified colorimetric method for the estimation of N-acetyl amino sugars. *J. Biol. Chem.* **217**: 959-966.
- Roden L, Campbell P, Fraser JR, Laurent TC, Pertoft H, Thompson JN. (1989) Enzymic pathways of hyaluronan catabolism. *Ciba Found. Symp.* **143**: 60-76.
- Shi YP, Mohapatra G, Miller J, Hanahan D, Lander ES, Gold P, Pinkel D, Gray JW. (1997a) FISH probes for mouse chromosome identification. *Genomics* **45**: 42-47
- Shi YP, Naik P, Dietrich WF, Gray JW, Hanahan D, Pinkel D. (1997b) DNA copy number changes associated with characteristic LOH in islet cell carcinomas of transgenic mice. *Genes Chromosomes Cancer* **19**: 104-111.
- Schuler GD, Boguski MS, Stewart EA, Stein LD, Gyapay G, Rice K, White RE, Rodriguez-Tome P, Aggarwal A, Bajorek E, Bentolila S, Birren BB, Butler A, Castle AB, Chiannilkulchai N, Chu A, Clee C, Cowles S, Day PJ, Dibling T, Drouot N, Dunham I, Duprat S, East C, Hudson TJ, et al. (1996) A gene map of the human genome. *Science* **274**: 540-546.

- Tolksdorf S, McCready MH, McCullagh DR, Schwenck E, Bloomfield NJ. (1949) The turbidimetric assay of hyaluronidase. *J. Lab. Clin. Med.* **34**: 74-89.
- Toole BP, Biswas C, Gross J. (1979) Hyaluronate and invasiveness of the rabbit V2 carcinoma *Proc. Nat. Acad. Sci. USA* **76**: 6299-6303.
- Wei MH, Latif F, Bader S, Kashuba V, Chen JY, Duh FM, Sekido Y, Lee CC, Geil L, Kuzmin I, Zabarovsky E, Klein G, Zbar B, Minna JD, Lerman MI. (1996) Construction of a 600-kilobase cosmid clone contig and generation of a transcriptional map surrounding the lung cancer tumor suppressor gene (TSG) locus on human chromosome 3p21.3: progress toward the isolation of a lung cancer TSG. *Cancer Res.* **56**: 1487-1492.
- Wilkinson CR, Bower LM, Warren C. (1996) The relationship between hyaluronidase activity and hyaluronic acid concentration in sera from normal controls and from patients with disseminated neoplasm. *Clin. Chim. Acta.* **256**: 165-173.
- Zhang L, Underhill CB, Chen L. (1995) Hyaluronan on the surface of tumor cells is correlated with metastatic behavior. *Cancer Res.* **55**: 428-433.

Chapter-5

HYAL1^{LuCa-1}, A Candidate Tumor Suppressor Gene on Chromosome 3p21.3, Is Inactivated In Head And Neck Squamous Cell Carcinomas Through Incomplete Pre-mRNA Splicing

Preface

My contributions to this work have included: culturing and preparation of HNSCC cell extracts and neonatal foreskin keratinocyte explant cultures; analysis of HYAL1 enzyme activity in HNSCC extracts and normal keratinocytes; generation of RNA, genomic DNA, and cDNA libraries; preparation of monoclonal and rabbit polyclonal antibodies to recombinant HYAL1; RT-PCR analysis of the full length and 5' UTR of HYAL1; sequencing of HYAL1 cDNA and genomic DNA from normal and HNSCC lines; transfection and generation of ecdysone-inducible subclones of the HSC-3 line. This work tested my hypothesis as to whether the inactivation of HYAL1 had a molecular-genetic basis in head and neck squamous cell carcinomas.

Major contributors to this work were:

Gayatry Mohapatra and Joe W Gray (Cancer Genetics Program, UCSF Cancer Center, University of California, San Francisco) for the comparative genomic hybridization analysis and fluorescence *in situ* hybridization analysis on HNSCC lines and normal keratinocytes

Tim M. Wong (Department of Pathology, University of California, San Francisco) examined anti-HYAL1 immunoprecipitates of HNSCC and keratinocyte extracts by substrate gel and western blot analysis.

Tony B. Csóka (Department of Pathology, University of California, San Francisco) generated the human 3p21.3 PAC probe, the HYAL1 cDNA probe, and constructed the ecdysone-inducible construct

Abstract

HYAL1 is a glycosaminoglycan-degrading enzyme expressed in many somatic tissues. The HYAL1 gene (also known as LuCa-1) maps to human chromosome 3p21.3 within a candidate tumor suppressor gene locus defined by homozygous deletions and functional tumor suppressor activity. Hemizyosity in this region of 3p21.3 occurs in many malignancies, including head and neck squamous cell carcinomas (HNSCC). We investigated whether HNSCC lines still expressed functional HYAL1 compared to normal keratinocyte controls. HYAL1 enzyme activity and protein were absent or markedly reduced in six of the seven lines examined. Comparative genomic and fluorescence *in situ* hybridization analysis identified chromosomal deletions of one allele of HYAL1 in six of the seven cell lines. Initial RT-PCR based analysis showed clear discrepancies between HYAL1 mRNA levels and protein, yet no mutations were found. Surprisingly, analysis of the HYAL1 5' untranslated region identified two species of transcripts. The predominant mRNA species did not correlate with protein translation and retained an apparent intron within the 5'-UTR. A second spliced form of HYAL1 lacking this intron was found only in cell lines producing HYAL1

protein and activity. We therefore suggest that the inactivation of HYAL1 in HNSCC lines is a result of incomplete splicing and is epigenetic in nature.

Introduction

The discovery of many tumor suppressor genes (TSG's) has been facilitated by the identification of either homozygous chromosomal deletions or hemizyosity at a particular locus, with functionally inactivating point mutations in the remaining allele. It is now recognized that alternative pathways, such as hypermethylation of CpG islands can also silence tumor suppressor genes in the process of carcinogenesis (1,²). Nevertheless, functionally inactivating point mutations are generally viewed as the critical "smoking gun" when defining a novel TSG.

We recently mapped the HYAL1 gene to human chromosome 3p21.3 (3), confirming its identity with LuCa-1, a candidate tumor suppressor gene frequently deleted in small cell lung carcinomas (SCLC) (4). The HYAL1 gene resides within a commonly deleted region of 3p21.3 where a potentially informative 30kb homozygous deletion has been found in one SCLC line (5). The position of HYAL1 within this 30kb homozygous deletion and the larger overlapping homozygous deletions in the NCI H740 and GLC20 SCLC lines leaves this gene a strong candidate TSG. A recent study identified a 220kb homozygous deletion on 3p21.3 in a breast carcinoma line (6). The telomeric breakpoint resides

approximately 4kb centromeric to the HYAL1 open reading frame, and overlaps with the centromeric region of the SCLC deletions. In addition to the chromosomal aberrations, the region encompassing 3p21.3 has functional tumor suppressor activity *in vivo* as determined by monochromosome mediated transfer in a nasopharyngeal carcinoma line (7). Despite the frequency of homozygous deletions on 3p21.3 in various carcinomas, no mutations have been reported with high frequency in any of the candidate genes examined to date. Hemizyosity over the candidate TSG locus on 3p21.3 has also been reported in head and neck squamous cell carcinomas (HNSCC's) (8). As normal keratinocytes produce HYAL1, the analysis of HYAL1 in head and neck malignancies was a rational approach to further characterize this candidate TSG on 3p21.3.

Mammalian hyaluronidases are family of β , 1-4 endoglucosaminidases that degrade hyaluronan and chondroitin sulfates (9,10). Until recently, mammalian hyaluronidases were uncharacterized enzymatic activities present in many tissues, characterized only on the basis of the enzyme pH optima for activity. Humans are now known to possess at least four hyaluronidases, PH-20, HYAL2, MGEA5 and HYAL1. PH-20 is GPI-anchored hyaluronidase located on chromosome 7q31 that is normally restricted in expression to testes (11). HYAL2

is a recently identified lysosomal hyaluronidase (12) that resides immediately centromeric to HYAL1 on 3p21.3. HYAL2 possesses an apparent specificity for high molecular weight hyaluronan (>20kDa) and is expressed in all tissues except the brain. MGEA5 is a hyaluronidase-like protein structurally unrelated to the PH20 family that was identified as a novel immunogenic antigen expressed in meningioma (13). HYAL1 is a secreted somatic tissue hyaluronidase, and the predominant hyaluronidase found in human plasma (14). Transcripts for HYAL1 are also found in most tissues. Paradoxically, although HYAL1 is predominantly secreted, it displays an acid pH dependence for activity, at least *in vitro*. HYAL1 was considered a candidate tumor suppressor gene in small cell lung carcinomas based upon homozygous deletion studies (15). Our study was designed to examine specifically whether HYAL1 could be directly involved with the large chromosomal aberrations on 3p21.3 that are found in HNSCC.

Results

HYAL1 enzyme activity and protein are absent in most cultured HNSCC lines-

We compared levels of HYAL1 in normal primary human keratinocyte cultures with a panel of seven head and neck squamous cell carcinoma lines derived from primary tumors (SCC-9, SCC-10a, SCC-15, SCC-25) and lymph node metastasis (SCC-10b, HOC-313, HSC-3). HYAL1 enzyme activity was measured by immunoprecipitation with the 17E9 anti-HYAL1 monoclonal antibody and detected by substrate-gel zymography and a microtiter-based assay using biotinylated hyaluronan. Substrate-gel zymography of anti-HYAL1 immunoprecipitates from serum-free cultured SCC lines and normal human foreskin keratinocytes revealed that only one laryngeal carcinoma line, SCC-10a expressed hyaluronidase levels comparable to normal keratinocyte controls (Fig.1). All other cell lines either showed drastically reduced or lacked any detectable activity by both HA-substrate gel zymography and by the microtiter-based enzyme assay (Fig.2). In contrast to the SCC10a line, the SCC-10b line, which was derived from a lymph node metastasis from the same patient as the SCC-10a at a later point in disease, showed no detectable activity in either assay. The microtiter-based assay used was sensitive enough to accurately

detect at least 1/100th the activity found in the SCC-10a line. Substrate gel zymography of the cell layer immunoprecipitates from normal keratinocytes and the SCC-10a line possessed an additional ~45kDa lower molecular weight isoform of HYAL1 which appeared similar to a proteolytically processed form of HYAL1 found in human urine (16). As no hyaluronidase activity could be found in the 17E9-supernates, changes in the 17E9 reactive epitope on HYAL1 in the deficient cell lines would appear unlikely.

Immunoblotting of the 17E9-immunoprecipitates from conditioned media and cell layers with polyclonal antibodies against HYAL1 were also examined (Fig.-3). HYAL1 protein levels were in agreement with the enzyme assays. HYAL1 protein was seen only in the SCC10a line and in normal keratinocyte cultures. These results would make postranslational inactivation or the presence of an inhibitor unlikely for the absence of enzymatic activity in the majority of cell lines.

RT-PCR analysis of HYAL1 reveals discrepancies between mRNA and protein-

To our surprise, RT-PCR analysis of HYAL1 transcripts from 482-2278 bp showed that all cells, with the exception of the HOC-313 cell line, produced

mRNA transcripts for HYAL1 (Fig.4). Although the HOC-313 line showed no detectable mRNA with 40 cycles of RT-PCR, extended cycles did reveal a weak transcript of the correct size (data not shown). Levels of β -actin from all cell-lines showed no appreciable differences within the cDNA library preparations.

Comparative Genomic Hybridization (CGH) And Fluorescence In Situ Hybridization (FISH) analysis of HNSCC cell lines-

The apparent discrepancy between HYAL1 protein levels and mRNA transcripts lead to an examination of the HYAL1 gene on chromosome 3p21.3 in these HNSCC lines. We assessed the status of the HYAL1 gene by FISH using a 100kb genomic PAC probe and compared this to the entire chromosome 3 by CGH. Representative FISH images from each cell line (200 nuclei scored) and CGH revealed a loss of 3p21 and one copy of HYAL1 in the SCC-9, SCC-10a, SCC-15, SCC-25, SCC-10b and HSC-3 relative to the chromosome 3 centromeric probe. The HNSCC lines were generally tetraploid with respect to the centromeric chromosome 3 probe and several other centromeric chromosome markers, but showed varying losses of 3p21.3 from ratios of 4/2 to 4/1 (chromosome-3/.3p21.3). Interestingly, the HOC-313 cell line possessed

equal ratios of centromeric 3p to HYAL1 by both FISH analysis and CGH. The HOC-313 line was diploid in DNA content. Surprisingly, this was the only cell line that did not show mRNA, protein or activity for HYAL1. The SCC-10a line on the other hand, expressed high levels of HYAL1 mRNA, protein and enzyme activity, but displayed a clear loss of HYAL1 by FISH and CGH. This would exclude hemizyosity at 3p21.3 as sufficient to inactivate HYAL1 in these cell lines, and would rule out imprinting of this particular gene on 3p21.3.

The HSC-3 HNSCC line is capable of synthesizing functional HYAL1 under an inducible promoter-

Given the discrepancies between HYAL1 mRNA levels and protein, we wished to investigate whether the HNSCC lines were capable of producing functional HYAL1 under an inducible promoter. We therefore subcloned the HYAL1 open reading frame into an ecdysone inducible vector (HYAL1 pIND) and cotransfected it with the pVgRXR vector into the HSC-3 HNSCC line. As shown in Fig.6, one of the HSC-3 subclones examined was fully capable of expressing HYAL1 activity and protein in an inducible fashion in response to muristerone. The majority of the activity and protein was recovered in the conditioned media.

As the HSC-3 line showed chromosomal aberrations surrounding the HYAL1 gene and produced endogenous transcript for HYAL1 without activity, we postulated that mutations could be responsible for the loss of immunoreactive protein.

Sequencing of the full length cDNA fails to identify mutations in the open reading frame

In light of the apparent discrepancy between mRNA levels and protein, we sequenced the HYAL1 RT-PCR products from NFK's, SCC-9, SCC-10a, SCC-15, SCC-25, SCC-10b and HSC-3 from bp 482-2278. Sequencing of these RT-PCR products failed to produce any mutations or polymorphisms that could explain our findings.

RT-PCR analysis of the 5' untranslated region of HYAL1 reveals a novel spliced form that correlates with enzyme and protein levels-

We noted that the 5' UTR of HYAL1 was unusually long (611bp). In addition, the 5' UTR contained eight methionines, placing the assumed HYAL1 open reading frame in poor context for expression assuming the ATG at 611bp

as the initiation codon. An expressed sequence tag for HYAL1 from neuroepithelial cells (AA223264) was found in the EST database that skipped 103-585bp, suggesting that this portion of the 5' UTR might be a retained intron. The previous primers would not have amplified this spliced form, as the forward primer was within this potential intron. Primers were therefore designed that amplified the HYAL1 5'UTR from 15 to 606bp. RT-PCR based analysis identified a shortened 109bp product in the keratinocytes and the SCC-10a line in addition to the expected 591bp product. Sequencing of the two PCR products from the keratinocyte 5' UTR showed that the splicing occurred between bp's (103) to (585). This spliced form of HYAL1 correlated very well with the protein and enzyme activity levels found in Figure-1 and Figure-3. There was a mixture of these two forms in normal keratinocytes and the SCC-10a line, whereas all other lines except the HOC-313 showed predominantly transcripts containing the 5' UTR with the retained intron. Northern blots from normal human tissues also identified 1.9 and 2.5kb transcripts that correlated with the spliced and unspliced 5' untranslated region of HYAL1 (Fig-8). We therefore concluded that these two forms naturally occur *in vivo* but that only the spliced form produces the functional enzyme protein.

Sequencing of HYAL1 genomic DNA fails to demonstrate mutations in introns or exons-

Sequencing of the full length genomic DNA from all eight cell lines failed to identify any mutations within the intron/exon boundaries that could explain the failure of the majority of HNSCC lines to splice out the retained intron within the 5' UTR. The HOC-313 line, which showed neither transcript by RT-PCR also lacked any detectable mutations.

Summary of HYAL1 in HNSCC lines-

A summary of the analysis of HYAL1 in HNSCC is given in Table-1. Only normal keratinocytes and the SCC-10a line produced comparable levels of enzyme activity, protein, and the spliced form of HYAL1 transcript. The SCC-9, SCC-15, SCC-25, SCC-10b, and HSC-3 lines showed very weak or absent levels of the spliced form of HYAL1, but levels of the unspliced form were at levels comparable to that found in the cells producing functional protein. The HOC-313 lines, however, produced neither transcript at levels detectable under the number of cycles examined

TABLE-1

Cell Line	HYAL1 Activity Cell Layer	HYAL1 Activity Media	Protein	mRNA 611bp 5' UTR	mRNA 129bp 5' UTR	CGH 3p21	FISH Cen/HY1
Keratinocyte	+	+	+	+	+	2	2/2
SCC-9	-	-	-	+	-	1	3/2
SCC-10a	+	+	+	+	+	1	4/1
SCC-15	-	-	-	+	-	1	4/2
SCC-25	-	-	-	+	-	1	4/2
SCC-10b	-	-	-	+	-	1	4/2
HOC-313	-	-	-	-	-	2	2/2
HSC-3	-	-	-	+	-	1	4/2

Discussion

The existence of acquired, somatic homozygous deletions over 3p21.3 in human malignancies is suggestive of a tumor suppressor gene locus. The presence of a functional tumor suppressor activity encompassing this region supports such a hypothesis. The homozygous deletions have been described both *in vitro* and *in vivo* (17), but no mutations of any of the genes in this deleted region have been reported with high frequency in carcinomas in which loss of heterozygosity has occurred. Knudson's "two hit hypothesis" (18) explaining the inactivation of two alleles of a recessive oncogene has generally held true for the classic tumor suppressor genes, such as the retinoblastoma gene product and p53. There has however, been considerable debate recently as to the stringency of defining what a tumor suppressor gene is (19). Although the HYAL1 gene product is not produced in the majority of HNSCC lines examined, the mechanism does not appear to have a molecular genetic basis. Therefore, the inactivation of HYAL1 in HNSCC could be independent of the tumor suppressor gene locus on 3p21.3.

Several factors hinder the refinement of the 3p21.3 candidate TSG locus. First, the density of gene transcripts arising from 3p21.3 has made it difficult to identify a particular gene, even with a 30kb homozygous deletion. Second, many genes on chromosome 3p21 are silenced at least in small cell lung carcinoma by unknown mechanisms (20). Finally, chromosome 3p is postulated to harbor other tumor suppressor gene loci i.e. Fragile Histidine Triad (FHIT) region at 3p14-p12 and the von Hippel-Lindau (VHL) disease region at 3p25, (21), making larger chromosomal deletions difficult to interpret.

The lack of a functional HYAL1 gene product in the majority of HNSCC lines examined is still intriguing, given that this gene resides within a potentially informative 30kb homozygous deletion. Although large chromosomal aberrations over 3p were found in the HNSCC lines, hemizyosity did not necessarily correlate with the loss of enzyme or protein. The SCC-10a line produced enzyme activity and properly spliced the 5'UTR. However, this line showed clear deletions of the 3p21.3 locus by FISH and CGH analysis. This demonstrates that one copy of the HYAL1 gene is sufficient to generate normal levels of enzyme activity.

The SCC-9, SCC-15, SCC-25, SCC-10b and HSC-3 lines showed only mRNA transcripts containing the unspliced 5' UTR. The unspliced 5' UTR leaves the transcript in a poor context for expression. Curiously, a mixture of the spliced and unspliced 5'UTR were found in normal keratinocytes and in human tissues by northern blot, demonstrating that this unspliced form is not exclusive to malignancies, but is rather the predominant species. Few examples of post-transcriptional regulation such as this exist in eukaryotic biology. The sex-lethal autoregulatory circuit in *Drosophila* is one such model in which 5' UTR splice variants regulate gene expression (22). Aberrant or alternative splicing of other candidate tumor suppressor genes such as FHIT and TSG101 have been reported, and generally appear to be epigenetic rather than mutations at intron-exon boundaries (23).

In contrast, the HOC-313 line lacked either one of the two transcripts for HYAL1 and yet was normal by both CGH and FISH. Preliminary studies showed a clear dose dependent reactivation of HYAL1 enzyme activity in this cell line following a 72 hr treatment with 5-aza-2'-deoxycytidine (data not shown). This raises the possibility that the HYAL1 gene is hypermethylated in the HOC-313

line. However, this has not been verified by sequencing metabisulfite treated DNA to confirm that the CpG island immediately upstream of HYAL1 is affected.

We have not examined the status of other hyaluronidase activities such as HYAL2, immediately adjacent to HYAL1 on 3p21.3. Our assays have been unable to detect recombinant HYAL2 enzymatic activity using either the microtiter-based or substrate gel assays. The covalently-bound biotinylated substrate may not serve as an available substrate. Nevertheless, all enzyme activity in both assays could be immunoprecipitated with the 17E9 mAb. There did not appear to be a cofactor required for enzyme activity, as the HSC-3 line was capable of producing HYAL1 protein as well as activity when the gene was introduced without the 5'UTR. These studies point towards the 5'UTR as the rate-limiting step in the production of enzyme activity.

In conclusion, it appears that in the HNSCC lines, the HYAL1 gene is silenced by either aberrant splicing or possibly by hypermethylation. The HYAL1 gene was inactivated or suppressed in six of the seven cell lines examined, but functionally inactivating mutations were not the basis of such phenomena. Both hypermethylation and the splicing deficiency could be explained as bystander effects that are not directly related to the inactivation of the HYAL1 gene.

Without evidence for a functional role of HYAL1 in suppressing tumorigenicity, these findings are simply associative in nature. In conclusion, although the HYAL1 gene is inactivated in HNSCC lines, the mechanisms responsible for such inactivation do not appear to be directly associated with the chromosomal aberrations at 3p, but warrant further investigation of this candidate tumor suppressor gene along with the other candidate genes in this region.

Materials and Methods

Cell Culture- SCC-9, SCC-15, SCC-25 squamous cell carcinoma lines were from the ATCC. SCC-10a, SCC-10b, HSC-3 and HOC-313 cell lines were kindly provided by R.H. Kramer (UCSF, O.C.R.C.). Normal human foreskin primary keratinocyte cultures (HFK) were obtained from Clonetics (San Diego, CA). HFK's were routinely cultured in serum-free defined keratinocyte basal media (Life Technologies) with antibiotics except for experiments for comparison of SCC lines. SCC lines were cultured in DME H21/F12 50:50 mix with 10% FBS plus antibiotics. For the analysis of serum-free cultures, all cells were grown in DMEH21/F12 50:50 mix plus antibiotics with insulin, transferrin and selenium.

Analysis of HYAL1 hyaluronidase activity in HNSCC lines- Hyaluronidase activity was measured using the microtiter-based assay as described (24), with biotinylated human umbilical cord HA as a substrate (ICN). SDS-HA substrate gel zymography was measured as previously described (25) using 100µg/ml hyaluronan final concentration. HNSCC lines or normal keratinocytes were seeded at 2×10^6 cells in the presence of serum or KGM respectively, and were cultured overnight. Cells were washed x5 with serum-free media and were then

incubated for 48 h in DME H21/Hams F12 50:50 with antibiotics and insulin transferrin and selenium. After 48 h cell layers were harvested with 3ml/T75 with PBS + 60mM octylglucoside (Boehringer-Mannheim) and protease inhibitors (Complete Boehringer-Mannheim) plus 100U/ml DNAase (Boehringer-Mannheim) and extracted for 1 hr on ice. Octyl glucoside and protease inhibitors were also added to conditioned media samples. Samples were then immunoprecipitated with 17E9 IgG2a anti-hyaluronidase antibodies conjugated to protein-A beads (1.5µg IgG2a/ mg cellular protein) and were incubated overnight at 4°C. Beads were collected by centrifugation and washed once with PBS. Immunoprecipitates were then measured for enzyme activity by zymography or by the microtiter-based assay. For zymography, immunoprecipitates were incubated with 5% SDS without reducing agents at room temperature. Beads were pelleted by centrifugation and supernatants electrophoresed on 10% SDS gels impregnated with 100µg/ml hyaluronan (ICN, Costa Mesa, CA). Gels were then incubated with 3% Triton-X 100 followed by incubation overnight in formate buffer pH 3.7 with 0.15M NaCl. Enzyme degradation was then detected with Alcian blue staining followed by Coomassie blue counterstaining. For the microtiter based assay, immunoprecipitates were brought up into 0.1 M formate

pH 3.7 with 0.1M NaCl and 3% Triton-X 100 and incubated in the microtiter based assay for 45 minutes against a standardized curve of human plasma hyaluronidase dilutions. Enzyme activity was described as relative TRUs (rTRU) based upon a standard curve of calibrated commercial enzyme.

Western blot analysis of HYAL1- Immunoprecipitates of HYAL1 using the 17E9 monoclonal antibodies from 1mg of total cellular protein or equivalent conditioned media were electrophoresed on 12% gels and blotted to PVDF membranes. Membranes were blocked with 5% milk block followed by probing with rabbit polyclonal antibodies diluted 1:2,000 raised against immunoaffinity-purified recombinant enzyme from HEK cells overexpressing HYAL1 and detected with ECL (Amersham).

RT-PCR analysis of HYAL1- Cytoplasmic RNA was isolated from normal keratinocytes and HNSCC lines by NP-40 lysis and was purified with the Qiagen RNA isolation kit. RNA was reverse transcribed using the Thermoscriptase kit (Life Technologies) and 3µg of total RNA per cell line. For amplification of the HYAL1 open reading frame from (482 to 2278) bp, RT-PCR was performed using

Expand® High Fidelity polymerase mix (Boehringer Mannheim) for 40 cycles using HYAL1F1 (CAGAGCAGCGGTGGATTAATGCG) and HYAL1R1 (AAGTCCACATAAAACGCTTAGCACGG) with a 95°C denaturing step for 3 min, followed by 95°C 30 sec, 62°C 30 sec 72°C for 2 min plus an additional 5 sec/cycle from cycles 10-30 and a final extension of 10 min at 72°C. Control β -actin primers were β AF (AACACCCCAGCCATGTACGTTGC) and β AR (TCCTTCTGCATCCTGTCGGCAA) and run under the same conditions as HYAL1F1 and HYAL1R1. For examination of the HYAL1 5' untranslated region from (15 to 606) bp, primers used were HYAL1F2 (GCAGCTGGGGTGGAAATCTGGC) and HYAL1R2 (CGGGACTGGTCGAGGACAACCT) with a 95°C denaturing step for 3 min followed by 95°C 30 sec, 63°C 30 sec 72°C for 1min plus an additional 5 sec/cycle from cycles 10-30, and a final extension of 10 min at 72°C. For amplification of the genomic HYAL1 sequence from (-104 to 2278bp), primers HY1F3 (CTGGCCTGGCCTCCTAATCCAAG) and HY1R1 were used with a 95°C denaturing step for 3 min followed by 95°C 30 sec, 62°C 30 sec 72°C for 2 min plus an additional 5sec/cycle from cycles 10-30 and a final extension of 10 min at 72°C. For sequencing PCR products, bands were excised, eluted with the Gel

Extraction Kit (Boehringer-Mannheim). All sequencing reactions were performed on double stranded DNA with the *Taq* dye deoxy terminator cycle sequencing kit (Applied Biosystems) according to the manufacturers instructions, and run on an ABI Prism™ automated sequencer (Applied Biosystems).

Generation of an Ecdysone Inducible HYAL1 Construct in HSC-3- The HYAL1 construct used previously for expression (Frost et al., 1997) was subcloned from the PCR3.1-Uni vector into the Ecdysone-responsive pIND vector (Invitrogen). The HYAL1 pIND vector was cotransfected into the HSC-3 line with the pVgRXR vector using lipofectin (Life Technologies). Cells were selected in 500µg/ml G418/ 500µg/ml Zeocin and cloned by limiting dilution. Clones overexpressing HYAL1 were screened using the microtiter-based assay in the absence and presence of muristerone. A dose response of muristerone (0-10µM) was used to examine HYAL1 activity. HYAL1 protein levels were examined by immunoprecipitation and western blot analysis as described above.

Fluorescence *In Situ* Hybridization Analysis of HYAL1 in Head and Neck

SCC- A PAC probe spanning HYAL1 on 3p21.3 (2) was biotinylated with dATP

using the BRL BioNick labeling kit (Life Technologies) and used for FISH analysis of normal keratinocytes and HNSCC lines as described (26). 200 nuclei were scored for each cell line as a ratio of chromosome 3p centromeric probe to the HYAL1 PAC signal.

Comparative Genomic Hybridization of HNSCC Lines- Comparative genomic hybridization of HNSCC lines and normal keratinocytes was performed as described previously (27).

Northern Analysis of HYAL1 mRNA forms in human tissues- A human multiple tissue poly-A⁺ Northern blot (Clontech) was probed using ³²P random primed HYAL1 cDNA excised and gel purified from a PCR 3.1-UNI vector. Blots were exposed for 19 hours.

Legends to The Figures

Figure.1. HA Substrate Gel Zymography of HYAL1 in HNSCC Lines. 17E9 mAb immunoprecipitates from 1mg cellular protein or corresponding conditioned media was examined on 10% HA substrate gels. Enzyme activity corresponds to clearings in the Alcian blue gel.

Figure.2. Microtiter-based assay of 17E9 cell layer for hyaluronidase activity. 17E9 immunoprecipitates in cell layer, conditioned media or cell layer supernates were examined. Activity is expressed as relative TRU's.

Figure.3. Western Blot analysis of 17E9 immunoprecipitates using polyclonal antibodies against recombinant HYAL1. 17E9 immunoprecipitates were probed with polyclonal antibodies to HYAL1.

Figure.4. RT-PCR analysis of HYAL1 reveals transcript in all cell lines except the HOC-313. Primers amplifying HYAL1 from 482 to 2278bp were used. β -actin controls were examined to control for RNA.

Figure.5a. The HSC-3 HNSCC line is capable of producing HYAL1 protein under an inducible promoter. An HSC-3 subclone transfected with HYAL1 under an ecdysone inducible construct. Conditioned media and cell extracts with and without induction were analyzed by 17E9 IP and Western blot with rabbit anti-HYAL1 Polyclonal Abs.

Figure.5b. The HSC-3 HYAL1 inducible subclone is capable of synthesizing HYAL1 in a dose dependent fashion in response to muristerone. Cells were cultured with varying concentrations of inducing agent (muristerone-A) and assayed for 17E9 reactive hyaluronidase activity after 48hr.

Figure.6.(a-h) FISH analysis of HYAL1 using a 100kb probe and comparative genomic hybridization of chromosome-3. 200 nuclei from each line were scored as a ratio of chromosome 3 centromeric probe to 3p21.3. CGH analysis of chromosome 3 using genomic DNA from HNSCC lines and normal keratinocytes were examined. Deletions are represented as regions scoring below the normalized line (---).

Figure.7. RT-PCR analysis of the HYAL1 5' UTR reveals two variants of the HYAL1 5'UTR. Lower 109bp band corresponds to spliced form of HYAL1. The 591bp band represents the unspliced form.

Figure.8. Northern analysis of HYAL1 in human tissues reveals two species of HYAL1 in normal tissues. Lane-1 Heart, Lane-2 Brain, Lane-3 Placenta, Lane-4 Lung, Lane-5 Liver, Lane-6 Skeletal Muscle, Lane-7 Kidney, Lane-8 Pancreas.

FIGURE-1

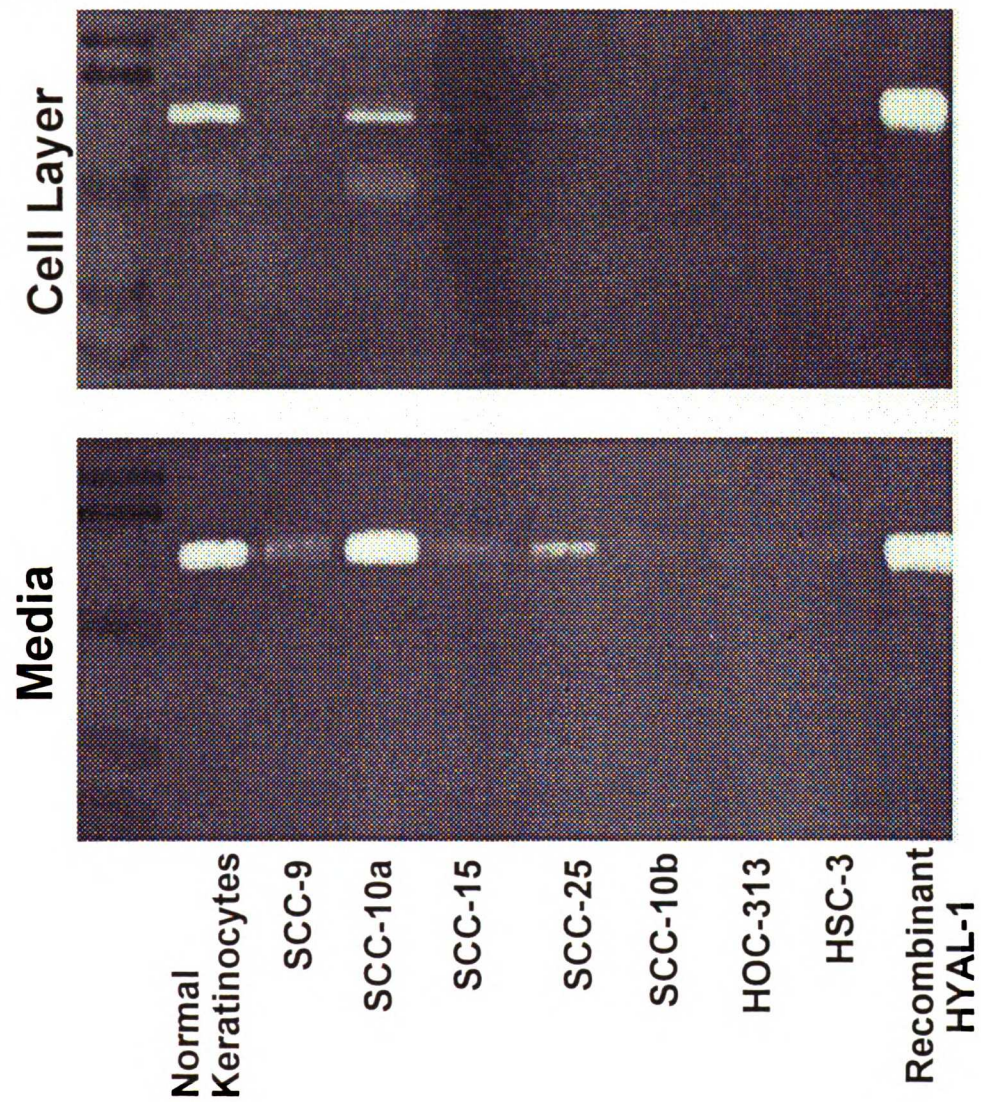


FIGURE-2

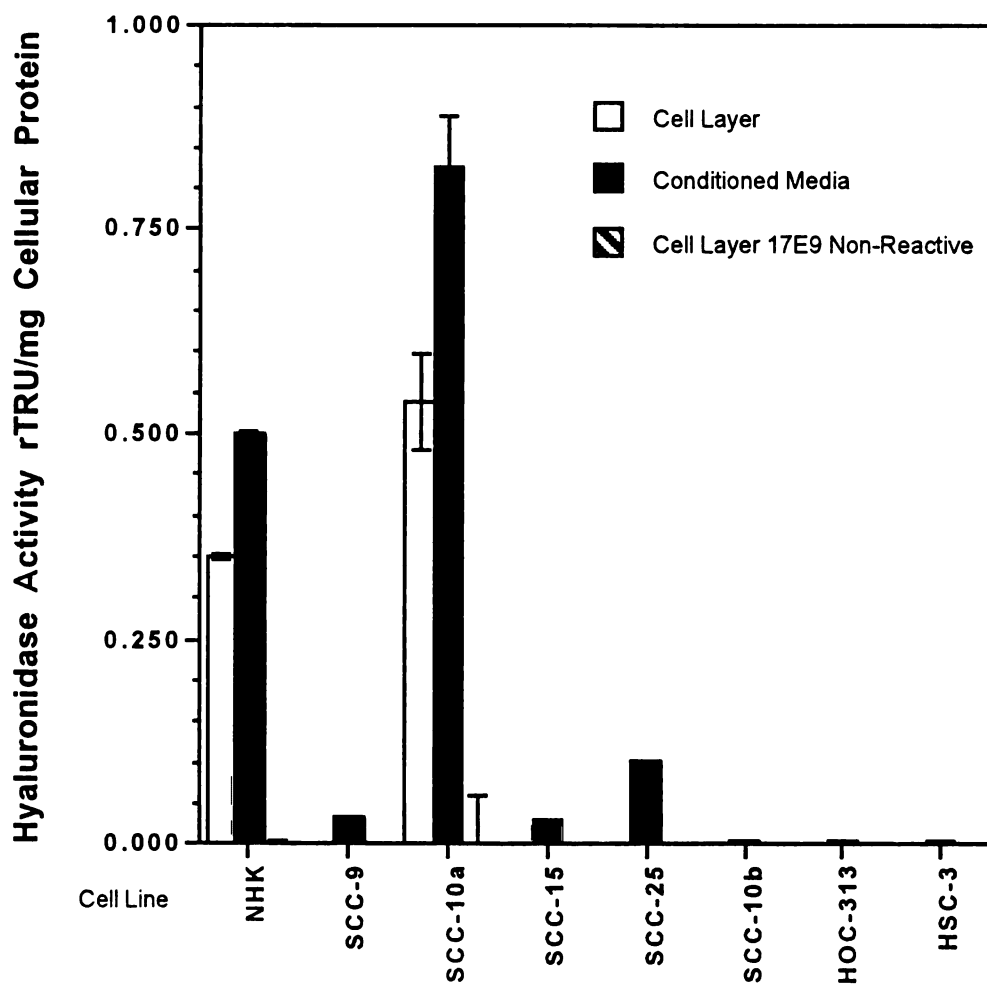


FIGURE-3

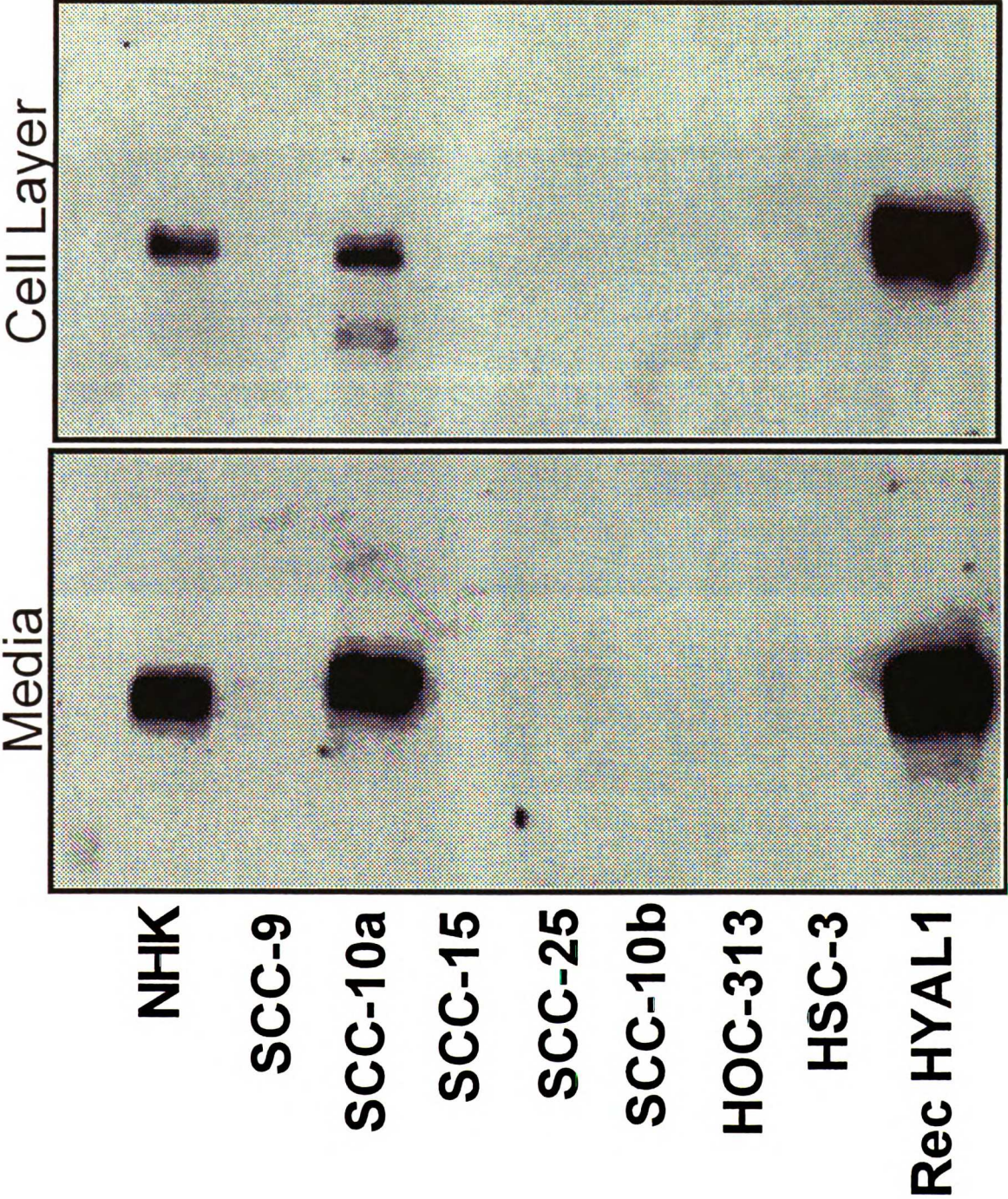


FIGURE-4

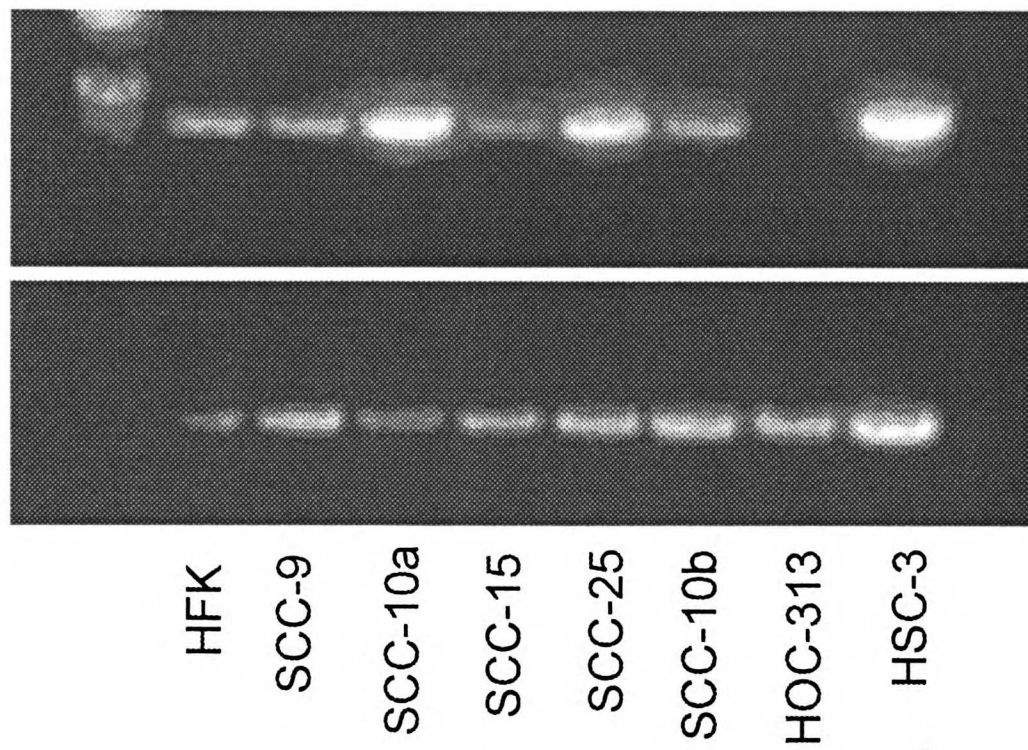
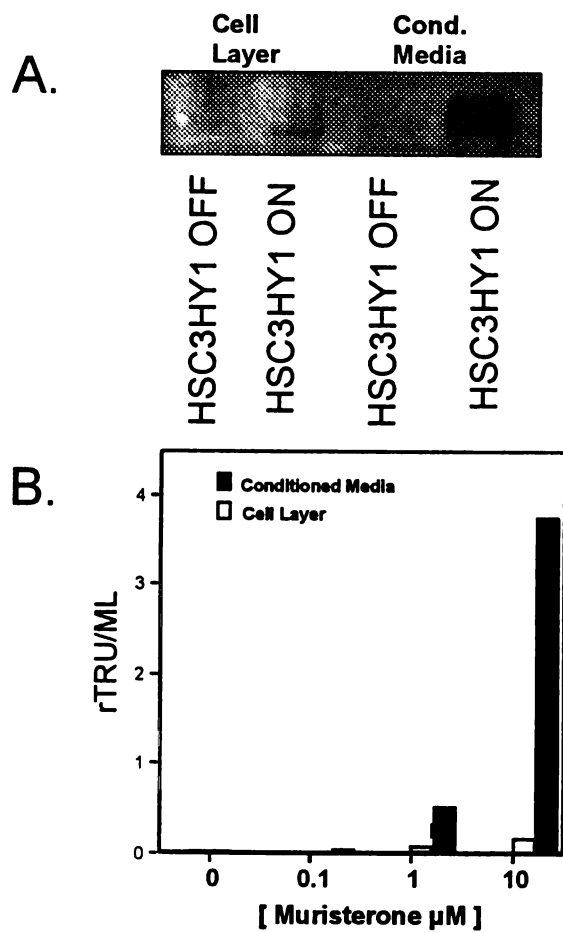
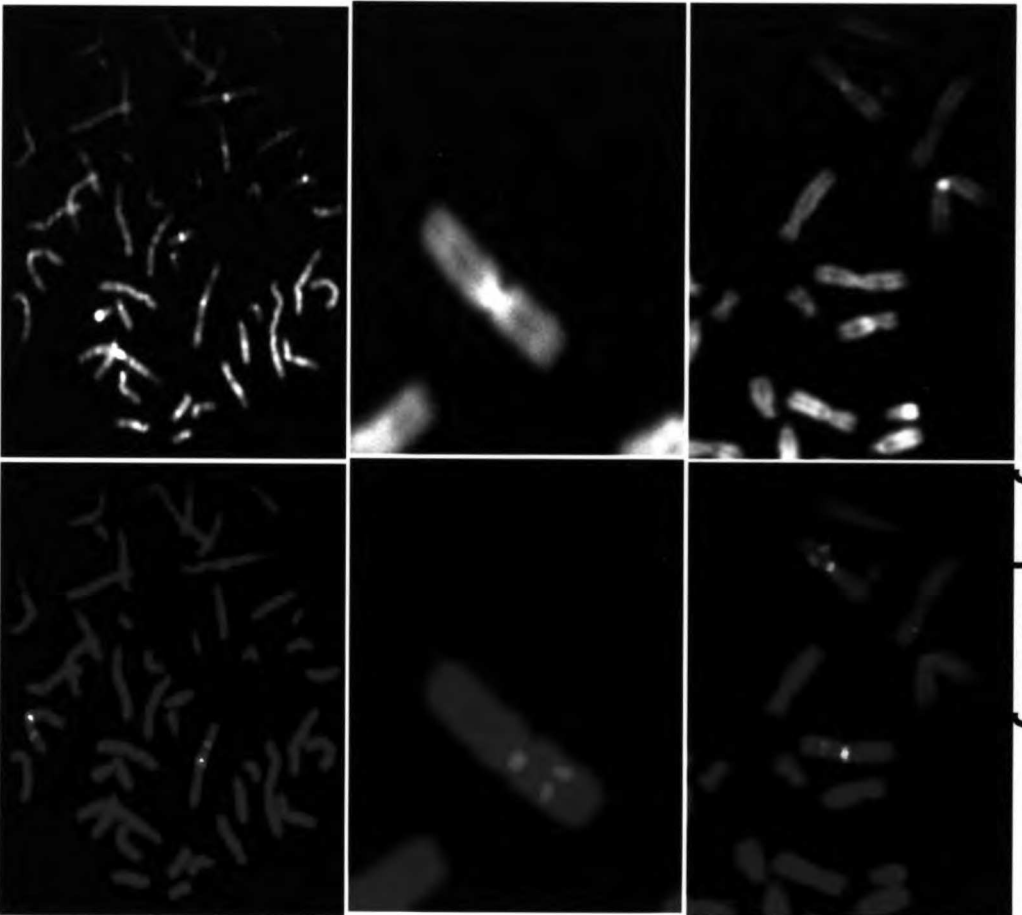


FIGURE-5

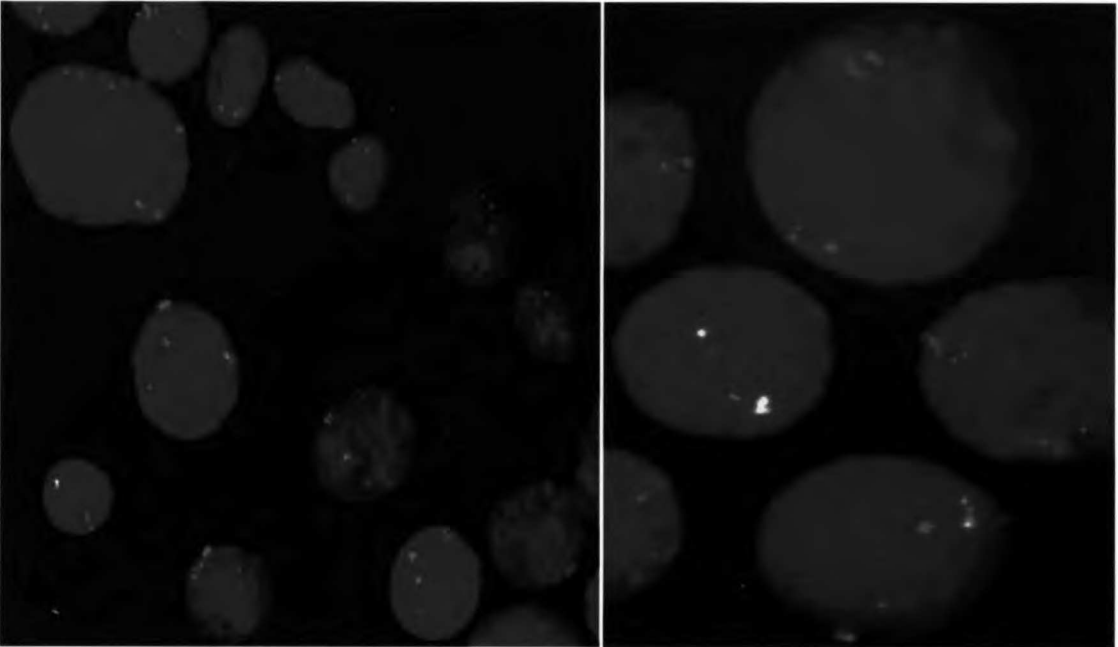


6a

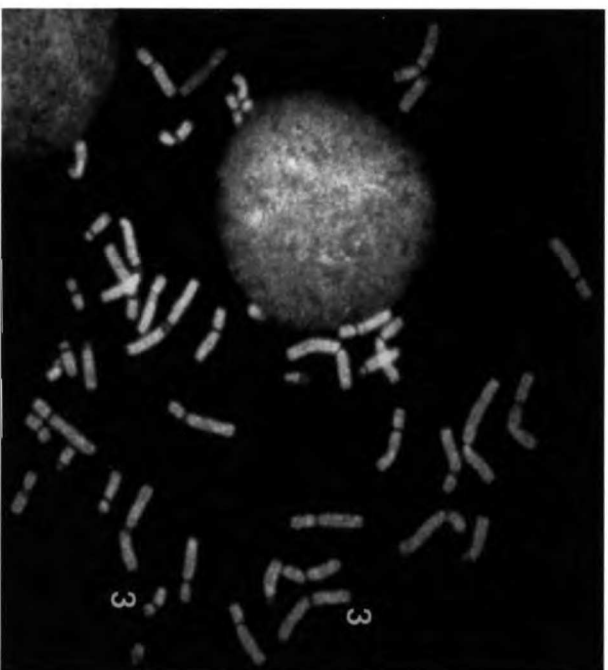
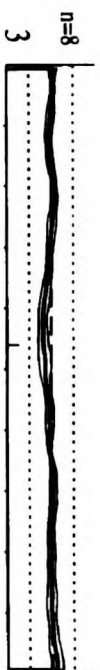
Normal Lymphocytes



6b

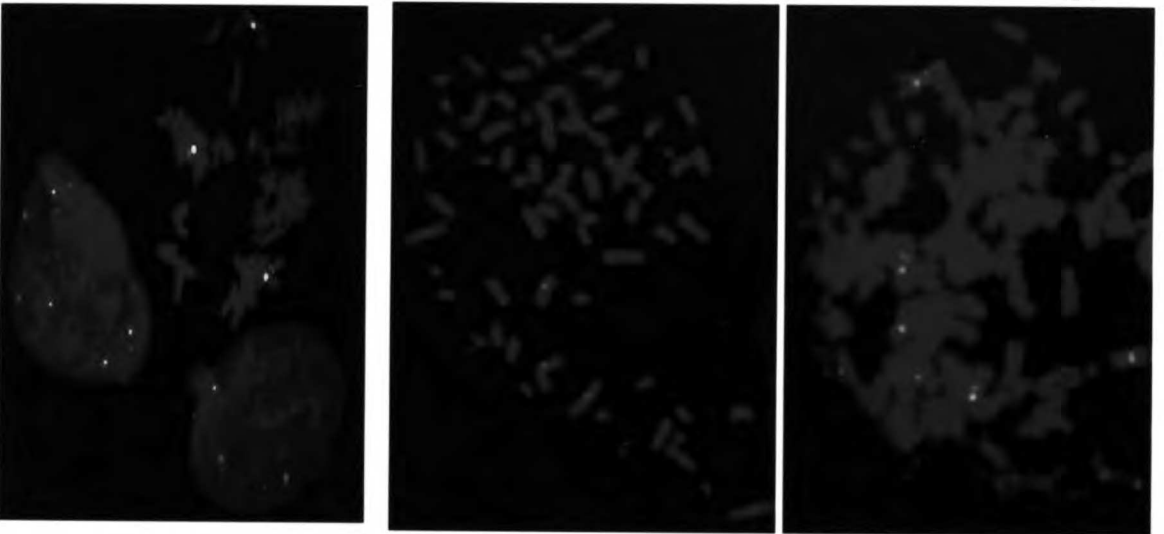


Keratinocytes



2/2=246
2/1=12

6C

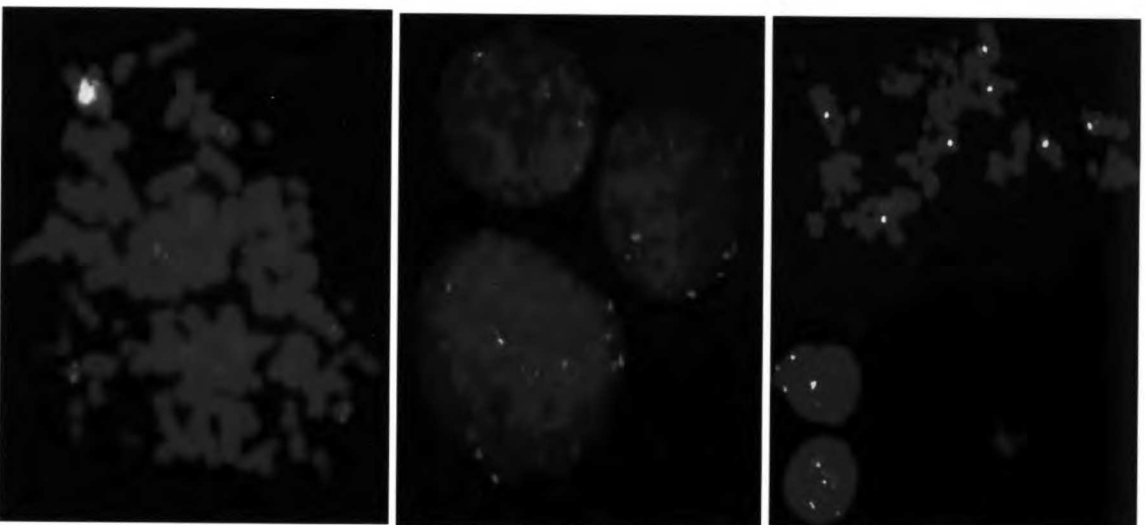


SCC-9

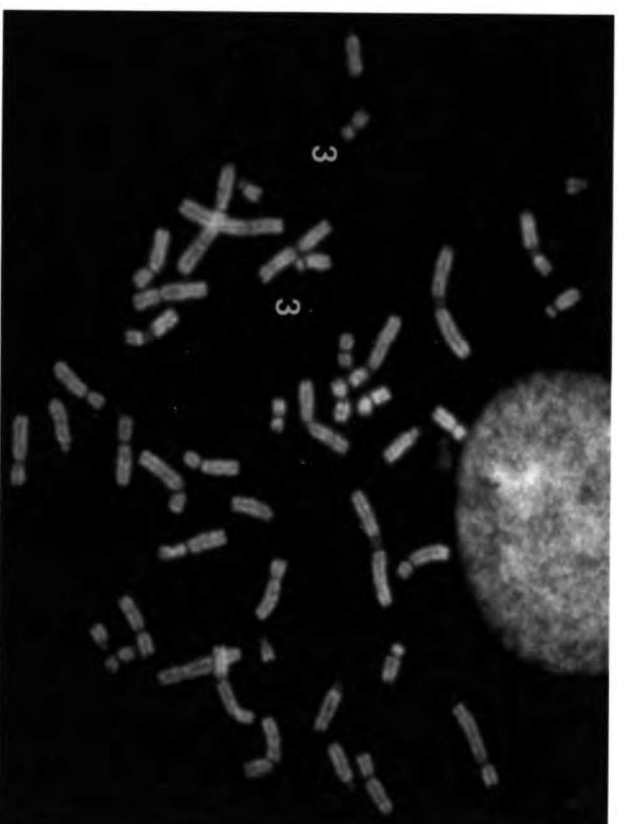
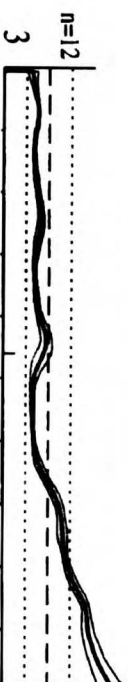


3/1=67
3/2=86
4/2=10

6d



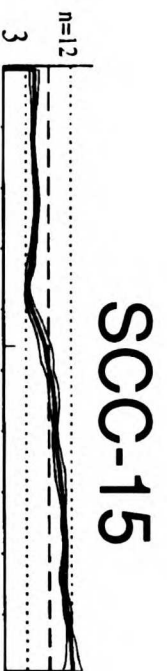
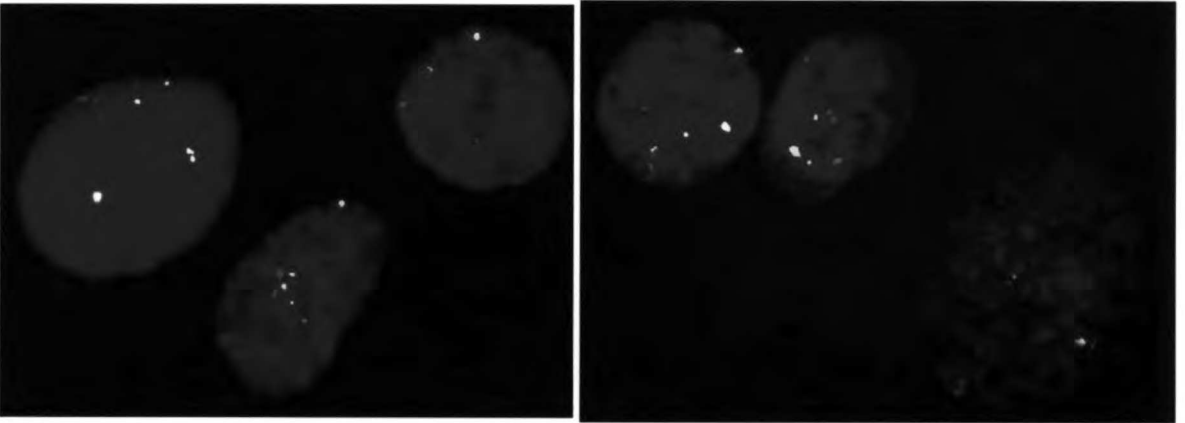
SCC-10a



4/1=87
3/1=31
4/2=27

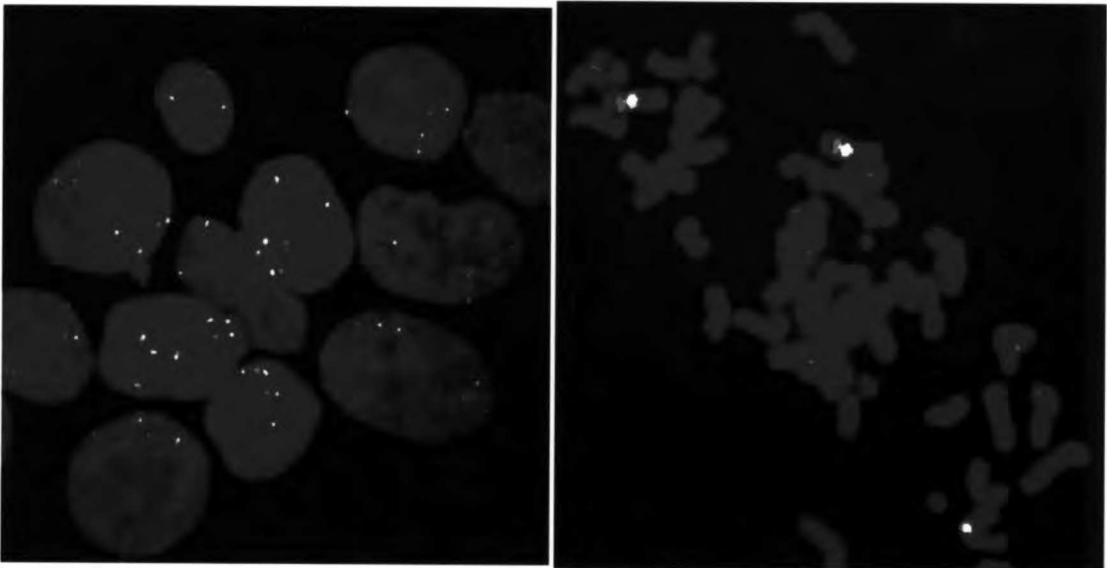
3/2=18
2/1=14

6e

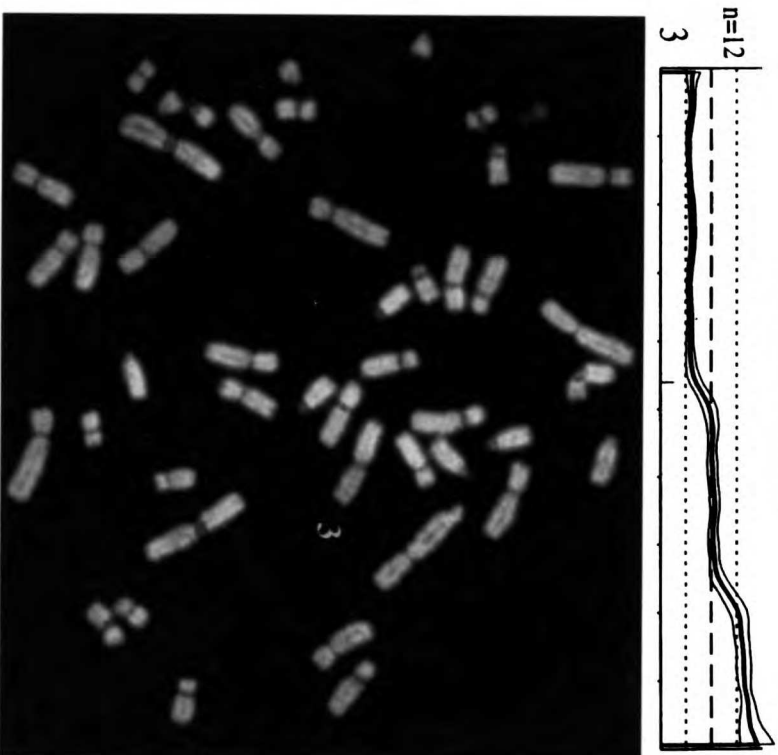


4/2=108 4/1=10
5/2=37 2/1=2
3/2=27

6f



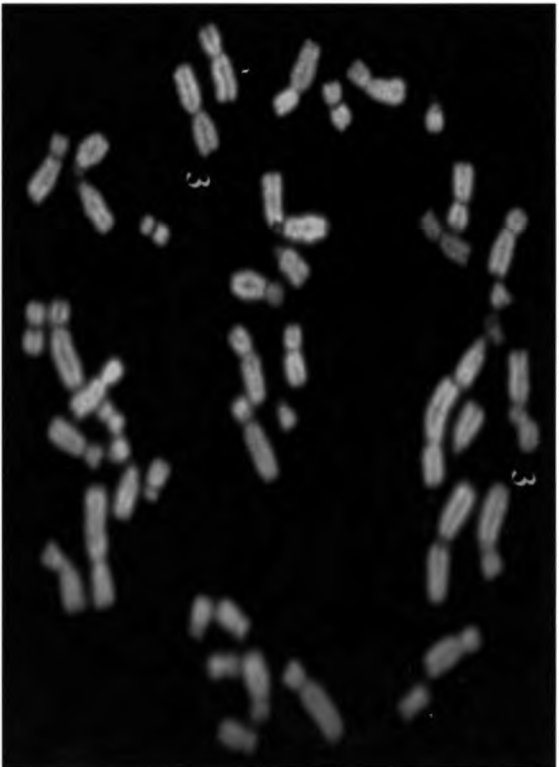
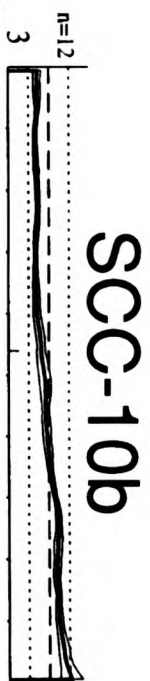
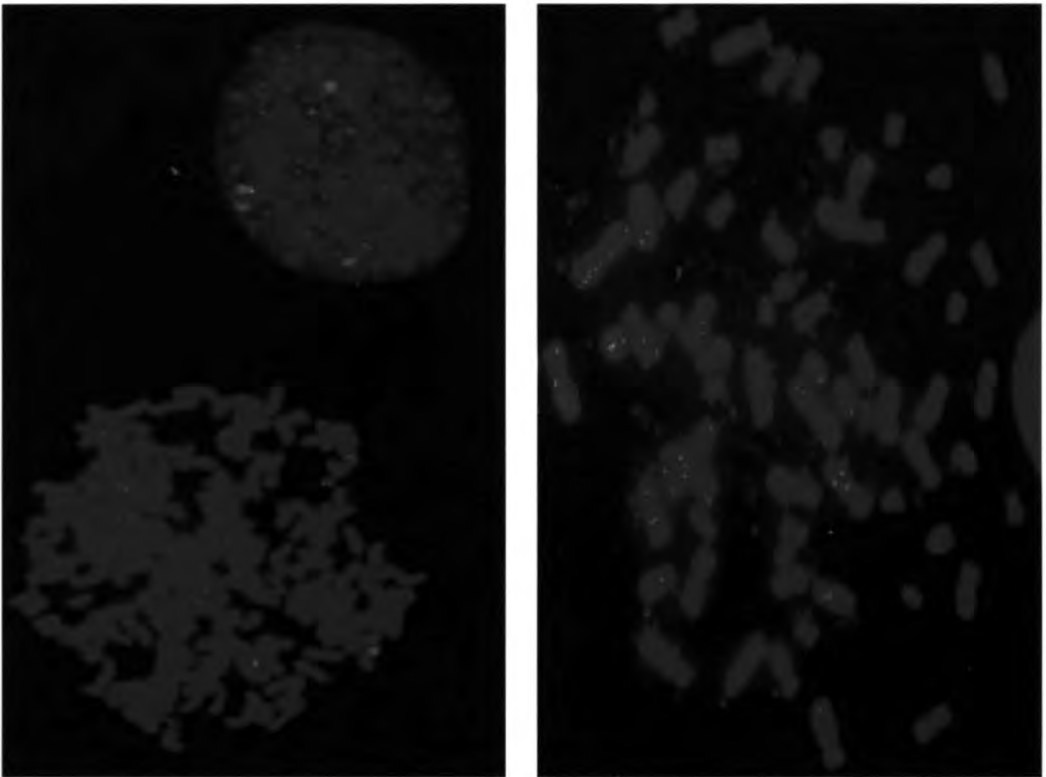
SCC-25



4/2=110
4/1=45

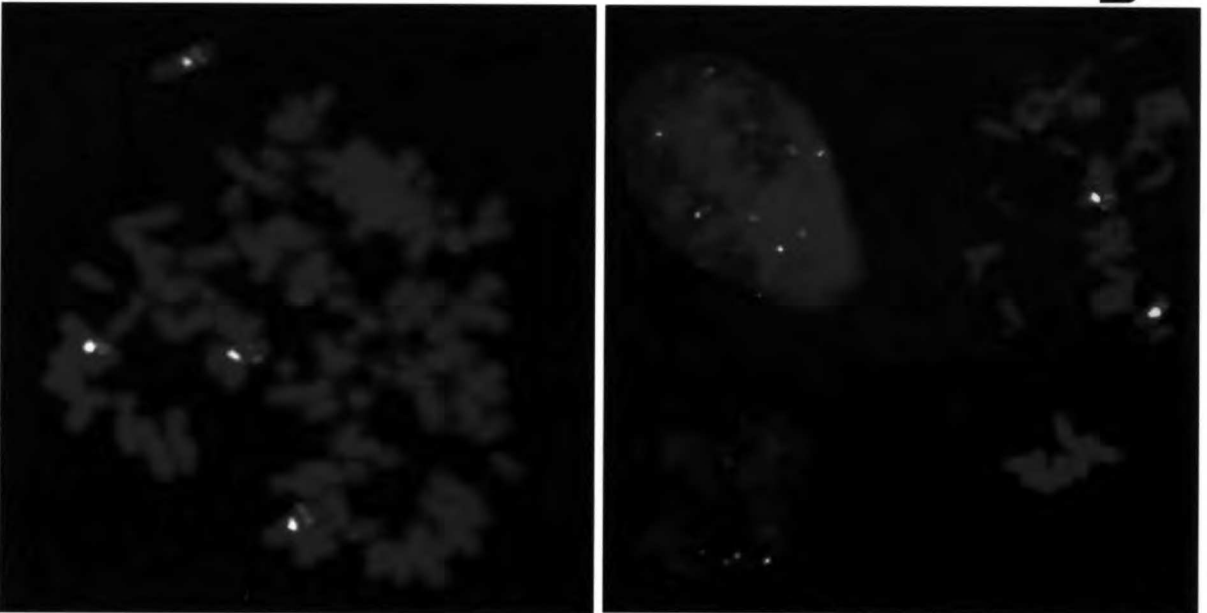
5/2=14
3/2=14

6g

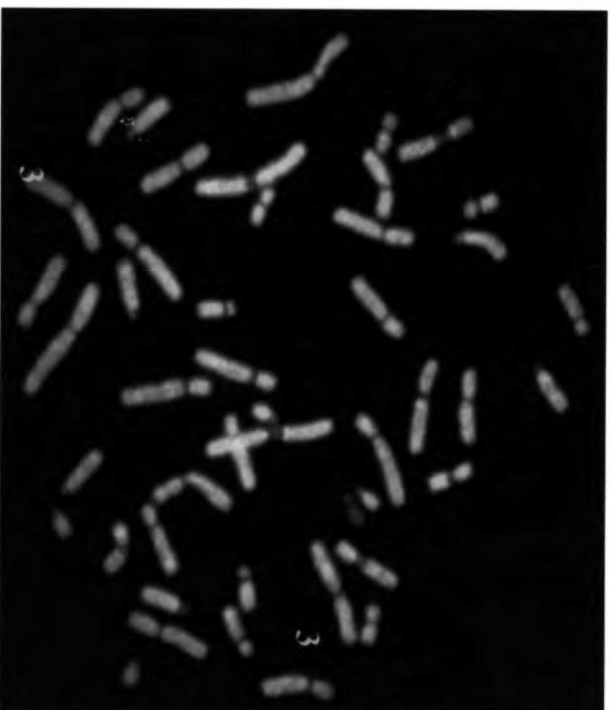


4/2=175
3/2=23

6h

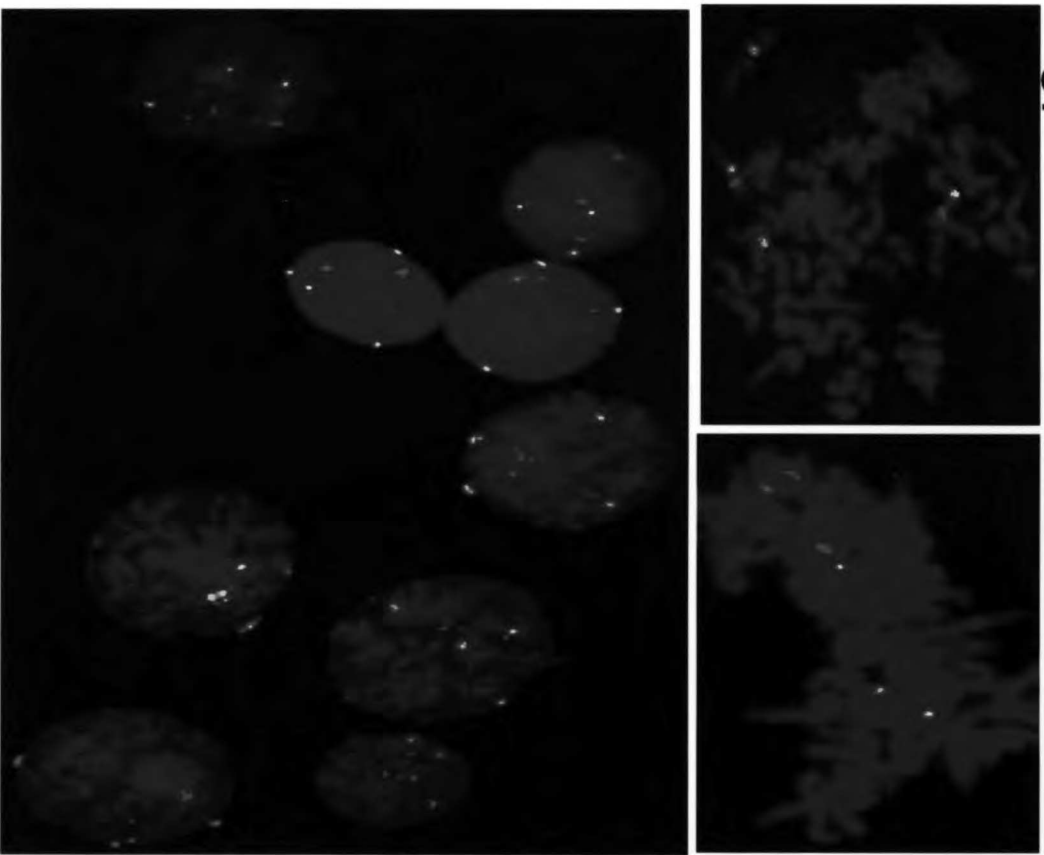


HOC-313

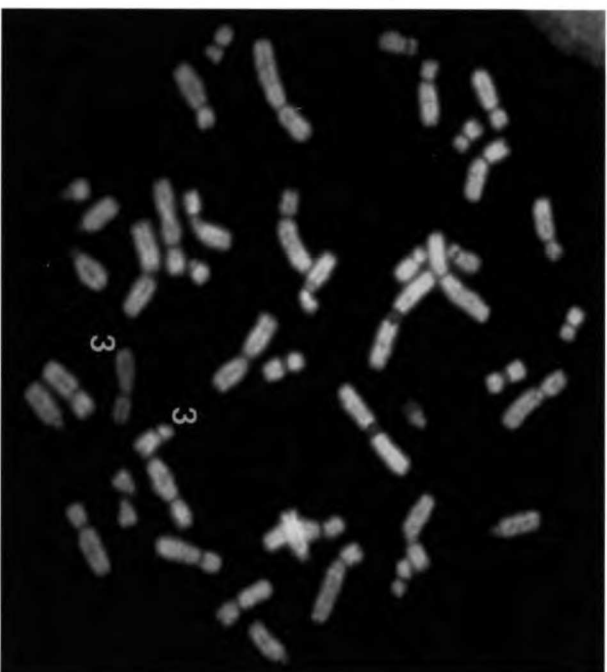


$3/2=60$	$4/4=24$
$2/2=136$	$3/3=11$

6i



HSC-3



4/2=240

4/1=5

3/2=2

10

FIGURE-7

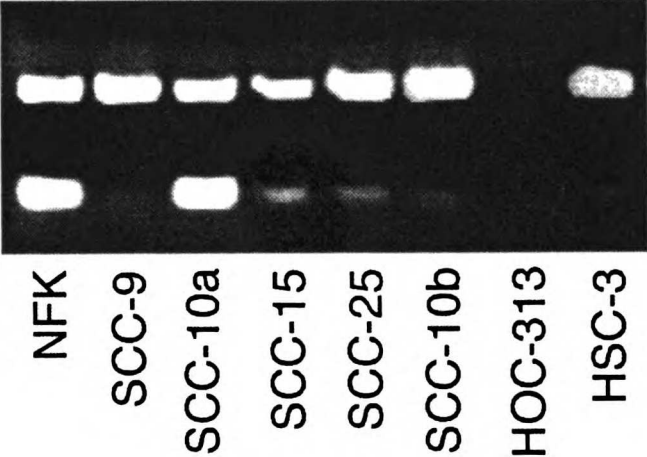
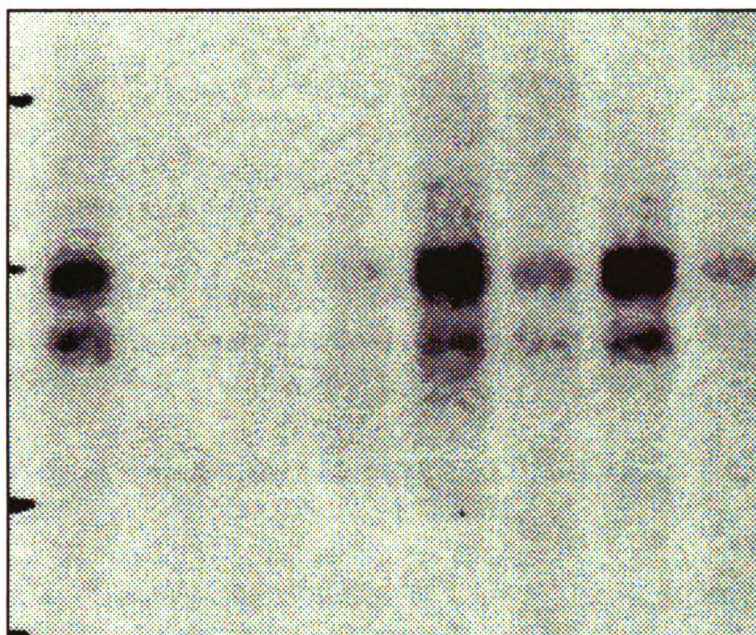


FIGURE-8



1 2 3 4 5 6 7 8

References

1. Baylin, S.B., Herman, J.G., Graff, J.R., Vertino, P.M. & Issa, J.P. (1998). *Adv Cancer Res*, **72**, 141-96.
2. Sager, R. (1997). *Proc Natl Acad Sci U S A*, **94**, 952-5.
3. Csoka, T.B., Frost, G.I., Heng, H.H., Scherer, S.W., Mohapatra, G. & Stern, R. (1998). *Genomics*, **48**, 63-70.
4. Wei, M.H., Latif, F., Bader, S., Kashuba, V., Chen, J.Y., Duh, F.M., Sekido, Y., Lee, C.C., Geil, L., Kuzmin, I., Zabarovsky, E., Klein, G., Zbar, B., Minna, J.D. & Lerman, M.I. (1996). *Cancer Res*, **56**, 1487-92.
5. Latif, F., Duh, F.M., Bader, S., Sekido, Y., Li, H., Geil, L., Zbar, B., Minna, J.D. & Lerman, M.I. (1997). *Hum Genet*, **99**, 334-41.
6. Sekido, Y., Ahmadian, M., Wistuba, II, Latif, F., Bader, S., Wei, M.H., Duh, F.M., Gazdar, A.F., Lerman, M.I. & Minna, J.D. (1998). *Oncogene*, **16**, 3151-7.
7. Cheng, Y., Poulos, N.E., Lung, M.L., Hampton, G., Ou, B., Lerman, M.I. & Stanbridge, E.J. (1998). *Proc Natl Acad Sci U S A*, **95**, 3042-7.
8. Buchhagen, D.L., Worsham, M.J., Dyke, D.L. & Carey, T.E. (1996). *Head Neck*, **18**, 529-37.
9. Frost, G.I., Csoka, T.B. & Stern, R. (1996). *Trends in Glycoscience and Glycotechnology*, **8**, 419-434.
10. Kreil, G. (1995). *Protein Sci*, **4**, 1666-9.
11. Gmachl, M., Sagan, S., Ketter, S. & Kreil, G. (1993). *FEBS Lett*, **336**, 545-8.
12. Lepperdinger, G., Strobl, B. & Kreil, G. (1998). *J Biol Chem*, **273**, 22466-70.
13. Heckel, D., Comtesse, N., Brass, N., Blin, N., Zang, K.D. & Meese, E. (1998). *Hum Mol Genet*, **7**, 1859-72.
14. Frost, G.I., Csoka, T.B., Wong, T. & Stern, R. (1997). *Biochem Biophys Res Commun*, **236**, 10-5.

-
15. Wei, M.H., Latif, F., Bader, S., Kashuba, V., Chen, J.Y., Duh, F.M., Sekido, Y., Lee, C.C., Geil, L., Kuzmin, I., Zabarovsky, E., Klein, G., Zbar, B., Minna, J.D. & Lerman, M.I. (1996). *Cancer Res*, **56**, 1487-92.
 16. Csoka, T.B., Frost, G.I., Wong, T. & Stern, R. (1997). *FEBS Lett*, **417**, 307-10.
 17. Todd, S., Franklin, W.A., Varella-Garcia, M., Kennedy, T., Hilliker, C.E., Jr., Hahner, L., Anderson, M., Wiest, J.S., Drabkin, H.A. & Gemmill, R.M. (1997). *Cancer Res*, **57**, 1344-52.
 18. Knudson, A.G., Jr. (1971). *Proc Natl Acad Sci U S A*, **68**, 820-3.
 19. Haber, D. & Harlow, E. (1997). *Nat Genet*, **16**, 320-2.
 20. Scaloni, A., Jones, W., Pospischil, M., Sassa, S., Schneewind, O., Popowicz, A.M., Bossa, F., Graziano, S.L. & Manning, J.M. (1992). *J Lab Clin Med*, **120**, 546-52.
 21. Hibi, K., Takahashi, T., Yamakawa, K., Ueda, R., Sekido, Y., Ariyoshi, Y., Suyama, M., Takagi, H., Nakamura, Y. & Takahashi, T. (1992). *Oncogene*, **7**, 445-9.
 22. Granadino, B., Penalva, L.O.F., Green, M.R., Valcarcel, J. & Sanchez, L. (1997). *Proc Natl Acad Sci U S A*, **94**, 7343-8.
 23. Gayther, S.A., Barski, P., Batley, S.J., Li, L., de Foy, K.A., Cohen, S.N., Ponder, B.A. & Caldas, C. (1997). *Oncogene*, **15**, 2119-26.
 24. Frost, G.I. & Stern, R. (1997). *Anal Biochem*, **251**, 263-9.
 25. Guntenhoner, M.W., Pogrel, M.A. & Stern, R. (1992). *Matrix*, **12**, 388-96.
 26. Mohapatra G, Moore DH, Kim DH, Grewal L, Hyun WC, Waldman FM, Pinkel D, Feuerstein BG. (1997) *Genes Chromosomes Cancer*. , **20**(4):311-9.
 27. Mohapatra G, Kim DH, Feuerstein BG. (1995) *Genes Chromosomes Cancer*. **13**(2):86-93.

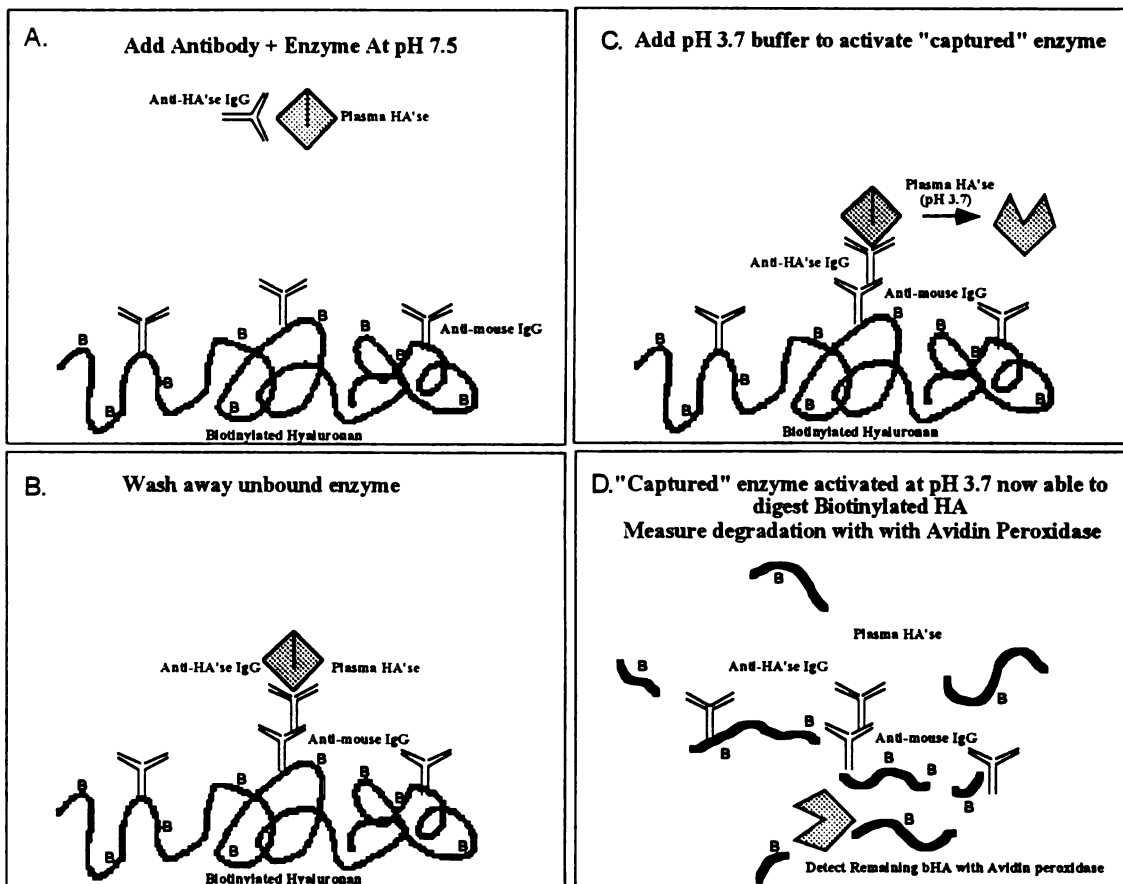
Appendix

A. Generation of anti-HYAL1 Monoclonal Antibodies-

Monoclonal antibodies against biochemically purified plasma hyaluronidase were generated by use of a novel enzyme capture assay. Six-week old Balb/c mice were inoculated i.p. with 25 μ g injections of purified antigen from 20-liters of human plasma in Freund's complete adjuvant, followed by three boosts over a three month period in Freund's incomplete adjuvant. Tail vein bleeds were assayed for anti-hyaluronidase antisera by use of an immunoenzyme capture assay developed for screening monoclonal antibodies.

Biotinylated HA 10 μ g/well was crosslinked on Covalink NH-ELISA plates with 1.25 μ g/well goat antimouse-IgG using an EDAC reaction and Sulfo-NHS. Immunized sera or pre-immune control was mixed with human plasma, followed by incubation in the anti-mouse IgG bHA plates. Non-immunoprecipitated enzyme was removed by washing under stringent conditions at neutral pH, followed by acidification to pH 3.7 which activates the immunoprecipitated enzyme and allows degradation of biotinylated substrate to occur (See diagram below).

Anti-Hyaluronidase Monoclonal Antibody Enzyme Capture Screening Assay



After the final boost of antigen (intravenously without adjuvant), two animals with the highest titers were sacrificed and two spleens were fused with SP2/0 myeloma cells by PEG-fusion. SP2/0-splenocyte hybridomas were plated out into 1,900 wells and grown in HAT-containing media for 10 days. Eight strongly positive colonies were recloned to ensure monoclonality. One clone of the IgG2a-kappa subclass was expanded for ascites production. Murine IgG2a was purified through protein-A affinity chromatography. All eight clones

immunoprecipitate all detectable hyaluronidase activity from human plasma using the microtiter assay.

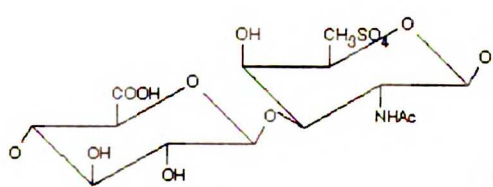
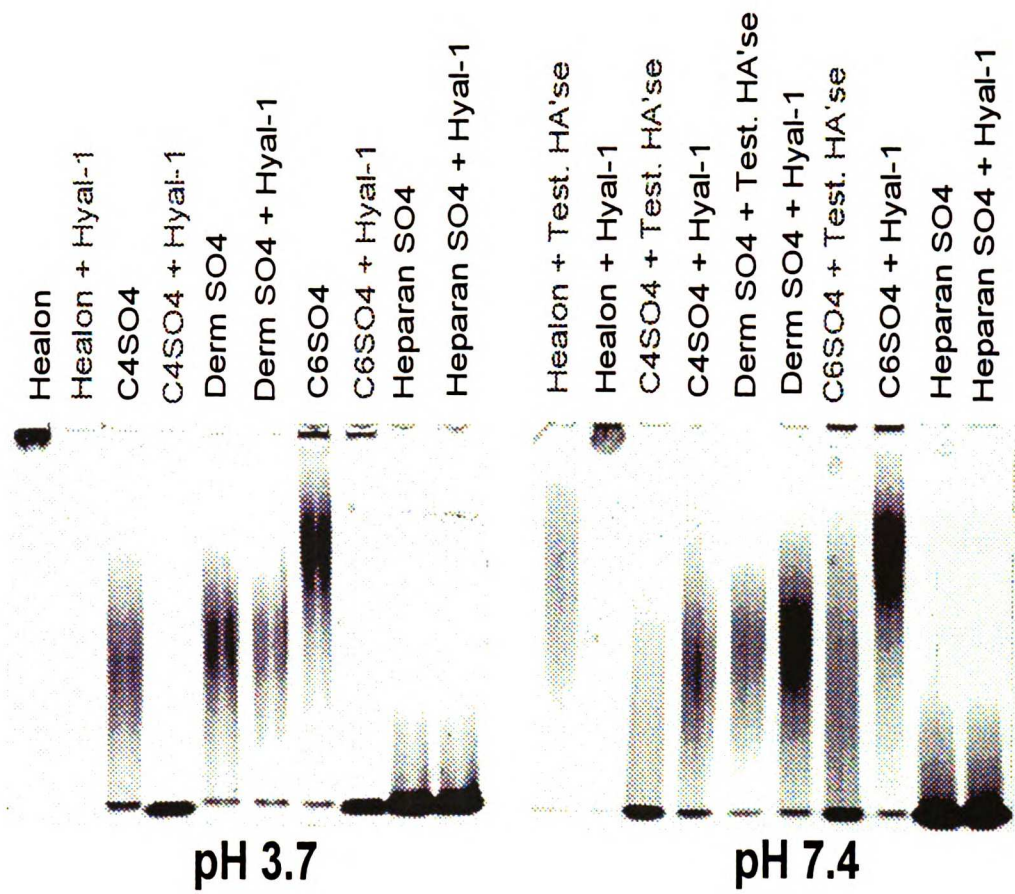
B. Substrate And pH Specificity of HYAL1

The substrate and pH specificity of immunoaffinity-purified recombinant HYAL1 towards various glycosaminoglycans was investigated by use of a gel shift assay.

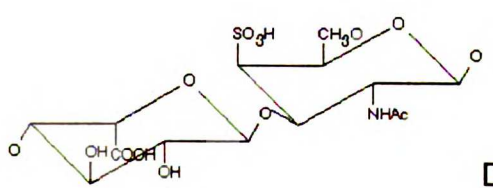
HYAL1 had endo-glycosidase activity towards HA, chondroitin-4 sulfate and chondroitin-6 sulfate, with no apparent hydrolysis of dermatan or heparan sulfate.

This substrate specificity is identical to that of testicular hyaluronidase preparations (mainly PH-20) aside from the pH dependence on such interactions.

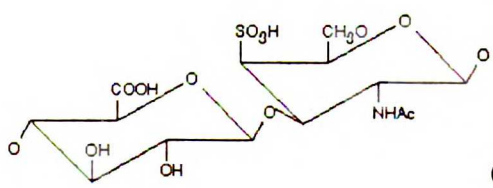
Although HYAL1 had no hydrolytic capacity towards heparan sulfate, the enzyme was capable of binding heparin at neutral pH as determined by heparin sepharose affinity chromatography.



Chondroitin 6-Sulfate



Dermatan Sulfate

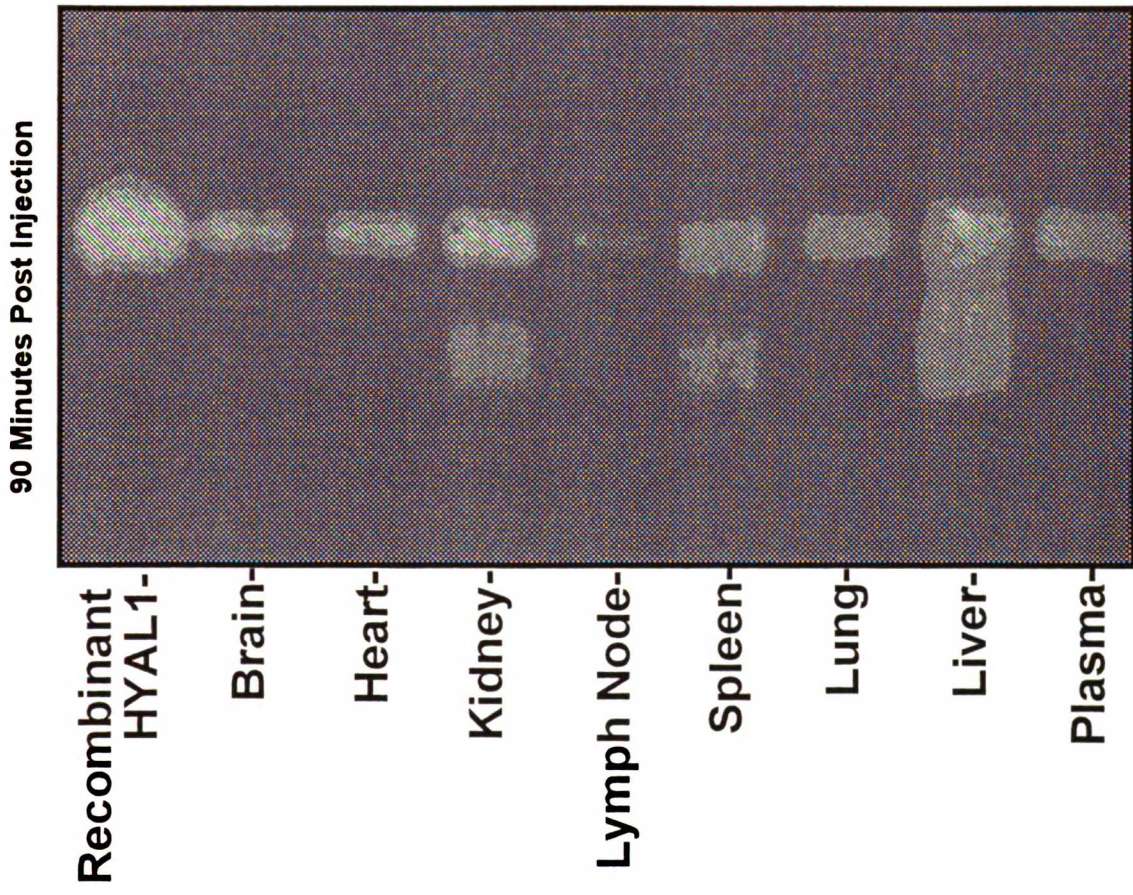


Chondroitin-4 Sulfate

C. Uptake of Immunoaffinity Purified HYAL1 in Mouse

To examine the fate of recombinant HYAL1 administered systemically in mice, 5,000 rTRU corresponding to approximately 50 μ g of enzyme was injected i.v. into C57B mice. Animals were sacrificed at 90 min. and tissues from liver, spleen, kidney, heart, lung, brain, lymph nodes and plasma were prepared. Organs were lysed in octylglucoside with protease inhibitors and enzyme was immunoprecipitated with the 17E9 conjugated to protein-A beads. HYAL1 activity recovered from immunoprecipitates of each organ was then measured by zymography and the microtiter-based assay. The majority of activity was recovered initially in the liver, followed by the kidney, spleen and lungs. On the basis of specific activity (activity/ mg protein), the liver kidney and spleen had essentially a similar specific activity. At 90 min. following administration of 5,000 rTRU's, greater than 50% of the enzyme remained in circulation. In each tissue, an additional 47kDa band was found in the tissue extracts of liver, kidney and spleen, which appeared to be identical in size to the lower MW, proteolytically processed form of HYAL1 found in human urine.

UPTAKE OF IV ADMINISTERED HYAL1 (5,000 Units)



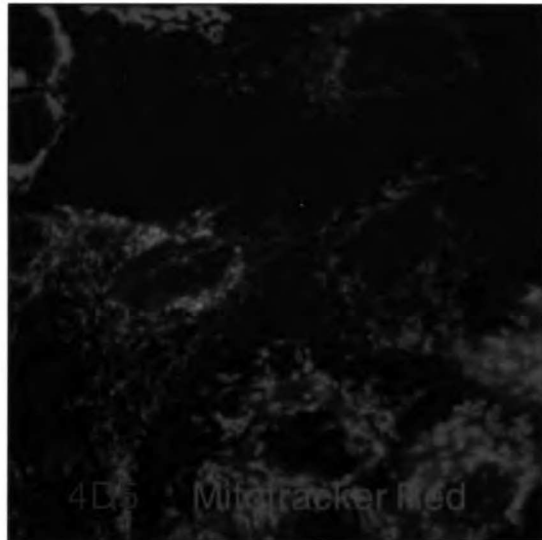
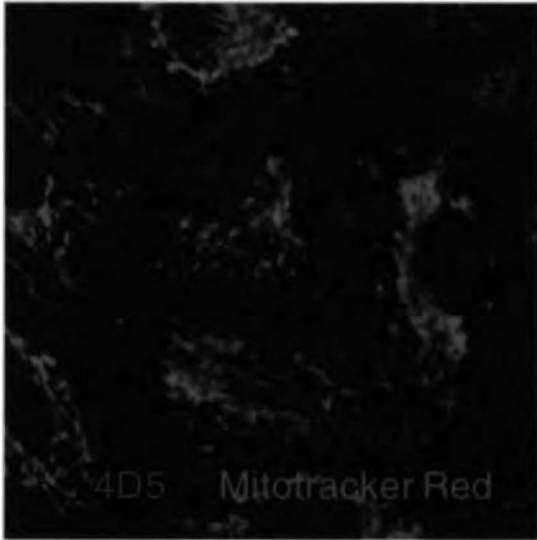
D. Immunoreactivity of HYAL1 in MDCK Cells

For the detection of HYAL1 immunoreactivity in MDCK cells, HYAL1 PCR3.1-CMV as described in Chapter-3 was transiently transfected into MDCK cells using Superfect reagent (Qiagen). Twelve hours following transfection, cells were trypsinized and replated into 8-well chamber slides. For the control of organelle structures, cells were incubated with Mitotracker-Red (Molecular Probes) for 30 min prior to fixation. Forty eight hours post transfection, cells were washed twice with cold PBS, fixed in 4% PFA, washed again with PBS, permeabilized with 0.1% Triton-X100 and blocked with 10% normal goat serum in PBS for one hour. 4D5 mAb ascites (which does not immunoprecipitate canine HYAL1 from MDCK cells) was applied in 10% NGS at a final IgG concentration of 5 μ g/ml for one h at 4°C. Mouse IgG was detected with FITC labeled goat anti-mouse IgG at a concentration of 20 μ g/ml for 45 min. Cells were mounted in Vectashield, sealed and processed for confocal microscopy.

Analysis of HYAL1 immunoreactivity in transfected MDCK cells revealed a perinuclear staining pattern that appeared to be vesicles of the Golgi. Weaker punctate nuclear staining was found in both controls and transfectants, which was much more pronounced using the 17E9 mAb. It appears that either HYAL1 is exclusively secreted from cells following synthesis or that the mAb epitope is lost following modifications in the Golgi.

Control

HYAL1 CMV



The first part of the document discusses the general principles of the proposed system. It is intended to provide a comprehensive overview of the various aspects involved in the implementation of the new regulations. The following sections will detail the specific measures to be taken, the responsibilities of the various departments, and the timeline for the completion of the project.

The second part of the document outlines the specific measures to be taken. These measures are designed to ensure the smooth and efficient operation of the system. The following sections will detail the specific measures to be taken, the responsibilities of the various departments, and the timeline for the completion of the project.

The third part of the document outlines the responsibilities of the various departments. These responsibilities are designed to ensure the smooth and efficient operation of the system. The following sections will detail the specific measures to be taken, the responsibilities of the various departments, and the timeline for the completion of the project.

The fourth part of the document outlines the timeline for the completion of the project. This timeline is designed to ensure that the project is completed on time and within budget. The following sections will detail the specific measures to be taken, the responsibilities of the various departments, and the timeline for the completion of the project.

The fifth part of the document outlines the budget for the project. This budget is designed to ensure that the project is completed on time and within budget. The following sections will detail the specific measures to be taken, the responsibilities of the various departments, and the timeline for the completion of the project.

The sixth part of the document outlines the conclusion of the project. This conclusion is designed to ensure that the project is completed on time and within budget. The following sections will detail the specific measures to be taken, the responsibilities of the various departments, and the timeline for the completion of the project.

The seventh part of the document outlines the appendix. This appendix is designed to provide additional information on the project. The following sections will detail the specific measures to be taken, the responsibilities of the various departments, and the timeline for the completion of the project.

The eighth part of the document outlines the index. This index is designed to provide a comprehensive overview of the various aspects involved in the implementation of the new regulations. The following sections will detail the specific measures to be taken, the responsibilities of the various departments, and the timeline for the completion of the project.

The ninth part of the document outlines the glossary. This glossary is designed to provide a comprehensive overview of the various aspects involved in the implementation of the new regulations. The following sections will detail the specific measures to be taken, the responsibilities of the various departments, and the timeline for the completion of the project.

The tenth part of the document outlines the bibliography. This bibliography is designed to provide a comprehensive overview of the various aspects involved in the implementation of the new regulations. The following sections will detail the specific measures to be taken, the responsibilities of the various departments, and the timeline for the completion of the project.

For Not to be taken
from the room.
reference

6861408



3 1378 00686 1408

